DISSERTATIONES
MEDICINAE
UNIVERSITATIS
TARTUENSIS
235

ANDRES LUST

Water mediated solid state transformations of a polymorphic drug – effect on pharmaceutical product performance

DISSERTATIONES MEDICINAE UNIVERSITATIS TARTUENSIS
235

DISSERTATIONES MEDICINAE UNIVERSITATIS TARTUENSIS
235

ANDRES LUST

Water mediated solid state transformations of a polymorphic drug – effect on pharmaceutical product performance

UNIVERSITY OF TARTU
PRESS
1632

Department of Pharmacy, University of Tartu, Estonia

Dissertation is accepted for the commencement of the degree of Doctor of Philosophy in Pharmacy on 17.06.2015 by the Council of the Faculty of Medicine, University of Tartu, Estoniaa.

Supervisors: Senior Researcher Karin Kogermann, PhD, Department of Pharmacy, University of Tartu, Estonia

Professor Peep Veski, Dr. Pharm, Department of Pharmacy, University of Tartu, Estonia

Reviewed by: Associate Professor Uno Mäeorg, PhD, Institute of Chemistry, University of Tartu, Estonia

Senior Researcher Meeme Utt, PhD, Institute of Biomedicine and Translational Medicine, University of Tartu

Opponent: Professor Guy Van Den Mooter, PhD, Laboratory for Pharmacotechnology and Biopharmacy, Department of Pharmaceutical and Pharmacological Sciences, Catholic University of Leuven, Belgium

Commencement: August 27, 2015

This study was supported by the European Union through the European Social Fund.

ISSN 1024-395X
ISBN 978-9949-32-871-0 (print)
ISBN 978-9949-32-872-7 (pdf)

Copyright: Andres Lust, 2015

University of Tartu Press
www.tyk.ee

CONTENTS

LIST OF ORIGINAL PUBLICATIONS

Given thesis is based on the following original publications referred to in the text by Roman numerals (I–III).

I **Lust, A.**, I. Laidmäe, M. Palo, A. Meos, J. Aaltonen, P. Veski, J. Heinämäki, and K. Kogermann, 2013. Solid-state dependent dissolution and oral bioavailability of piroxicam in rats: *European Journal of Pharmaceutical Sciences*, v. 48, p. 47–54.

II **Lust, A.**, C. Strachan, P. Veski, J. Aaltonen, J. Heinämäki, J. Yliruusi, and K. Kogermann, 2015. Amorphous solid dispersions of piroxicam and Soluplus®: Qualitative and quantitative analysis of piroxicam recrystallization during storage: *International Journal of Pharmaceutics*, v. 486, p. 306–314.

III **Lust, A.**, S. Lakio, J. Vintsevits, J. Kozlova, P. Veski, J. Heinämäki, and K. Kogermann, 2013. Water-mediated solid-state transformation of a polymorphic drug during aqueous-based drug-layer coating of pellets: *International Journal of Pharmaceutics*, v. 456, p. 41–48.

Contribution of Andres Lust to original publications

Study I: participation in study design; performing the experiments and data analysis; writing the paper.

Study II: participation in study design; preforming the experiments and data analysis; writing the paper.

Study III: participation in study design; performing the experiments and data analysis; writing the paper.

ABBREVIATIONS

3D	Three dimensional
AH	Piroxicam anhydrate form I
API	Active pharmaceutical ingredient
ATR-FTIR	Fourier transform infrared spectroscopy equipped with attenuated total reflection accessory
AUC_{0-12}	Area under the plasma concentration versus time curve
BCS	Biopharmaceutics classification system
CSD	Cambridge Structure Database
DSC	Differential scanning calorimetry
Cl/F	Hybrid constant clearance/bioavailability fraction
C_{max}	Maximum plasma drug concentration
FTIR	Fourier transform infrared spectroscopy
HPLC	High performance liquid chromatography
HPMC	Hydroxypropyl methylcellulose
HR-SEM	high-resolution scanning electron microscope
IDR	Intrinsic dissolution rate
LOD	Limit of detection
LOQ	Limit of quantification
MCC	Microcrystalline cellulose
MCR	Multivariate curve resolution
MCR-ALS	Multivariate curve resolution alternating least squares
MH	Piroxicam monohydrate
PC	Principal component
PCA	Principal component analysis
PITs	Process induced transformations
pK_a	Logarithmic acid-ionization constant
PLS	Partial least squares
PM	Physical mixture
PM AH	Physical mixture of piroxicam AH and Soluplus® in 1 to 4 weight ratio
PM MH	Physical mixture of piroxicam MH and Soluplus® in 1 to 4 weight ratio
PRX	Piroxicam
PVP	Polyvinylpyrrolidone
RCF	Relative centrifugal force
RH	Relative humidity

SD	Amorphous solid dispersion of piroxicam and Soluplus® in 1 to 4 weight ratio
SE	Standard error
SEM	Scanning electron microscopy
SNV	Standard normal variate
$t_{1/2}$	Half-life
Tg	Glass transition temperature
t_{max}	Time at maximum plasma drug concentration
Vd/F	Hybrid constant volume of distribution/bioavailability parameter
XRPD	X-ray powder diffraction

1. INTRODUCTION

Many drugs can exist in different solid-state forms (e.g., crystalline, amorphous, hydrates/solvates, co-crystals). Given forms differentiate from each other by the arrangement of molecules towards each other in three-dimensional (3D) space. In case of crystalline material the molecules have very well defined three dimensional long range arrangement in 3D space whereas the amorphous form is defined by the lack of long range order of molecules. The solvates are crystalline matter that contains solvent molecules in a host crystal lattice. In case of crystal hydrates water molecules are incorporated to the structure.

Due to different arrangement of molecules towards each other, given solid state forms have different physicochemical properties. Most important to pharmaceutical processes are the differences in the dissolution rate, solubility and physical stability. Less stable forms have usually faster dissolution and higher apparent solubility compared to the more stable forms at given conditions. The possibility to obtain supersaturated solution and faster dissolution rate is the main benefit which can be obtained by using less stable solid state forms.

As amorphous form is usually thermodynamically very unstable several different formulation-based and processing-based approaches have been proposed in order to stabilize it. One of the methods used is a solid dispersion approach. Given method involves dispersing the active pharmaceutical ingredient (API) in a suitable carrier, which is usually a hydrophilic polymer. The kinetic barrier or reduced molecular mobility and specific interactions between the carrier polymer and drug molecules are the two factors that can stabilize the solid dispersions.

In case of metastable crystalline solid state forms, adding amphiphilic polymers to solutions has been shown to have a good stabilizing effect. The amphiphilic polymers can absorb to crystals and thus stabilize them. As metastable solid state forms can produce supersaturated solutions towards the most stable form, the amphiphilic polymer molecules can stabilize the metastable form also through solubilization process which lowers the degree of supersaturation and hence the driving force to crystallization.

It is known that introducing water to the metastable solid state forms can compromise the stability even further. Thus it is important to study the effect of aqueous media and water vapour to the physical stability of solid state forms. As during pharmaceutical processes the drug substance(s) are also often exposed to water and elevated temperatures which can lead to water-mediated process induced transformations (PITs), it is essential to monitor the solid state form also during processing. Present thesis is aiming to gain further knowledge and understanding on these topics.

Present research work focused on investigating the solid state forms of piroxicam (PRX) and its possible phase transformations during processing and storage. The different solid state forms studied were PRX anhydrate form I (AH), PRX monohydrate (MH), and amorphous solid dispersion of PRX and

Soluplus® in 1 to 4 weight ratio (SD). In order to determine the effect of Soluplus® as an excipient in a formulation, also the respective physical mixture of AH and Soluplus® (PM AH) was studied. The aim of this study was to gain understanding about the effects of different solid-state forms of a poorly water-soluble PRX on the drug dissolution and oral bioavailability in rats. Also the stability of different solid state forms in a relevant dissolution medium was studied. The second aim of the present study was to carry out qualitative and quantitative analysis of the physical solid-state stability of the SD during storage. The third aim was to study the stability of PRX solid state forms during a pharmaceutical process that involves exposition of material to water and elevated temperatures.

2. LITERATURE REVIEW

2.1. Solid state forms and their properties

Many drugs can exist in different solid-state forms (e.g., crystalline, amorphous, hydrates/solvates, co-crystals). Given forms differentiate from each other by the arrangement of molecules towards each other in three dimensional (3D) space (Chieng et al., 2011; Lu and Rohani, 2009). In case of crystalline material, the molecules have very well defined 3D long range arrangement built up by fixed repeating unit cells which form a crystal lattice (Lin, 2015). The polymorphism can be defined as the ability of any compound to crystallize in more than one distinct crystal structures. Thus the polymorphic forms are solid state forms that differentiate from each other by the arrangement and/or confirmation of molecules in crystal lattice (Aaltonen et al., 2009). If the crystal structure is built up by host molecules that contain guest molecules, the resulting solid is called co-crystal or solvate depending on the state of guest molecule in ambient conditions. If the guest molecule is solid in ambient conditions the solid is called co-crystal and in case of liquid the resulting solid is called solvate (Vishweshwar et al., 2006). If the adducted molecule is water the resulting solid is called hydrate. It is noteworthy that the solvates/hydrates can also exhibit polymorphism (Aaltonen et al., 2009). The amorphous form is defined by the lack of long range ordered arrangement of molecules (Hilden and Morris, 2004).

Due to different arrangement of molecules in the lattice, the solid state forms can have different properties (Datta and Grant, 2004). Among others the differences can be found in unit cell volume (only in case of crystalline matter), density, refractive index, hygroscopicity, melting point, enthalpy, entropy, free energy, solubility, spectroscopic properties, dissolution rate, stability, surface free energy, interfacial tensions, crystal habit, hardness, flowability and compactability (Aaltonen et al., 2009; Vippagunta et al., 2001). As given properties affect the processability (tableting, granulation etc.) and the release of the active pharmaceutical ingredient (API) from dosage form, it is vital to use the most suitable solid state form (Hickey et al., 2007). Since different solid state forms have different stabilities, the metastable forms can convert to the most stable form at given conditions. Thus it is also vital to monitor the solid state form stability during manufacture and storage (Byrn et al., 1995). Possible solid state phase transitions include polymorphic interconversions, hydrate-anhydrate transformations, order-disorder transformations and polyhydrate interconversions (Hickey et al., 2007).

Among the properties of solid state forms the aqueous solubility and dissolution rate are crucial as they can have a direct impact on the bioavailability of a polymorphic drug after oral administration (Aaltonen et al., 2009; Newman and Byrn, 2003). To date, several studies have been reported on oral administration and bioavailability of different solid-state forms of drugs both in humans and animals (Hurst et al., 2007; Janssens and Van den Mooter, 2009; Vasconcelos et

al., 2007). The first pioneering work on the influence of solid state forms to bioavailability was reported by Aguiar et al., who described the effect of chloramphenicol palmitate polymorphism on bioavailability (Aguiar et al., 1967). As the number of poorly water soluble APIs and drug candidates has been growing significantly during past decade (Buckley et al., 2013) new and novel methods that can improve the dissolution characteristics have been searched for and thus also the interest in different solid state forms has grown. If the oral absorption of a drug is solubility-limited, one could use more soluble solid-state form(s) to achieve the systemic exposure required for therapy (Huang and Tong, 2004; Singhal and Curatolo, 2004). The difference in solubility and dissolution rate arise from the different bonding strength of molecules in different solid state forms. Usually the smaller is the bonding energy between the molecules at given conditions the faster is the dissolution and the higher is the probability of obtaining supersaturated solution. Unfortunately this also means that the solid state forms which are dissolving faster are less stable and tend to recrystallize as more stable and less soluble forms (Burger and Ramberger, 1979). Little attention, however, has been paid on the potential solid-state transformations after oral administration, and subsequent implications on the bioavailability of drugs. In addition, the effect of excipients on the performance of different solid-state forms has not been very much studied. As different solid state forms can have different dissolution profiles and bioavailability, it is important to monitor the solid-state stability of metastable and amorphous materials during storage (Weuts et al., 2005). Since different excipients (polymers) can have quite specific interactions with drug molecules (Wen et al., 2008), it is also important to study how excipients affect *in vitro* and *in vivo* dissolution behavior of solid state forms. The physical instability of metastable and amorphous materials has to be taken into an account during the formulation of these materials (Janssens and Van den Mooter, 2009).

2.1.1. Crystalline polymorphs

Different polymorphs can be obtained by changing the crystallization conditions like temperature, solvents where crystallization takes place, and additives in crystallization medium (Llinàs and Goodman, 2008). Also interconversions between polymorphic forms are possible when pressure is applied during tableting and grinding. For example, given transformations have been shown to take place in case of paracetamol (Boldyreva et al., 2002). Due to the different arrangement of the molecules in crystal lattice, the polymorphs can also have different properties (Sheth and Grant, 2005). For example the differences in unit cell usually manifest also in different crystal habits. As with other solid state forms the most stable polymorph at given conditions is usually the least soluble. This arises from the difference of bonding strength between the molecules making up the crystal lattice. The most stable polymorphs have the strongest bonding between the molecules at given conditions (Chemburkar et al., 2000).

Polymorphs can be classified as enantiotropes and monotropes, depending on whether or not the interconversion can take place reversively. In case of the monotropic polymorphic forms only one of the polymorphic forms is stable at all conditions. In case of enantiotropic polymorphic forms different polymorphic forms are stable at different temperatures below melting temperature. In case of monotropic systems there is only one stable polymorph below melting temperature and all metastable forms will recrystallize to given form over time or when they are subjected to temperature corresponding to their melting point (Sheth and Grant, 2005). The recrystallization of metastable polymorphic forms as stable forms in solid state are mechanistically rather complex reactions, and their kinetics is usually described by Arrhenius type equations (Lin, 2015). Because of the activation energy associated with them, the solid-solid transformations are kinetically hindered and they occur only at the temperature that provides the system with sufficient thermal energy to cross the activation energy barrier (Lohani and Grant, 2006).

The crystallization itself is a multi-step process which includes nucleation and subsequent crystal growth. In the solutions the driving force for crystallization arises from supersaturation. The prerequisite of crystallization is the formation of stable nucleus, which is dependent on the volume free energy that favors aggregation and the surface free energy that favors dissolution of the molecular clusters. Given two factors are dependent on the size of the nucleus. The bigger the nucleus the smaller is the influence of surface free energy and thus more stable is the nuclei. Thus, there is a critical radius of nuclei above which it is stable. The activation energy barrier related to obtaining this state can be overcome in supersaturated solutions (Lohani and Grant, 2006; Rodríguez-Sponga et al., 2004). Once there is presence of stabile nuclei in the solution, the process of crystal growth starts. As the nucleation and crystal growth compete for solute in terms of their respective dependence on supersaturation, the rates of given processes determine the crystal size. Crystal growth is dependent on internal factors such as three dimensional structure of the crystal and external factors such as temperature, solvent and degree of supersaturation. Mechanistically the growth process involves several steps through which the growth unit pass. These include the transport from the bulk of the solution to the site at crystal surface, adsorption of the growth unit onto the impingement site, diffusion from the impingement site to growth site and incorporation to crystal lattice. Each of given steps can be rate-limiting depending on the internal and external factors (Rodriguez-Hornedo and Murphy, 1999). It is also vital to mark that the optimum conditions for nucleation and crystal growth may not be the same (Yu, 2001).

2.1.2. Crystal hydrates

The crystal hydrates can be classified by the way the water molecules are incorporated in 3D space relative to host molecules. In case of isolated site hydrates the water molecules are isolated from each other by host molecules and in case of channel hydrates the water molecules sit next to each other in rows (Gillon et al., 2003). The amount of solvent or water molecules per host molecule can be stoichiometric or nonstoichiometric (Sheth and Grant, 2005). The properties of hydrates are closely related to the arrangements of molecules. In case of isolated site hydrates the removal of water can usually happen only when the overall structure is broken up whereas in case of channel hydrates the dehydration can also take place without breaking up the host crystal lattice. Thus the water removal is more easily facilitated in case of channel hydrates. This also means that the dehydration of the channel hydrates can occur at lower temperatures (Petit and Coquerel, 1996).

As the hydrates are the most stable solid state forms in aqueous media, they are the least soluble and other forms tend to transform to those. This means that hydrates can be obtained by mixing anhydrous solid state forms with water. The stability of hydrate form arises from the properties of water molecules. The water molecules stabilize the crystal lattice as they have small size and multidirectional hydrogen bonding capability (Aaltonen et al., 2009; Gillon et al., 2003). The hydrate formation in solution can take place as solid to solid transformation or it can be solution mediated. In case of channel hydrates both processes could take place, while for isolated hydrates it is more common that the hydrate formation is solution mediated. In case of isolated site hydrate formation the structure of anhydrate form has to be broken up, while the tunnel hydrate can be formed by simply absorbing water (Datta and Grant, 2004; Zhang et al., 2004). In case of solution mediated process the overall crystallization process of hydrate from solutions follows the same basic principles as the crystallization of anhydrates.

2.1.3. Amorphous materials

Solid material may by intrinsically amorphous at ambient conditions. For example polymers like polyvinylpyrrolidone (PVP) and polyethylenglycole are in amorphous form at room temperature. (Craig et al., 1999). This is the case for molecules that pack poorly or have many internal degrees of freedom. Kinetically the slow crystallization rate will result in material becoming “frozen liquid” without crystallization (Yu, 2001). One general cause of the physical stability of given amorphous materials arises from conformational flexibility of given molecules (Yu et al., 2000). However the amorphous form is thermodynamically unstable for most of the small organic molecule APIs and can only be obtained by special production methods. For example quench-cooling of the melt, mechanical activation (via ball-milling), rapid precipitation from solution and continuous concentration processes (e.g., lyophilization or spray-

draying) have been used for obtaining amorphous form (Hilden and Morris, 2004). Amorphous forms can also be formed accidentally during processing, examples including milling, compression and drying (Craig et al., 1999). The lack of crystal structure means that amorphous materials are physically unstable and they tend to crystallize over time in case of small organic molecule API-s. On the other hand that also means that they have higher solubility and fastest dissolution rate compared to other solid state forms (Hancock and Parks, 2000). Lack of structure also means that amorphous materials are more hygroscopic compared to other solid state forms (Aaltonen et al., 2009).

As the amorphous form does not have a crystal structure it does not have a definite melting point. One of the more important properties of amorphous solid is a glass transition temperature (Tg). Tg is a temperature where the material goes from rubbery state to brittle glassy state. In glassy state the rotational and translational motions of molecules are greatly reduced while the bonding remains similar to the liquid state. Thus the glass transition is characterized by a step change of heat capacity of given material (Craig et al., 1999). Due to increased molecular motions above Tg, the probability of crystallization is also significantly higher (Craig et al., 1999; Hancock and Zografi, 1997). The overall nucleation and crystal growth theory also applies to amorphous to crystalline conversion (Hancock and Zografi, 1997; Yu, 2001). It has to be noted that the Tg of the mixtures is dependent on the Tg of the components according to Gordon-Taylor equation (Craig et al., 1999). Thus adding a component with a low Tg will compromise the stability of the component with higher Tg. As the Tg of water is approximately –135 °C and it can be quite easily absorbed by amorphous materials, the high humidity can compromise the physical stability of given material (Craig et al., 1999; Haque and Roos, 2008; Heljo et al., 2012).

2.1.4. Water mediated solid state transformations and their impact on the performance of active pharmaceutical ingredients

Although amorphous and metastable polymorphic forms have solubility and dissolution benefits, their instability during storage and in the presence of aqueous media (gastric fluid and dissolution environment) could lead to the recrystallization of crystalline form with lower solubility. Hydrate formation during dissolution testing has been reported with many drugs (Aaltonen et al., 2006; Alonzo et al., 2010; Lehto et al., 2009; Paaver et al., 2012) and amorphous drugs are extremely prone to this kind of solid-state transformation. It has to be emphasized that given solid-state transformations may also occur during the drug absorption *in vivo*. To date, the consequences of such solid-state changes on oral bioavailability are not fully understood (Greco and Bogner, 2011). Possible solid-state transformations to a less stable form during dissolution could lead to an unexpectedly low bioavailability. Hence, if the transformation takes longer to occur, the estimated dissolution and bioavailability

could be achieved with a less stable amorphous form. These phenomena have not been thoroughly investigated in the literature, and there are no direct correlations between *in vitro* and *in vivo* performance of metastable solid forms. Therefore it is important to study the *in vivo* absorption of the drugs that exhibit solid-state transformations during *in vitro* dissolution.

Also the exposure of the API to water and high temperature during pharmaceutical processes could present higher risks for process induced transformations (PITs) in the solid-state of drugs and/or excipients which in turn may ultimately affect the processability and final dosage form quality and performance (Morris et al., 2001; Nikowitz et al., 2013; Zhang et al., 2004). Several recent reports provide evidence that unexpected solvent-mediated transformations of APIs may be induced, especially during manufacturing of pharmaceuticals in wet conditions and/or in high relative humidity. For example, given transformations have occurred during wet granulation (Airaksinen et al., 2005; Jørgensen et al., 2002). Also dissolving or suspending the drug in an aqueous liquid during coating can greatly increase the potential for PITs to occur through the solution or solution-mediated mechanisms (Zhang et al., 2004). These types of PITs include polymorphic transformations, hydration/ dehydration, and/or amorphous crystallization. For example, the hydration of drugs typically proceeds via solution or solution-mediated mechanisms, and different hydrate forms can differ markedly from each other with respect to their physical, chemical, and biological properties (Sheth et al., 2004c; Zhang et al., 2004). In addition, the rapid water removal during coating or drying phase of wet granulation may result in fast crystallization of a metastable crystal form of drug, or may lead to the formation of an amorphous phase in the drug layer via the solution mechanism (Zhang et al., 2004). The kinetics of the possible phase transitions (such as solution-mediated transformations, solvate formation) in aqueous-based manufacturing processes determines whether or not the PITs will be completed during the time scale of the process (Morris et al., 2001).

2.2. Amorphous solid dispersions

The solid dispersion approach has been successfully used to stabilize the materials in amorphous form. Given method involves dispersing the API in a suitable carrier, which is usually a hydrophilic polymer (Leuner and Dressman, 2000). This kind of stabilization method was first used by Sekiguchi et.al. (Sekiguchi and Obi, 1961). While the pioneering works used small well soluble molecules, nowadays amphiphilic polymers are usually applied as carrier polymers (Leuner and Dressman, 2000). For example synthetic polyvinyl polymers and polyethylene glycols have been successfully used as carriers in pharmaceutical solid dispersions since they have significant inhibitory effects on the crystallization of drugs both in solution and solid state (Gupta et al., 2004).

The kinetic barrier or reduced molecular mobility and specific interactions between the carrier polymer and API are the two factors that can stabilize the solid dispersions (Vasconcelos et al., 2007). For example the main mechanisms of crystallization inhibition in solid state have been reported to be due to the antiplasticizing effect of the polyvinyl polymer (e.g., PVP), and steric and specific interactions occurring between the drug and PVP (Khougaz and Clas, 2000). As molecular mobility governs the diffusion and surface integration, it influences the phase separation and subsequent crystallization of solid dispersions (Janssens and Van den Mooter, 2009). The nucleation and crystal growth require correct orientation and conformation of the molecules, both of which are also governed by the molecular mobility. Furthermore, the number of contacts between the molecules that lead to the formation of hydrogen bonds depend on the molecular mobility (Janssens and Van den Mooter, 2009). Hence, the probability of crystallization is lower if the system has lower molecular mobility.

Some small molecules are known to increase the molecular mobility of amorphous systems (by acting as plasticizers), and they can cause the crystallization (Hancock and Zografi, 1994; Heljo et al., 2012; Janssens and Van den Mooter, 2009). For hydrophilic polymers, the water is well known to act as a plasticizer (Blasi et al., 2005; Lai et al., 1999). The hydrogen bonding and specific interaction between carrier polymer and API has been shown to stabilize the solid dispersions (Bhugra and Pikal, 2008). Formation of the hydrogen bonds between an API and polymer can inhibit the formation of hydrogen bonds between two API molecules. Also the relative bonds strength in the crystalline API compared to the hydrogen bonds in solid dispersion can affect the thermodynamic crystallization driving force (Janssens and Van den Mooter, 2009). As hydrogen bonding between an API and polymer can inhibit the diffusion of API molecules, it is evident that this also affects the molecular mobility (Bhugra and Pikal, 2008).

In addition to the effect on physical stability of the solid state form, the amorphous solid dispersions may also improve the apparent solubility of the poorly soluble drug molecules. (Brouwers et al., 2009). Since SDs approach aims at improving the solubility and dissolution of drugs, it is foremost effective in enhancing the bioavailability of drugs belonging to biopharmaceutical classification system (BCS) Class II which have low solubility and high permeability (Kawabata et al., 2011). Amorphous solid dispersions generate high or even supersaturated concentrations of poorly soluble drugs by increasing their apparent solubility and dissolution rate. In addition, the hydrophilic carrier polymer can increase the wettability and surface area available for dissolution. Hydrophilic carrier polymers used in solid dispersions can also inhibit the precipitation by reducing the degree of supersaturation of the solutions (Brouwers et al., 2009).

In conclusion, the SD approach is a promising formulation strategy to improve the oral bioavailability of poorly water-soluble drugs (Janssens and Van den

Mooter, 2009; Kawabata et al., 2011; Vasconcelos et al., 2007) since APIs formulated in SDs have a higher physical stability compared to pure amorphous compounds and they still have a faster dissolution compared to their crystalline counterparts. The other advantage of the SDs over the pure amorphous compounds is that the carrier polymer can solubilize the poorly water-soluble compound during dissolution and thus inhibit the crystallization.

2.3. Properties of piroxicam

Piroxicam (PRX) was used as a poorly soluble polymorphic drug in this study. PRX is a well-known long-acting non-steroidal anti-inflammatory drug used in the treatment of rheumatic disease.

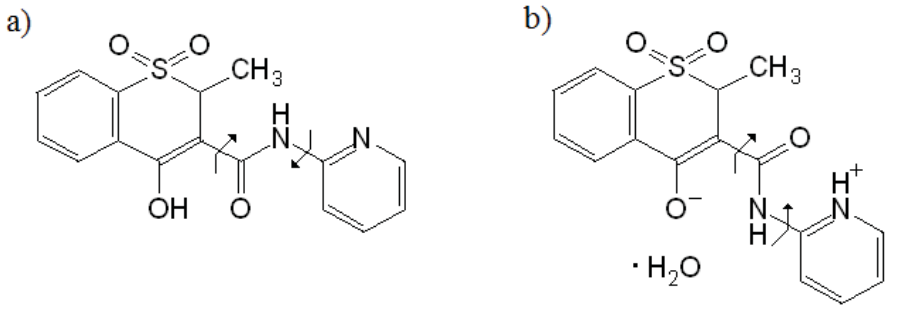

Figure 1. a) Chemical structure of piroxicam anhydrate form I (AH). **b)** Chemical structure of piroxicam monohydrate. The arrows show internal rotations about the C8–C9 and N10–C11 bonds.

Since PRX has such a low water solubility and high permeability, it belongs to class II in BCS (Amidon et al., 1995). PRX has two pK_a values: pK_{a1}=1.86 and pK_{a2} = 5.46 (Jinno et al., 2000). PRX has four known crystal forms: PRX anhydrate form I (AH), II, III and PRX monohydrate (MH) (Kogermann et al., 2011; Vrečer et al., 2003). The chemical structures of AH and MH are shown on Figure 1a and Figure1b, respectively. PRX can also be converted to the amorphous form. Pure amorphous PRX has been reported to be very unstable (Kogermann et al., 2011; Sheth et al., 2004a; Sheth et al., 2004b; Sheth et al., 2004c) and it transforms quickly to MH in a dissolution medium (Naelapää et al., 2012). The PITs associated to the ball milling and cryomilling, melt spinning and nanocrystallization of PRX have been widely reported (Drebushchak et al., 2006; Kogermann et al., 2011; Lai et al., 2011; Shakhtshneider et al., 2007; Sheth et al., 2004c). It has been reported that the solubility of AH in artifical gastric fluid at 37 ºC is 184.9 mg/l and that the solubility of MH in the same conditions is 84.5 mg/l (Vrečer et al., 2003). Also it is known that AH has faster dissolution and higher solubility compared to a MH in solutions with

biorelevant pH. It is well known that all anhydrous polymorphic forms of PRX (AH, II and III) can undergo the solid-state transformation to PRX MH (Jinno et al., 2000; Naelapää et al., 2012; Sheth et al., 2004c). In water, AH recrystallizes as a MH, and at room temperature it takes more than one hour for this process to start (Paaver et al., 2012). In MH the PRX is in the zwitterionic form (with ZZZ configuration) which structure differs significantly from anhydrous forms (with EZE configuration) by internal rotations about the C8–C9 and N10–C11 bonds and by proton transfer from O17 to N16 (Kojic-Prodic and Ruzic-Toros, 1982; Reck et al., 1988; Reck and Laban, 1990; Taddei et al., 2001). According to the Sheth et al. (2004c), the dehydration behaviour of MH is consistent with its underlying crystal structure, which is characterized by the absence of tunnels and a complicated hydrogen-bond network (Sheth et al., 2004c). Since AH and MH have completely different unit cells, it is obvious that the AH dissolves in a dissolution medium before it can recrystallize as a MH. It could be expected that different solid-state forms could also show different rate and extent of dissolution and oral bioavailability. Hence possible solid-state transformations that could also occur during dissolution *in vivo* can decrease the bioavailability of a better dissolving form. The same applies to PITs and solid state transformations that occur during storage. Thus it is important to monitor the stability of solid state of API and excipients during processing, dissolution and storage.

2.3. Properties of Soluplus®

As the instability of amorphous PRX is well known the solid dispersion approach was chosen in order to stabilise it in this study. Polyvinyl-caprolactame-polyvinylacetate-polyethyleneglycole graft copolymer (Soluplus®) was used as a carrier polymer. This is a novel hydrophilic pharmaceutical excipient that is specially tailored to be applied as a carrier polymer in the SDs of poorly water-soluble APIs.

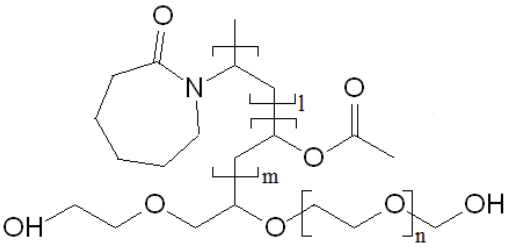

Figure 2. Chemical structure of Soluplus®

To date Soluplus® has been successfully used to obtain SD-s of several different API-s (Djuris et al., 2013; Linn et al., 2012; Nagy et al., 2012; Shamma and Basha, 2013). The average molecular weight of Soluplus® is in the range of

90 000 to 140 000 g/mol. Soluplus® has relatively low Tg of 68 °C (Lim and Hoag, 2013), and to date it has been mostly used for preparing SDs by melting method. Soluplus® is known to absorb water readily from air: at 40% relative humidity (RH) its water content is about 4% and at 75% RH about 12% by weight in ambient room temperature . Soluplus® has a lower critical solution temperature of 40 °C, and adding electrolytes to the aqueous solutions of Soluplus® can result in lower critical solution temperature and cause its salting out (Hughey et al., 2013).

2.5. Common analytical techniques used in solid state form analysis

The physical characterization of solid state forms can be performed with many different techniques which enable to analyse different properties (Aaltonen et al., 2009). Perhaps the oldest method used for characterization of solid state forms and especially the crystalline matter is optical microscopy. In its basic form it enables to register the crystal habit. By using polarized light microscopy it is possible to determine the optical properties of the material. Also amorphous form can be distinguished from crystalline material with given technique (Alonzo et al., 2010). It is also possible to study solid state transformations with optical and polarized light microscopy when the hot stage accessory is used (Rustichelli et al., 2000). The optical microscopy can be substituted with methods that have much higher magnification such as scanning electron microscopy (SEM) and atomic force microscopy (Danesh et al., 2001; Rasenack and Muller, 2002).

Single crystal X-ray diffractometry is indispensable in studying crystalline material as all crystalline materials have distinctive diffraction pattern. As the diffraction pattern arises from constructive interference of the X-rays diffracted from crystal planes, given analytic tool enables to determine the unit cell constants. As it can be relatively hard to obtain single crystals that are large enough to carry out single crystal X-ray diffraction experiment, one could use X-ray powder diffraction method (XRPD) (Yu et al., 2003). This method is also capable of distinguishing the amorphous form from crystalline solid state forms, since amorphous materials display amorphous halo instead of diffraction pattern (Newman et al., 2008).

Thermal methods are also quite often used in the characterization of solid state forms. The differential scanning calorimetry (DCS) is suitable for defining the changes in enthalpy, melting temperatures, Tg-s and dehydration temperatures. The DSC can be used for detecting the interaction between the API and excipients as interaction can change the given properties. Also given properties can be used for the identification of different solid state forms as these are material properties that are related to the interaction of the molecules in solid state (Chadha and Bhandari, 2014). Also thermogravimetry is useful additional technique that can be used in studying the behaviour of the crystal hydrates as it

enables to determine the weight loss upon dehydration (Han and Suryanarayanan, 1998).

The vibrational spectroscopy techniques (mid-infrared spectroscopy, near-infrared spectroscopy, pulsed terahertz spectroscopy and Raman spectroscopy are extremely useful in differentiating all solid state forms from each other as they are probing the inter- and/or intra-molecular bond vibrations (Bugay, 2001; Kogermann et al., 2007b). In addition, Raman and near-infrared spectroscopy carry the benefit of being applicable as process analytical technology tools since these methods do not need the preliminary sample preparation. Thus they can be used for detecting the solid state transformations during different pharmaceutical processes (Yu et al., 2004).

Solid state nuclear magnetic resonance spectroscopy is another method that has become quite common tool for studying the solid state forms in recent years. Given technique can be applied to very different kinds of analytical work ranging from polymorph identification and quantification to a final dosage form characterization. It is also possible to use it in order to distinguish amorphous material from crystalline material and detect the interactions between the solid state forms and excipients (Stephenson et al., 2001; Tishmack et al., 2003).

2.6. Multivariate data analysis methods- tools for monitoring the solid state stability

The interest in multivariate data analysis methods has substantially increased over the past decade due to the application of vibrational spectroscopic methods as process analytical tools. A number of multivariate data analysis methods coupled with vibrational spectroscopy have been successfully employed in the analysis of solid-state transformations of APIs (Aaltonen et al., 2007b; De Beer et al., 2009; Kogermann et al., 2008; Kogermann et al., 2007a; Kogermann et al., 2011; Naelapää et al., 2012; Paaver et al., 2012; Romero-Torres et al., 2007).

2.6.1. Principal component analysis

Principal component analysis (PCA) has been used in the qualitative analysis of solid-state forms during storage stability tests (Kogermann et al., 2011). PCA is a multivariate statistical analysis tool that can be used for data compression and information extraction. PCA finds combinations of variables that describe the major trends in the data set. Mathematically the PCA carries out eigenvector decomposition of the covariance or correlation matrix of the process variables (Wise et al., 1999). Thus in case of PCA the dimensions of the X matrix which corresponds to the number of X-variables are reduced to a fewer set of mutually orthogonal variables best describing the systematic variance in the data. Given new variables are uncorrelated with each other and they are called principal

components (PC). Each PC is the product of samples-score vectors and variables-loading vector. Plotting two score vectors against each other will give the positions of samples in that respective PC direction and plotting the loading vectors will describe the relationship between the original variables and the PC in question. Combining the scores and loadings plots will give the information on how the samples will behave compared to each other (Aaltonen et al., 2009; Abdi and Williams, 2010).

2.6.2. Multivariate curve resolution

For quantification of the solid-state transformations of APIs, partial least squares (PLS) regression has been successfully exploited (Aaltonen et al., 2007a; Paaver et al., 2012; Stephenson et al., 2001). The quantification of amorphous systems, however, can be challenging since most of multivariate analysis methods used for analysing spectroscopic data need the calibration model based on the instrumental measurements of calibration mixtures. As amorphous material can readily recrystallize when coming in contact with a crystalline matter, a method which does not need calibration models would be needed in order to carry out quantitative analysis. One method which can be used for this purpose is multivariate curve resolution (MCR). This method does not require a preliminary measurement of mixtures with specific composition (Christensen et al., 2013). The MCR mathematically decomposes instrumental responses of mixtures into the contributions of pure components and calculates the concentration profiles of them. In case of MCR alternating least squares (MCR-ALS), the equation of MCR is solved iteratively by using alternating least squares method (Tauler, 1995). While MCR is commonly used to obtain the quantitative information of the reagents during chemical reactions (de Juan and Tauler, 2006; Ruckebusch and Blanchet, 2013), lately it has been successfully used also in studying complex phase transitions of APIs during dehydration (Christensen et al., 2013) and freeze-drying (De Beer et al., 2007). The general theory and application of MCR-ALS as a quantitative analysis tool for solid mixtures has been discussed in several papers (Azzouz and Tauler, 2008; Garrido et al., 2004; Garrido et al., 2008).

3. AIMS OF THE STUDY

The main goal of the present study was to investigate the water-mediated solid state transformations of a poorly water-soluble model drug piroxicam (PRX) that may occur during pharmaceutical processing and storage. Furthermore, to reveal and understand the biopharmaceutical relevance of these solid state transformations *in vitro* and *in vivo*. The specific aims of the study were:

1. to prepare and characterize the different solid state forms of PRX (I, II, III)
2. to gain understanding about the effects of different solid-state forms of PRX on the *in v*itro dissolution (I, II, III) and to determine the physical stability of PRX solid state forms in dissolution medium (I)
3. to compare the *in vivo* bioavailability of different solid-state forms (AH *vs* MH *vs* amorphous PRX in a solid dispersion with polyvinylcaprolactame-polyvinylacetate-polyethylene-glycole graft copolymer (Soluplus®) (SD)) of a model drug PRX after oral administration to rats (I).
4. to investigate the physical solid-state stability of SDs of PRX and Soluplus® during a short-term storage in different humidity and temperature conditions and to determine the effect of possible crystallization on the dissolution of stored SDs (II).
5. to carry out qualitative and quantitative analysis of the physical solid-state stability of the SDs of PRX and Soluplus® (II).
6. to investigate the effects of aqueous drug-layer coating process of pellets (Cellets®) on the solid state forms of PRX in the miniaturized coating equipment and with free films and to determine the coating efficiency (III).

4. MATERIALS AND METHODS

4.1. Materials

Piroxicam (PRX) was used as a poorly water-soluble and polymorphic model drug. PRX anhydrate I (AH) was purchased from Letco Medical, Inc., USA. PRX monohydrate (MH) was obtained by recrystallization from water (Kogermann et al., 2007a). Soluplus® (polyvinyl caprolactam – polyvinyl acetate – polyethylene glycol graft copolymer) with a molecular weight range of 90000 – 140000 g/mol was obtained from BASF SE Pharma Ingredients & Services, Ludwigshafen, Germany. Tenoxicam was purchased from Sigma-Aldrich Corporation. Ketamin (Bioketan inj 100 mg/ml 10 ml) was purchased from Vetoquinol S.A., Lure Cedex, France. Hydroxypropyl methylcellulose (HPMC, Methocel E5) was purchased from Dow Chemicals, Midland, MI, USA. Microcystalline cellulose (MCC) neutral pellets (Cellets®) with the particle size distribution of 1000–1400 μm were obtained from Syntapharm Harke Group, Gesellschaft für Pharmachemie mbH, Germany. All other reagents were purchased from Sigma-Aldrich Co. and used without any further purification. Size number 1 and 3 hard gelatin capsules (PosilockTM, Elanco, USA) were used in *in vitro* dissolution tests. Purge gasses were obtained from Eesti AGA AS, Tallinn, Estonia.

4.2. Methods

4.2.1. Preparation of physical mixtures and solid dispersions (I, II, III)

Solid dispersion of AH and Soluplus® 1:4 (SD) was prepared using a solvent evaporation method (Tantishaiyakul et al., 1999). Soluplus® and AH were first dissolved in acetone. After evaporating the solvent at 40 ºC, the resulting SD was gently ground using a mortar and pestle. Four different ratios of PRX and Soluplus® were studied: 1:1, 1:2, 1:3, and 1:4. The 1:4 ratio was the first that resulted in amorphous PRX, therefore it was chosen for further investigation. Physical mixture (PM) of AH and Soluplus® 1:4 was obtained by mixing them in a mortar with pestle using geometric dilution.

All PRX samples were passed through a 150 μm sieve. The solid-state forms were prepared one day before *in vitro* and *in vivo* experiments. AH, PM and SD were stored in a desiccator at ~0% relative humidity (RH) under reduced pressure at room temperature. MH was stored at ~54% RH at room temperature.

The SDs of PRX and Soluplus® (1:4 weight ratio) for storage stability study were prepared by the following modified solvent evaporation method: 5 g of AH and 20 g of Soluplus® were dissolved in 250 ml of acetone. The solvent was evaporated at 40 ºC by using a Rotovapor® rotatory evaporator (Büchi, Switzerland). The rotation speed of the 1000-ml flask was set at 120 rpm. The SDs formed a solid foam which was removed from a flask using spatula and milled

gently by using mortar and pestle. After this the sample was placed under vacuum (50 mbar). All samples were passed through a 150-μm sieve.

4.2.2. Storage stability study (II)

The samples were investigated immediately after preparation and within regular time periods during a short-term (6-month) aging at the following storage conditions: ~0% RH / 6 °C ("low humidity-low temperature"), ~0% RH / 25 °C ("low humidity-intermediate temperature"), ~40% RH / 25 °C ("intermediate humidity-intermediate temperature"), and ~75% RH / 25 °C ("high humidity-intermediate temperature"). The stability study protocol involved ten sampling time-points after preparation: one day (1D), two days (2D), four days (4D), one week (W1), two weeks (W2), three weeks (W3), four weeks (4W), two months (2M), three months (3M), six months (6M). Raman spectroscopy and ATR-FTIR spectroscopy were used for the solid-state and drug-polymer interaction analyses of samples.

4.2.3. Preparation of coating suspensions (III)

The HPMC solution (5% w/w) was prepared as follows: approximately half of the calculated amount of distilled water (45 g) was heated (70 °C), and the polymer (5 g) was added to the hot distilled water under magnetic stirring. After the polymer was thoroughly dispersed, the remaining cold distilled water (50 g) was added, and the solution was continuously stirred for 48 hours before use. In order to obtain coating suspensions (50 g), the HPMC solution was loaded with different solid-state forms of PRX as follows: (1) 4% (w/w) AH in 5% (w/w) HPMC solution; (2) 4% (w/w) MH in 5% (w/w) HPMC solution; and (3) 10% (w/w) SD (2% (w/w) PRX) in 5% (w/w) HPMC solution. In case of SD, the coating suspension was charged with a drug load only half of that used with the other PRX solid state forms (since Soluplus® would have made the suspension too viscous to be sprayed).

4.2.4. Preparation of the free films (III)

Free films were prepared with an in-house set-up using a rotating plate made of Teflon and two drying heating units. A schematic diagram of the system is presented in Figure 3.

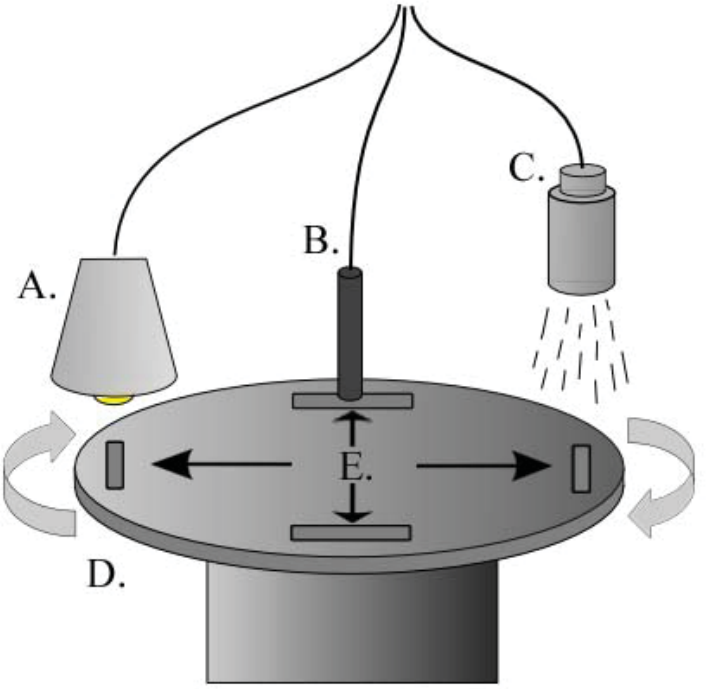

Figure. 3. A rotating plate set-up for preparing drug-loaded free films. Key: A. drying heating unit (60 W lamp), B. Raman spectrometer probe, C. drying heating unit (air flow unit), D. rotating Teflon plate, E. sample cups in the rotating plate.

The sample size for each film was 2 ml and a coating suspension was applied to the sample cups in the rotating plate. Two opposite cups were used for each drying cycle. In the next phase, rotating plate was turned on and both heating units (lamp and air flowing device) were switched on. The rotation speed of the plate was adjusted to 1.0 rpm. The air flow rate was 5 m/s and the output of the lamp was 60 W. The distance between the rotating plate and the lamp was 2.0 cm and between air flow unit and the plate 25 cm. The temperature at the sample level of the plate was 40 °C ± 2 °C. Raman spectra were measured from both of the samples. The spectra were also collected every 10 minutes during the drying phase. The distance between the Raman probe and sample was less than 1 mm. After the films were dried, they were gently removed from the sample cups using a spatula in order to carry out the differential scanning calorimetry (DSC) analysis.

4.2.5. Drug-layer coating of microcrystalline cellulose pellets (III)

The MCC neutral pellets (Cellets®) were drug-layer coated in a miniaturized top-spray air-suspension coating apparatus (Caleva Mini Coater, Caleva Process Solutions Ltd., Dorset, UK). Each small-scale coating batch comprised 20 g of

pellets. Film-coating parameters were adjusted as follows: inlet airflow rate 4–6 m/s, air flow temperature 30 °C, vibration 17 Hz, amplitude 17 mm, atomising air pressure (drum) 0.5 bar, height of spray nozzle 130 mm, and the flow rate of a coating suspension 35 ml/h. The walls of the coating chamber were pretreated with Tween 40 (10% solution in water) before the experiments to avoid the sticking of the pellets. Both uncoated and drug-layer coated pellets were weighed with analytical balance (d=0,1mg) (AB54, Mettler-Toledo International Inc., Switzerland) and the weight increase (%) and coating efficiency (%) was calculated (Table 1, see paragraph 5.4.2). In this study, "coating efficiency" was defined as a ratio of the weight gain of the coated pellets to the mass of the coating material added to the process. From the given ratio the coating efficiency (%) was calculated. The pellets were coated for 5 minutes followed by a 1-minute drying period. These cycles were repeated three or more times. Total coating time was 15 minutes for AH and MH, and 30 minutes for SD drug-layer coating. For Raman spectroscopy analysis and dissolution tests, the drug-layer coated pellet samples were collected at 5, 10, 15 and 30 minutes. In the prolonged drug-layer coating experiments (with a total coating time of 1 hour), multiple samples were taken at 10, 20, 30 and 60 minutes. In case of AH and MH loaded coatings, the theoretical amounts of coating after 15 and 60 minutes were 3.8% (w/w) and 15.2% (w/w) of the total weight of the pellets, respectively. In case of SD loaded coatings, the theoretical amount of coating after 30 minutes was 11.6% (w/w) of the total weight of the pellets.

4.2.6. Raman spectroscopy (I, II, III)

All solid-state forms of PRX were verified with Raman spectroscopy (BWS415 i-Raman Miniature Raman Spectrometer, B&W TEK inc., USA) equipped with a peltier-cooled CCD detector (2048x64), two-fiber coaxial optic probes and a 300-mW diode laser source operating at 785 nm. The analytical range was from 175 cm^{-1} to 3100 cm^{-1}. A total of 3 spectra with an integration time of 12 seconds were recorded from each sample. During slurry experiments, in-line Raman spectra were collected using the same parameters at a five-minute interval.

Raman spectroscopy analysis of storage stability study was performed using a Kaiser Raman PhAT spectrometer (Kaiser areospace &electronics company, USA) equipped with a RXN1-PhAT-785-D laser with 20 mW nominal power operating at 785 nm, PhAT system probe head (nominal focal length 250 mm, nominal beam diameter at focal position 6 mm, focal tolerance +/– 12mm) and CCD detector (1024x256 EEV MPP type) with minimum operating temperature at –50 °C. HoloGRAMS software was used for preliminary data processing. The useful analytical wavelength region ranged from approximately 200 cm^{-1} to 1920 cm^{-1} and the integration time of 0.5 second was used.

4.2.7. Fourier-transform infrared (FTIR) spectroscopy (I, II)

ATR-FTIR spectroscopy was performed on powders using a IRPrestige-21 spectrophotometer (Shimadzu Corp., Kyoto, Japan) and Specac Golden Gate Single Reflection ATR crystal, (Specac Ltd., Orpington, U.K). The analytical range was from 600 cm^{-1} to 4000 cm^{-1}.

ATR-FTIR spectroscopy analysis of storage stability study samples was performed using a Vertex 70 FTIR spectrophotometer (Bruker AXS GmbH, Germany) and MIRacleTM single reflection ATR crystal (Pike Technologies, Inc., USA). The analytical range was from 600 cm^{-1} to 4000 cm^{-1}, resolution was 4 cm^{-1} and a total of 70 scans were taken from each sample. Opus 5.5 programme was used for preliminary data processing.

4.2.8. X-ray powder diffractometry (XRPD) (I, III)

XRPD analysis was performed using a Bruker D8 Advanced diffractometer (D8 Advance, Bruker AXS GmbH, Germany) with Ni filtered Cu Kα1 radiation (λ=1.5406Å, 40 kV and 40 mA) and using 0.3° divergence slit, two 2.5° Soller slits and LynxEye line detector. Samples were measured in Bragg Brentano reflection mode in the 2θ–range 3 – 50°, with the step size of 0.01° 2θ. A total counting time of 8.8 seconds per step was used. The operating current and voltage were 40 mA and 45 kV, respectively. Experimental results were compared to the theoretical patterns in the Cambridge Structural Database (CSD, Cambridge, UK) (Allen, 2002). Refcodes BIYSEH (Kojic-Prodic and Ruzic-Toros, 1982), and CIDYAP01 (Bordner et al., 1984) were used as reference crystal structures, for AH, and MH, respectively.

4.2.9. Differential scanning calorimetry (DSC) (I, III)

Non-isothermal DSC was performed with a differential scanning calorimeter with refrigerated cooling system (DSC 4000, Perkin Elmer Ltd, Shelton, CT, USA). The DSC system was calibrated for temperature and enthalpy using indium as a standard. Samples were analyzed under dry nitrogen purge in crimped aluminium pans with 2 pinholes in a lid at a heating rate of 10 °C/minutes from 30 to 210 ºC. Temperatures are given as onset temperatures of the events unless mentioned otherwise.

4.2.10. Scanning electron microscopy (SEM) (III)

Particle size and surface morphology of the samples were investigated using HeliosTM NanoLab 600 (FEI Company, Hillsboro, Oregon USA) high-resolution scanning electron microscope (HR-SEM). Samples were mounted on aluminum stubs with silver paint and magnetron sputter coated with 3 nm gold layer in argon atmosphere prior to imaging. Pellets were measured using 75× and 175× magnification.

4.2.11 Dissolution studies (I, II, III)

Dissolution tests were carried out in a Distek Dissolution system 2100B (Distek, Inc., North Brunswick, New Jersey, USA) dissolution test apparatus using USP basket method. The samples were automatically taken with minipuls 3 peristaltic pump (Gilson, Middleton, WI, USA) and analyzed in-line with Uvikon spectrophotometer 922 (Kontron instruments, Ltd., Buckinghamshire, UK) at 354 nm. The extinction coefficient of PRX at given wavelenght was $1.5379\times10^4\ M^{-1}\ cm^{-1}$. It was confirmed that Soluplus® did not show any absorption at 354 nm at used concentration. The dissolution medium was 900 ml hydrochloric acid buffer (pH 1.2) (USP XXVIII) at 37 °C. The stirring rate was set to 50 rpm. Hard gelatin capsules (size 3) filled with 20 mg of AH, MH or equivalent amount of SD (mesh size 150 μm) were used for the dissolution testing of different PRX powder forms. Hard gelatin capsules (size 1) filled with 500 mg of drug-layer coated pellets were used for the dissolution tests of drug-layer coated pellets. All samples were tested immediately after preparation and dissolution tests were performed at least in triplicate.

In case of storage stability study the *in vitro* dissolution tests were performed using a paddle method (USP apparatus 2) and a Sotax AT7 (Switzerland) dissolution apparatus. In the dissolution experiments, 900 ml of hydrochloric acid buffer (pH 1.2) at 37 °C was used as the dissolution medium at a temperature of 37±0.5 ºC. Dissolution tests were performed in triplicate. Samples (3 ml, replaced) were withdrawn with a syringe at ten minutes intervals. After removal, the samples were immediately filtered through cellulose filters with a pore diameter of 45 μm and measured with a UV spectrophotometer (UV-1600PC Spectrophotometer, VWR International Europe) using an analytical wavelength of 354 nm.

4.2.12. Intrinsic dissolution testing (I)

Intrinsic dissolution testing was carried out using a Sotax 7A dissolution apparatus and Wood's intrinsic dissolution test apparatus (Sotax AG, Switzerland). 0.1 g of PRX solid-state forms were compressed into the die using a tabletop hydraulic press and 392.6 MPa of pressure for 30 seconds. The intrinsic dissolution rate (IDR) test was performed using the same experimental parameters as in the conventional dissolution tests described above. The solid-state form of the samples after the intrinsic dissolution test was verified by using Raman spectroscopy.

4.2.13. Slurry experiments (I)

In order to determine the possible phase transformations of PRX in hydrochloric acid buffer (pH 1.2) during dissolution testing, slurry tests were performed. Total 2 g of anhydrous PRX sample or PRX mixtures (AH/PM AH/SD) were dispersed

in 5 ml of hydrochloric acid buffer (pH 1.2). Continuous mixing (300 rpm) was performed using magnetic stirrer and in-line Raman spectra were collected.

4.2.14. Pharmacokinetic studies (I)

Experiments were approved by the Ministry of Agriculture Ethical Committee for Animal Experimentation. 12 male Wistar rats, weighing 250–300 g were obtained from Harlan laboratories, Sweden. At the start of the experiment the rats were nine weeks old. Rats were randomly divided into two groups, each with six animals. The first group was given AH and the second group MH by the oral route. After washout period, the first and second groups were given SD and PM AH, respectively. Prior to all experiments animals were fasted overnight, water was given *ad libitum*. Before oral administration of different solid-state forms of PRX, rats were anesthezised with ketamin. Each rat was given 20 mg/kg of AH/MH or equivalent amount of PRX mixtures dispersed in 1 ml of water with intragastric gavage. The dispersion of different solid-state forms of PRX in water took place within one minute prior to oral administration in order to minimize the possibility of solid-state form transformations *in vitro*. 0.2 ml of blood was taken from lateral tail vein in the following time points: 0, 15, 30, 60, 90, 120, 180, 480, 720 minutes after drug administration. Samples were mixed with 0.02 ml of 3.8% sodium-citrate solution and centifuged at for 10 minutes at 3500g (RCF). Plasma was separated from sedimented cells with a pipet. Samples were storaged deep frozen at –75 ºC.

4.2.15. Piroxicam assay (I)

Plasma samples were analyzed using a high performance liquid cromatography (HPLC) system as described by Gwak et al., 2005 (Gwak et al., 2005). The HPLC system consisted of a Shimadzu Prominence LC 20AD pump and Shimadzu Prominence SPD M20A PDA detector set at 230 nm. A base de-activated octadecylsilyl (ODS) column (Luna, 4.6mm × 250mm, 5µm, Phenomenex, USA) was eluted with a mixture of 0.05 M phophate buffer (pH 3.0) and acetonitrile (60:40 v/v) at a flow rate of 1 ml/minutes and at 40 ºC. After melting, 0.05 ml of plasma was taken from each sample and 0.15 ml of tenoxicam solution (250 µg/ml) was added to the sample as an internal standard. Thereafter 0.2 ml of 0.1 N HCl solution was added and samples were then extracted with 7 ml of diethyl ether for three minutes using Vortex mixer. Tubes were centrifuged for 10 minutes at 1100g (RCF), and after that the organic layer was separated and back-extracted with 0.2 ml of 0.02 N sodium hydroxide for three minutes using a Vortex mixer. After centrifuging for 10 minutes at 1100g (RCF), 0.02 ml of the aqueous layer was injeced into the HPLC system. Limit of quantification (LOQ; 1 µg/ml) and limit of detection (LOD; 0.1 µg/ml) were found to be similar as described by Gwak et al., 2005 (Gwak et al., 2005).

4.2.16. Pharmacokinetic and statistical analysis (I, II, III)

Analysis of pharmacokinetic data was carried out using a non-compartmental method. The area under the plasma concentration versus time curve ($AUC_{0–12}$) was calculated by the linear trapezoidal rule. The maximum plasma drug concentration (C_{max}) and the time at maximum concentration (t_{max}) were directly determined from individual plasma concentrations-versus-time curves. The half-life ($t_{1/2}$), hybrid constant volume of distribution/bioavailability parameter (Vd/F) and hybride constant clearence/bioavailability fraction (Cl/F) were calculated as described by Bauer et. al (Bauer, 2008). Statistical analysis of pharmacokinetic data was carried out using unpaired t-tests. Differences between pharmacokinetic parameters of study groups were considered as statistically significant if the p-value was less than 0.05.

PCA and MCR-ALS multivariate analysis methods were used to analyze the Raman spectra collected during the storage stability study. The spectral range from 1073 cm^{-1} to 1661 cm^{-1} was used for data analysis. PCA was carried out with Simca-P+ ® software (Version 12.0.1, Umetrics AB, Umea, Sweeden). The MCR-ALS was carried out with Unscrambler X® (Version 10.3, Camo software, Oslo, Norway). The Raman spectra were preprocessed using standard normal variate (SNV) correction. A linear baseline correction and baseline offset were also employed in order to minimize the effect of fluorecence on the multivariate data analysis. For MCR-ALS, pure Raman spectra of SD, PM AH and PM MH were used for initial estimates. Non-negativity of component concentrations and closure were applied as constraints. The R2X(cum) and Q2(cum) values were used to evaluate the PCA model. The R2X (cum) is a measure of explained overall variance of the data and it shows how well the data is explained by model. The Q2(cum) indicates how well the model predicts new data based on internal cross-validation. The MCR-ALS model performance was tested by comparing it to the PCA model. Since PCA provides the best possible fit along a set of orthogonal principal components (PCs), a similar number of PCs needed and also the similarity between the total variation described by the PCA and MCR-ALS show that the MCR-ALS model is performing reasonably well in terms of fit.

5. RESULTS AND DISCUSSION

5.1. Solid state characterization (I, II, III)

The formation of PRX solid state forms (AH, MH and amorphous SD) was verified by means of XRPD, Raman spectroscopy, FTIR-ATR and DSC.

5.1.1. XRPD (I, III)

XRPD patterns of solid state forms were in good agreement with the calculated theoretical patterns obtained from CSD and previously published diffraction patterns of PRX solid state forms (Kogermann et al., 2011).The XRPD pattern of PM showed peak positions identical to those of AH (Soluplus® as an amorphous polymer showed no peaks). The XRPD pattern of SD showed a characteristic halo thus verifying the presence of amorphous PRX (Fig. 4).

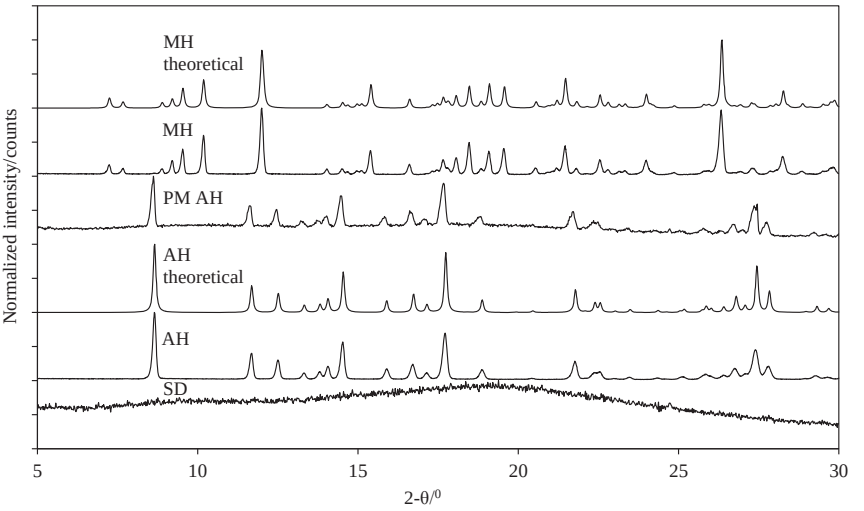

Figure 4. X-ray powder diffraction (XRPD) patterns of piroxicam anhydrate I (AH), piroxicam monohydrate (MH), physical mixture of AH and Soluplus® 1:4 (PM), and solid dispersion of AH and Soluplus® 1:4 (SD). Theoretical patterns of AH and MH are shown for comparison.

5.1.2. Raman spectroscopy (I, II, III)

Different solid-state forms of PRX exhibited differences in Raman spectra, and enabled their identification (Fig. 5). In addition, the Raman spectra of different PRX forms were in good agreement with the previously published Raman spectra of AH and MH (Kogermann et al., 2007a; Kogermann et al., 2011; Kogermann et al., 2007b). There were only minor differences in peak positions, probably due to variation between the equipment used. AH showed characteristic peaks

at 1235 cm^{-1}, 1279 cm^{-1}, 1334 cm^{-1}, 1433 cm^{-1} and 1522 cm^{-1}. As expected, peak positions in Raman spectrum of PM AH were identical to the peak positions of pure AH. The intensities of the peaks measured in PM AH were lower than in case of AH. Since the intensities of characteristic Soluplus® peaks were very low compared to the intensities of PRX peaks, the overall contribution of them to the Raman spectra of PM AH was almost non-existent. MH showed five characteristic peaks in a range of 1128 cm^{-1} – 1238 cm^{-1}. In addition, two higher peaks at 1401 cm^{-1} and 1463 cm^{-1} characteristic to MH were observed. Raman spectum of SD showed broader peaks (Fig. 5) being characteristic to the amorphous state (Bernstein, 2007). For example, the peaks seen at 1334 cm^{-1} and 1235 cm^{-1} were broader compared to AH. There were also some shifts in the peak positions of SD compared to AH and PM AH which is characteristic to the amorphous form (Kogermann et al., 2011). For example, the AH peaks at 1151 cm^{-1}, 1433 cm^{-1} 1473 cm^{-1} and 1558 cm^{-1} shifted to 1154 cm^{-1}, 1435 cm^{-1} 1476 cm^{-1} and 1561 cm^{-1}, respectively. In addition, the relative intensity of the peak at 1334 cm^{-1} in SD spectrum was considerably decreased compared to that observed in AH and PM AH spectra. Peak broadening and shifts in SD spectrum provide evidence that hydrogen bonding interactions between the polymer and PRX are present.

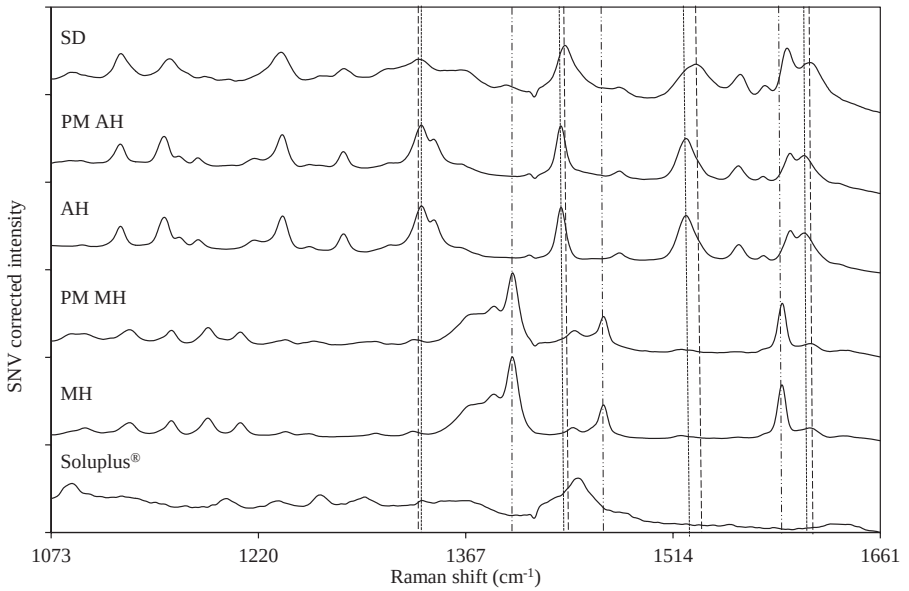

Figure 5. SNV corrected Raman spectra of piroxicam (PRX) solid-state forms measured immediately after preparation. Amorphous solid dispersion (SD) of PRX and Soluplus® graft co-polymer 1:4 (SD), physical mixture of PRX anhydrate form I (AH) and Soluplus® 1:4 (PM AH), PRX anhydrate form I (AH), physical mixture of PRX monohydrate (MH) and Soluplus® 1:4 (PM MH) and PRX monohydrate (MH). Characteristic peaks for amorphous PRX in SD are marked with dashes (—), for AH with dots (···) and for MH with dashes and dots (–··), respectively. All spectra are offset for clarity.

5.1.3. ATR-FTIR (I, II)

As seen in Figure 6, there are clear differences between the ATR-FTIR spectra of SD and corresponding physical mixtures (PM AH). The major difference between the spectra of PM AH and SD is the widening of the PRX N-H stretching vibration band in the SD spectrum (located at 3337 cm^{-1} in the PM AH spectrum). Several previous studies on the SDs of PRX and polyvinyl-pyrrolidone (PVP) have reported the widening of the PRX NH stretching vibration band in the region of the spectrum from 3000 cm^{-1} to 4000 cm^{-1} as a proof of hydrogen bonding between PRX and PVP in SDs (Banchero et al., 2009; Tantishaiyakul et al., 1999). It is evident that the hydrogen bonding between the NH group of PRX molecule and the >N– or C=O group of PVP might be strong enough to weaken the NH stretching of PRX resulting in a very weak and wide peak (Tantishaiyakul et al., 1999). Similarly to Tantishaiyakul et al. and Banchero et al. studies, vibrational band at 3337 cm^{-1} in the ATR- FTIR spectrum of SD has become widened. As the molecule of Soluplus® also possesses >N- and C=O functional groups, it is evident that hydrogen bonding is taking place between the present graft copolymer and PRX in SDs. The Raman spectrum of PM MH shows several specific vibrational bands in the spectral region from 3000 cm-1 to 4000 cm-1, which makes it easier to distinguish from the spectra of SD and PM AH.

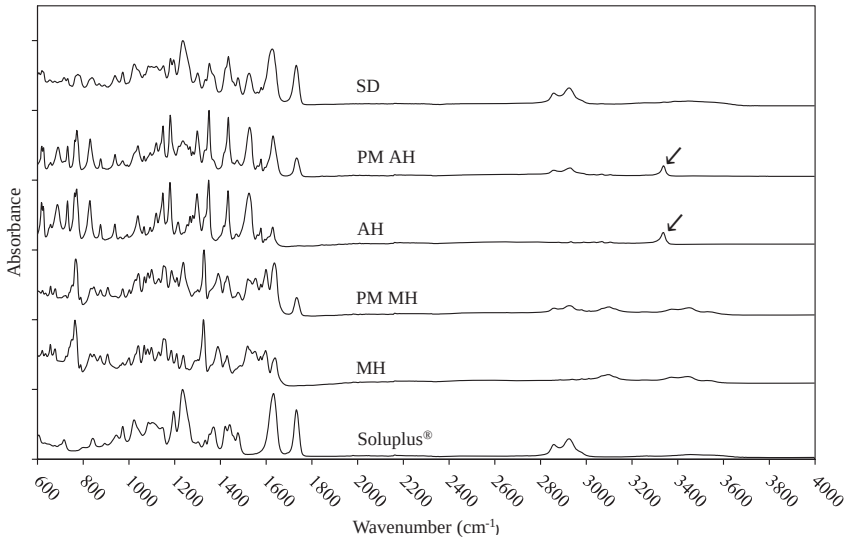

Figure 6. ATR-FTIR spectra of piroxicam (PRX) solid-state forms measured immediately after preparation. Amorphous solid dispersion of PRX and Soluplus® graft copolymer 1:4 (SD), physical mixture of PRX anhydrate form I (AH) and Soluplus® 1:4 (PM AH), PRX anhydrate form I (AH), physical mixture of PRX monohydrate (MH) and Soluplus® 1:4 (PM MH), and PRX monohydrate (MH). The arrows indicate the N-H stretching vibration band of PRX at 3337 cm^{-1}. All spectra are offset for clarity.

5.1.4. DSC (I)

DSC results verified the purity of AH and MH, and showed the thermal events (melting and dehydration endotherms) at expected temperature ranges (Fig. 7).

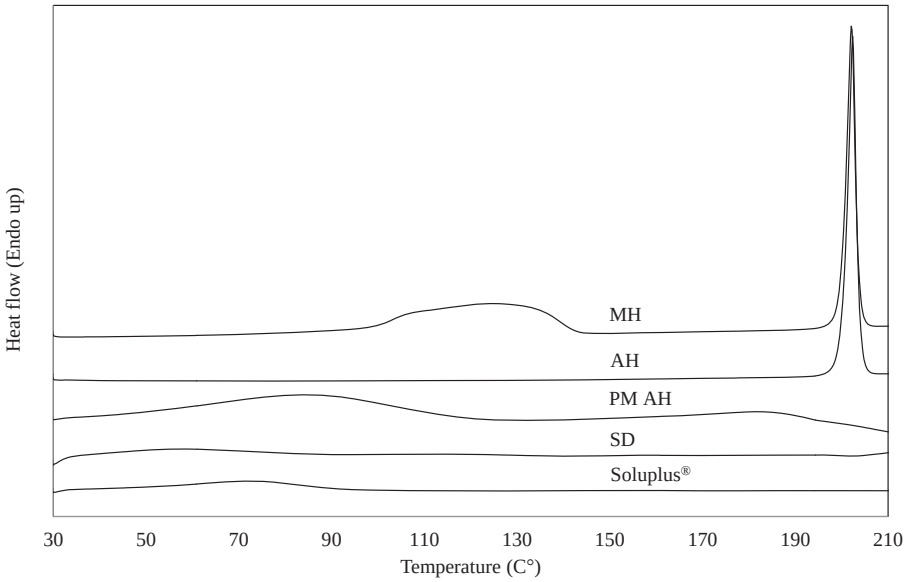

Figure 7. DSC thermograms of piroxicam anhydrate I (AH), piroxicam monohydrate (MH), physical mixture of AH and Soluplus® 1:4 (PM AH), and solid dispersion of AH and Soluplus® 1:4 (SD) and pure Soluplus®.

AH melting endotherm onset was observed at 199 ºC. Dehydration endotherm of MH was observed between 90 ºC and 149 ºC, and the subsequent melting endotherm onset of AH was recorded at 199 ºC. These results were in accordance with the previously reported values (Kogermann et al., 2007a; Vrečer et al., 2003), Soluplus® and PM AH showed a wide endotherm between 35 ºC and 110 ºC, which could be attributed to the removal of water absorbed by the polymeric excipient. In the thermogram of amorphous SD this endotherm was narrower, from 35 ºC to 90 ºC. This difference can be attributed to the increased temperature used to prepare SD, which can induce the removal of water. PM AH showed also another wide endotherm between 125 ºC and 185 ºC, which can be attributed to the fusion of PRX. The depression of fusion temperature of PRX in PM AH compared to the melting temperature of pure AH can be attributed to the interaction with Soluplus®. This kind of behavior is quite usual for systems composing of crystals of small organic drug molecules and amorphous polymeric excipients (Marsac et al., 2006; Zhao et al., 2011).

5.2. Physical solid state stability in aqueous media during dissolution testing (I, II, III)

5.2.1. Dissolution testing (I, II, III)

Significant differences were found in the rate and extent of *in vitro* dissolution of different PRX solid-state forms from capsules (Fig. 8). SD showed the highest dissolution rate compared to those obtained with the other samples (Fig. 8). The lowest rate of dissolution was observed with MH, which is the most stable form of PRX in aqueous conditions, and therefore it is the least soluble (Fig. 8). AH exists in the form of dimers, where two PRX molecules are joined together with two intermolecular hydrogen bonds (Vrečer et al., 2003). In AH, PRX molecules are neutral with an EZE conformation. MH exists in the form of two hydrogen bonded PRX dimers that are connected by a central tetramer that consists of four water molecules joined together by hydrogen bonds. Therefore, PRX molecules in MH are in a zwitterionic form with a ZZZ conformation. Water molecules in MH structure stabilize the zwitterionic PRX molecules and thus lower the free energy of MH relative to AH (Sheth et al., 2004c). The lower solubility of MH compared to AH has previously been reported (Paaver et al., 2012).

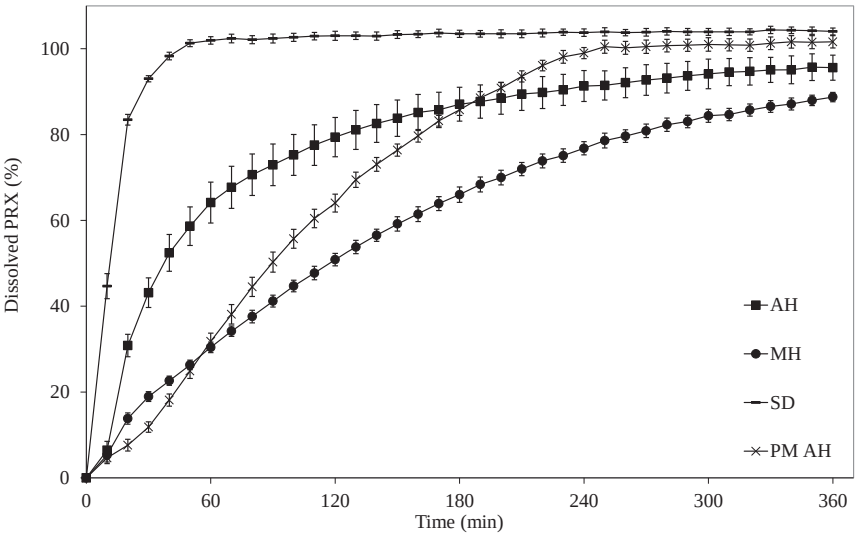

Figure 8. Dissolution of piroxicam (PRX) solid-state forms from hard gelatin capsules (size 3) in hydrochloric acid buffer (pH 1.2) at 37 °C (data are exhibited as mean (n=5)±S.E). Key: Piroxicam anhydrate I (AH), piroxicam monohydrate (MH), physical mixture of AH and Soluplus® 1:4 (PM AH), and solid dispersion of AH and Soluplus® 1:4 (SD).

In SD, PRX exists in an amorphous form, and consequently, dissolution does not need to overcome the energy barrier for breaking up the crystal lattice. In addition, amorphous SDs are known to generate high or even supersaturated concentrations of poorly soluble drugs by increasing their apparent solubility and dissolution rate (Brouwers et al., 2009). An amorphous solid may have some short-range molecular order and there could be a relationship between the neighboring molecules but there is no long-range order in their molecular packing (Yu, 2001). The lack of long range order in the molecular packing and thus lack of crystallinity results in higher free energy compared to the crystalline counterparts (Hancock and Zografi, 1997).

Additional experiment with PM AH was performed to investigate the effect of excipient (Soluplus®) on the dissolution behavior of PRX. Furthermore, it was hypothesized that an increase in the dissolution rate of PRX from SD (compared to AH) was due to PRX being amorphous, and not only by the solubilizing properties of Soluplus® (Fig. 8). The results suggest that the total amount of dissolved PRX was increased both with SD and PM AH compared to AH and MH. As seen in Figure 8, the release profile of PRX from PM AH was almost linear (zero-order kinetics). According to the literature, Soluplus® with an amphiphilic chemical structure has an excellent affinity to form a molecular dispersion with drugs which makes it a good solubilizer for poorly water-soluble drugs (Thakral et al., 2011). The Raman spectroscopy results showed that Soluplus® also prevents the water-mediated phase transformation of AH to MH in both PM AHs and SDs (this is described more precisely in the paragraph "Slurry Tests"). The present results are in accordance with previous studies reporting the dissolution of amorphous SDs containing PVP as a hydrophilic polymer (Tantishaiyakul et al., 1999).

Additional test was carried out with powders of PRX solid state forms introduced directly to the dissolution medium in order to detect the possible effect of capsule shell on the dissolution. Although the general trends were similar, also the formulation of drug (capsule vs. powder) turned out to be important (Figs. 8 and 9). As can be seen the SD introduced to dissolution medium as powders released all the PRX within 10 minutes while from capsules only 45% was relesed. Also the release of PRX from PM AH was significantly faster from powders. The slower release rate of PRX from amorphous SD in capsules was probably due to the effect of the capsule shell. This hinders the disintegration process of the SD which causes the formation of supersaturated PRX solution between the particles, leading to the partial crystallization of PRX as MH.

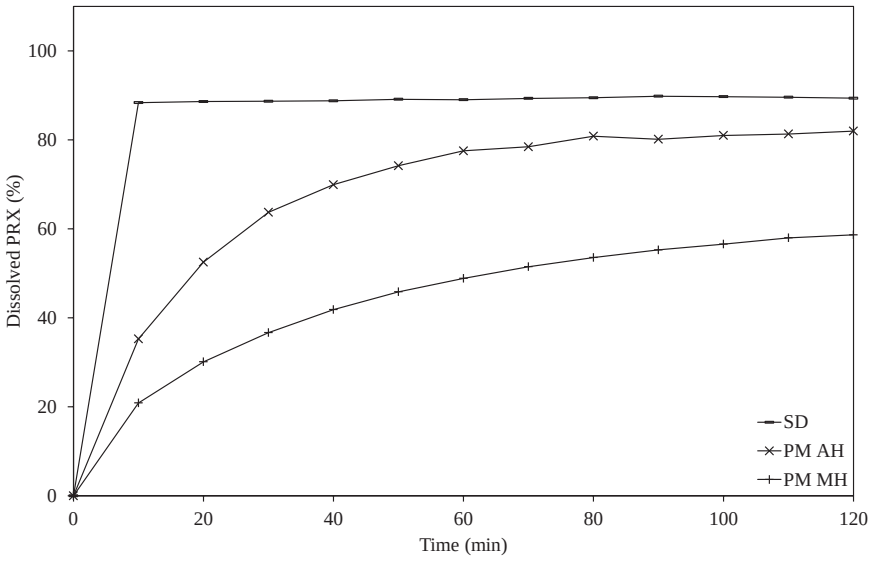

Figure 9. Dissolution profiles of piroxicam (PRX) solid state forms (as powders) in 900 ml of hydrochloric acid buffer (pH 1.2) at 37 °C (n = 3). Average standard error was ±0.49% and is not shown for clearance purposes. Key: Solid dispersion of PRX and Soluplus® graft co-polymer 1:4 (SD), physical mixture of PRX anhydrate I (AH) and Soluplus® 1:4 (PM AH), physical mixture of PRX monohydrate (MH) and Soluplus® 1:4 (PM MH).

5.2.2. Intrinsic dissolution test (I)

To get further insight into the solubility of different solid-state forms, intrinsic dissolution tests were performed (Fig. 10). As observed in the dissolution test with basket method, SD showed the highest intrinsic dissolution rate within the first 15 minutes (61.6 µg/min/cm2) after which a gradual decrease in IDR was determined up to 60 minutes sampling point. In the last phase of the test the intrinsic dissolution rate of SD was similar to MH (10.7 µg/min/cm^2). This is due to the conversion of amorphous PRX to MH which was confirmed by Raman spectroscopy. Such changes in the IDR are typical for APIs that exhibit solid-state transformations during dissolution testing (Greco and Bogner, 2011). Similar behavior has also been reported for amorphous indometacin and carbamazepine during IDR testing (Savolainen et al., 2009).

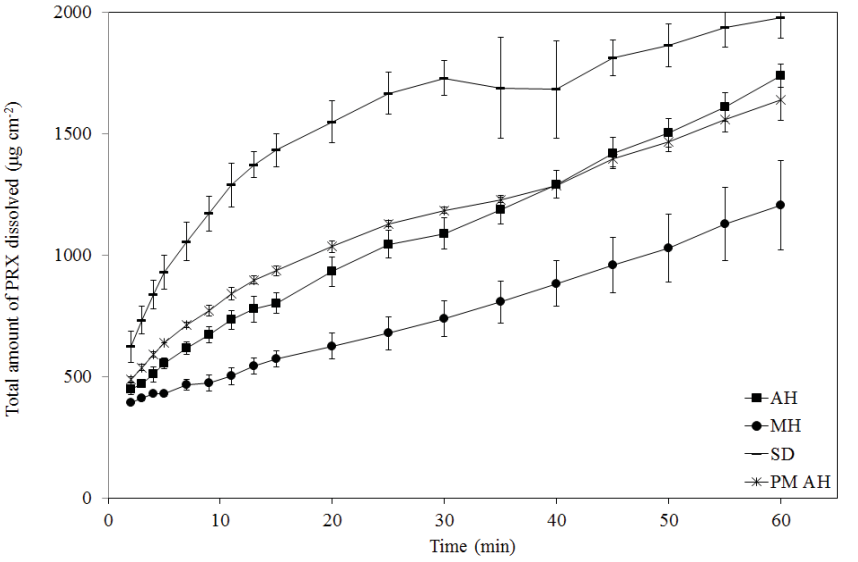

Figure 10. Intrinsic dissolution rate measurement of (PRX) solid-state forms in hydrochloric acid buffer (pH 1.2) at 37 °C (n=3). Key: Piroxicam anhydrate I (AH), piroxicam monohydrate (MH), physical mixture of AH and Soluplus® 1:4 (PM AH), and solid dispersion of PRX and Soluplus® 1:4 (SD).

The second highest IDR was measured with PM (26.2 µg/min/cm2), which was quite close to the IDR of AH (24.4 µg/min/cm2). This result, however, is in contrast to the results obtained in the dissolution test with basket method and this discrepancy is probably due to the rapid dissolution and solubility-enhancing effect of Soluplus® around PRX in the PM AH and the interaction between a polymer and gelatin capsule during dissolution testing with capsules. The lowest IDR was measured for MH (12.5 µg/min/cm2). It was expected that also the dissolution rate of AH would change during IDR testing, since MH formation has been reported to occur during solubility testing (Jinno et al., 2000) and IDR testing (Tsinman et al., 2009). However, in the time-scale of IDR testing performed in the present study (up to 120 minutes), this was not observed.

5.2.3. Slurry tests (I)

Slurry tests together with Raman spectroscopic monitoring were performed in order to investigate the solid-state transformations in the dissolution medium. In slurry tests AH and SD converted to MH at different rates.

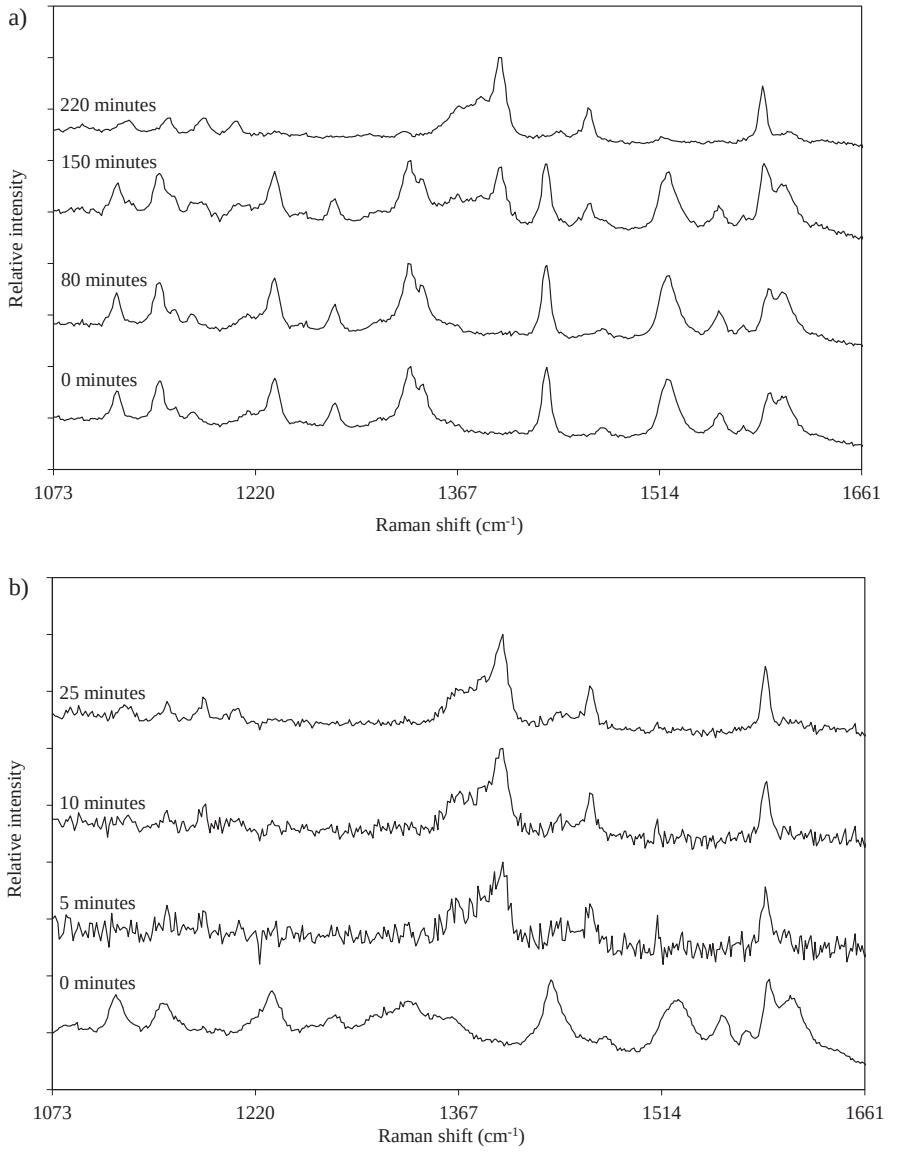

Figure 11. a) Piroxicam anhydrate (AH) conversion to piroxicam monohydrate (MH) in during slurry test monitored by means of Raman spectroscopy. **b)** Solid dispersion of PRX and Soluplus® 1:4 (SD) conversion to piroxicam monohydrate (MH) during slurry test monitored by means of Raman spectroscopy. Raman spectra are shown after different time-points during slurry testing (minutes).

As seen in Figure 11a, AH converted to MH within 220 minutes of mixing, which may explain the decrease in dissolution rate during the dissolution test with basket method (see Fig. 8). Amorphous PRX in SDs converted to MH after 10 minutes of mixing (Fig. 11b). These results are in accordance with previous study where amorphous PRX prepared by low temperature milling converted to MH in simulated gastric fluid (without pepsine) within few minutes of testing (Naelapää et al., 2012). These results were supported by the intrinsic dissolution rate measurements as the dissolution rate of SD was decreasing. Surprisingly, PM AH did not show any changes in the solid-state form during the slurry test within eight hours. This is probably due to the adsorption of amphiphilic Soluplus® onto PRX crystals and the formation of stabilizing hydrogen bonds, which can inhibit the recrystallization. This kind of recrystallization inhibition has also been reported with other polymers and APIs (Murdande et al., 2011). Formation of hydrogen bonds between PRX and Soluplus® may also increase the activation energy of nucleation (Brouwers et al., 2009).

5.3. Physical solid-state stability of solid dispersions during storage (II)

5.3.1. Effects of "low-humidity" storage conditions (II)

No significant changes in the ATR-FTIR spectrum of SDs were observed during a six-month short-term stability study when the samples were stored at low humidity and low temperature (~0% RH/ 6 °C) and at low humidity and intermediate temperature (~0% RH / 25 °C) conditions (Figs. 12a and 12b).

Similar results were obtained using Raman spectroscopy. The interpretation of Raman spectra collected during the storage of SDs was found to be more difficult than the interpretation of the corresponding ATR-FTIR spectra. Consequently, Raman spectroscopy was combined with PCA, which enabled better visualization and investigation of the possible solid-state transformations of PRX during storage (Fig. 13). Three PCs were needed to describe 99.8% of the chemically meaningful variation in all Raman spectra. PCA scores and loading vector of the first PC (PC 1) explained 97.9% of the variation in Raman spectra. The second PC (PC 2) and third PC (PC 3) explained 1.1% and 0.8% of the variation, respectively. The loading vector of PC 1 correlated positively to the spectrum of SDs, the loading vector of PC 2 correlated negatively to the spectrum of PM AH and positively to the spectrum of PM MH, and PC 3 correlated positively to the spectra of PM AH and PM MH (Fig. 13a and 13b).

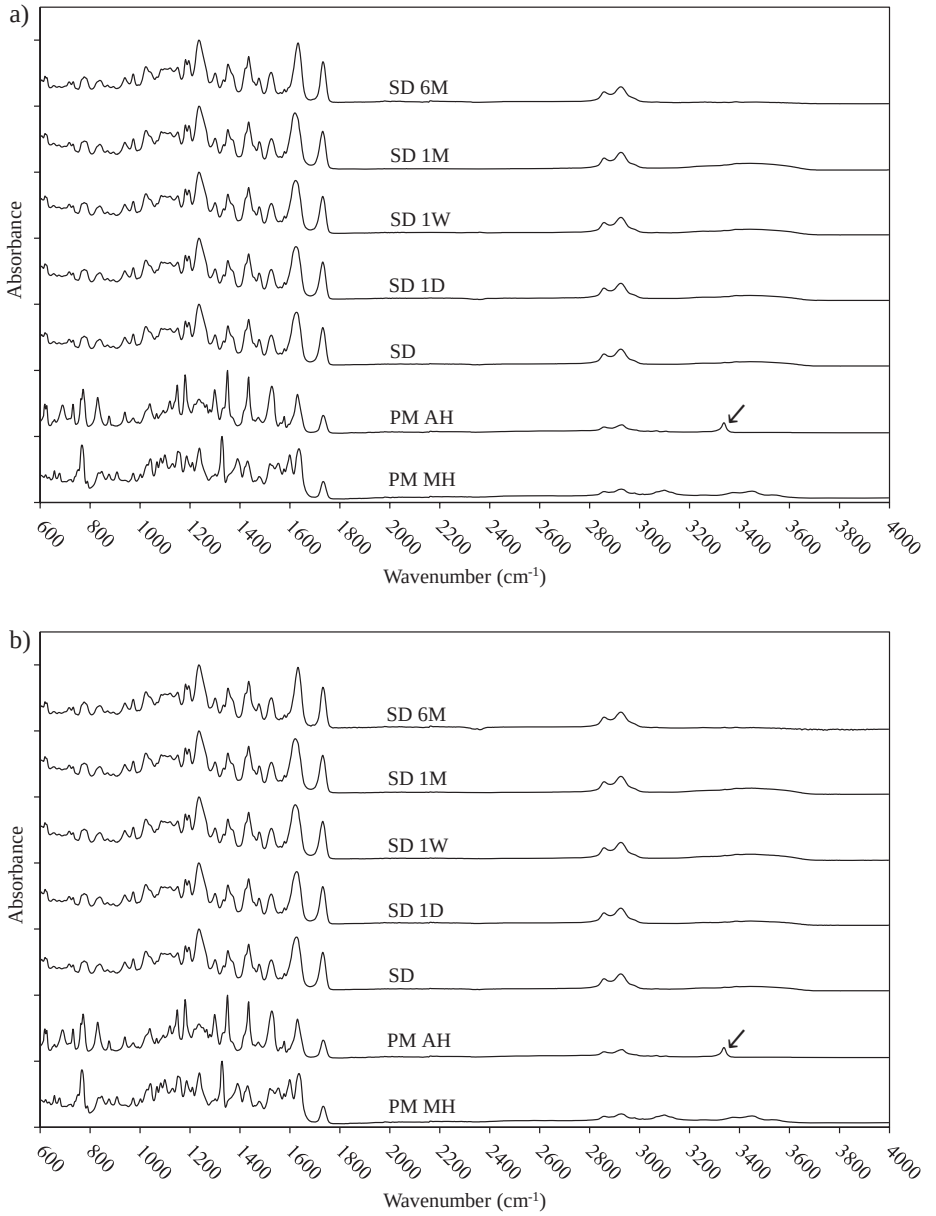

Figure 12. ATR-FTIR spectra of amorphous solid dispersions of piroxicam (PRX) and Soluplus® graft co-polymer 1:4 (SDs) stored at **a)** ~0% RH / 6 °C, **b)** ~0% RH / 25 °C, Key: The SDs stored for one day (SD 1D), one week (SD 1W), one month (SD 1M) and for six months (SD 6M). The respective spectrum of fresh SD (immediately after preparation), physical mixture of PRX anhydrate I (AH) and Soluplus® 1:4 (PM AH), and physical mixture of PRX monohydrate (MH) and Soluplus® 1:4 (PM MH) are shown as references. The arrows indicate the N-H stretching vibration band of PRX at 3337 cm^{-1}. All spectra are offset for clarity.

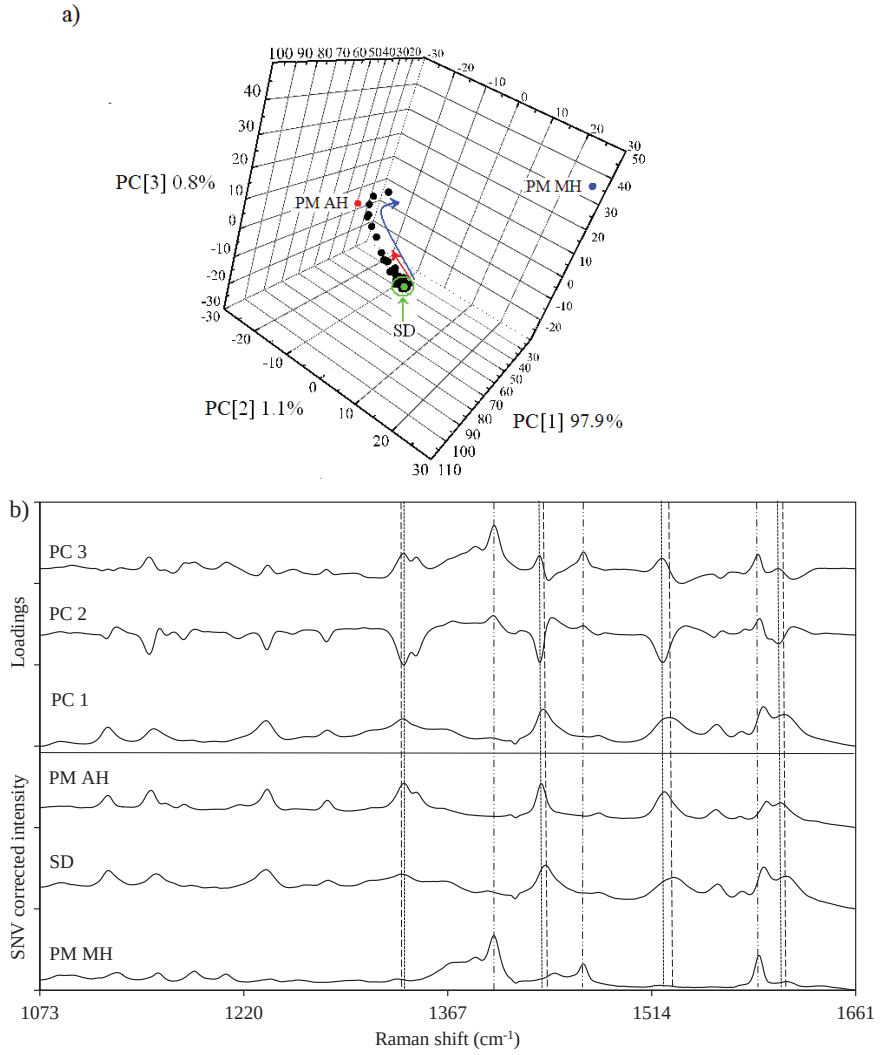

Figure 13. a) The 3D principal component analysis (PCA) scores plot for the first, second and third principal components (PC 1, PC 2 and PC 3, respectively) of solid dispersions (SDs) stored in different conditions together with pure forms: SD of piroxicam (PRX) and Soluplus® 1:4 (SD, marked with green dot and arrow), physical mixtures of PRX anhydrate I (AH) and Soluplus® (PM AH, marked with red dot) and PRX monohydrate (MH) and Soluplus® (PM MH, marked with blue dot). Cluster of principal components (PCs) of Raman spectra recorded from samples stored at low humidity is surrounded with green circle. The red arrow shows the evolution of PCs of Raman spectra recorded at intermediate humidity from first day up to six months of storage. The blue arrow shows the evolution of PCs of Raman spectra recorded at high humidity from first day up to six months of storage. **b)** Loadings of the PC1, PC2 and PC3. SNV corrected Raman spectra of AH PM, SD and MH PM are shown for comparison and all spectra are offset for clarity. Characteristic peaks for amorphous PRX in SD are marked with dashes (—), for AH with dots (···) and for MH with dashes and dots (–··) respectively.

In the 3D PCA scores plot, the dots representing the Raman spectra for the SD samples stored at low humidity formed a clear cluster around a dot representing the Raman spectrum of SD immediately after preparation (Fig. 13a). This indicates that no solid-state transformations had taken place in the SD samples stored at low humidity. The results of ATR-FTIR and Raman spectroscopy suggest that the SDs of PRX and Soluplus® prepared by a solvent evaporation method are physically stable in a powder form in the present storage conditions for at least six months. This is an interesting finding since previous studies have shown that the corresponding SDs of PRX and Soluplus® prepared by ball-milling recrystallize within two months (Kogermann et al., 2013). It is evident that the use of different methods for preparing SDs can result in different molecular arrangements and drug-polymer interactions in the final product. Different preparation methods can result in different sizes of nuclei and also the degree of mixing of polymer and API can be different. With ball milling, the molecular-level dispersion of drug molecules in carrier polymer can be limited which means that the physical stability is compromised.

5.3.2. Effects of "intermediate humidity" storage conditions (II)

The ATR-FTIR spectra of the SD samples stored at intermediate humidity conditions showed that PRX recrystallized out as PRX AH (Fig. 14).

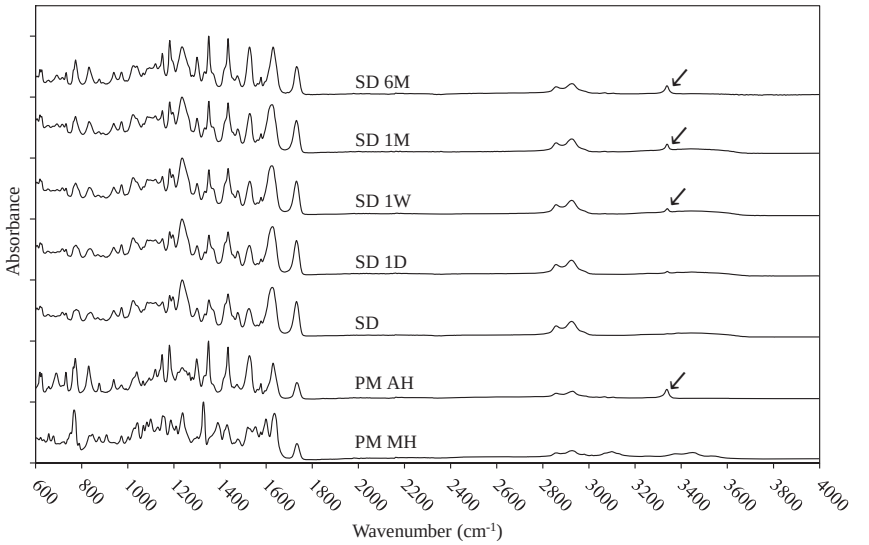

Figure 14. ATR-FTIR spectra of amorphous solid dispersions of piroxicam (PRX) and Soluplus® graft co-polymer 1:4 (SDs) stored at ~40% RH / 25 °C. Key: The SDs stored for one day (SD 1D), one week (SD 1W), one month (SD 1M) and for six months (SD 6M). The respective spectrum SD immediately after preparation, physical mixture of PRX anhydrate I (AH) and Soluplus® 1:4 (PM AH), and physical mixture of PRX monohydrate (MH) and Soluplus® 1:4 (PM MH) are shown as references. The arrows indicate the N-H stretching vibration band of PRX at 3337 cm^{-1}. All spectra are offset for clarity.

After four days of storage, the N-H stretching band characteristic to PRX AH appeared at 3337 cm^{-1}. Furthermore, there were also other changes of the peaks in the fingerprint area that were suggesting increased crystallinity in the SD samples.

Raman spectroscopy combined with multivariate analysis was used to further investigate the physical solid-state changes of PRX. PCA and MCR-ALS was used to carry out qualitative and quantitative analysis of the Raman spectra (Fig. 13a, 13b, 15a and 15b). In the PCA plots, the Raman spectra for the SD samples stored at intermediate humidity and temperature line up on a vector that points from the dot representing the Raman spectra of SDs towards the dot representing the Raman spectrum of PM AH (Fig. 13a and 13b). The present results confirmed the corresponding results obtained with ATR-FTIR. It can be concluded that the present SDs of PRX and Soluplus® are physically unstable when stored at higher humidity and temperature, and tend to recrystallize as PRX AH already after short-term aging (1 week). This is contrary to the results obtained with the SD samples stored at low humidity and low/intermediate temperature conditions.

Raman spectra for the SD samples stored at intermediate humidity and temperature conditions were investigated in more detail using MCR-ALS (Fig. 15a and 15b). This also allows (semi-) quantitative analysis of the physical solid-state changes in the aged SDs. Figure 15a shows the MCR-ALS calculated amounts of amorphous PRX and crystalline PRX and Figure 15b shows the MCR-ALS estimated Raman spectra of the components in the samples stored at the intermediate humidity and temperature conditions. Raman spectroscopy coupled with MCR-ALS was able to detect and quantify the crystallization of PRX already after one day of storage. After six months of storage, approximately 40% of PRX had crystallized as AH. The MCR-ALS model for Raman spectra collected from the samples stored at 40% RH / 25 °C showed that only two PCs existed in a given system and the model described 99% of the variation in the given data matrix. The present results were in good agreement with the PCA model for the Raman spectra obtained from the aged SD samples stored at 40% RH / 25 °C. In this model, two PCs described 99.6% of the total variation in the data (data not shown). As PCA provides the best possible fit along a set of orthogonal PCs, the similarity of the number of PCs needed and the similarity between the total variation (described by the PCA and MCR-ALS) provide evidence that the MCR-ALS model is also performing reasonably well in terms of fit.

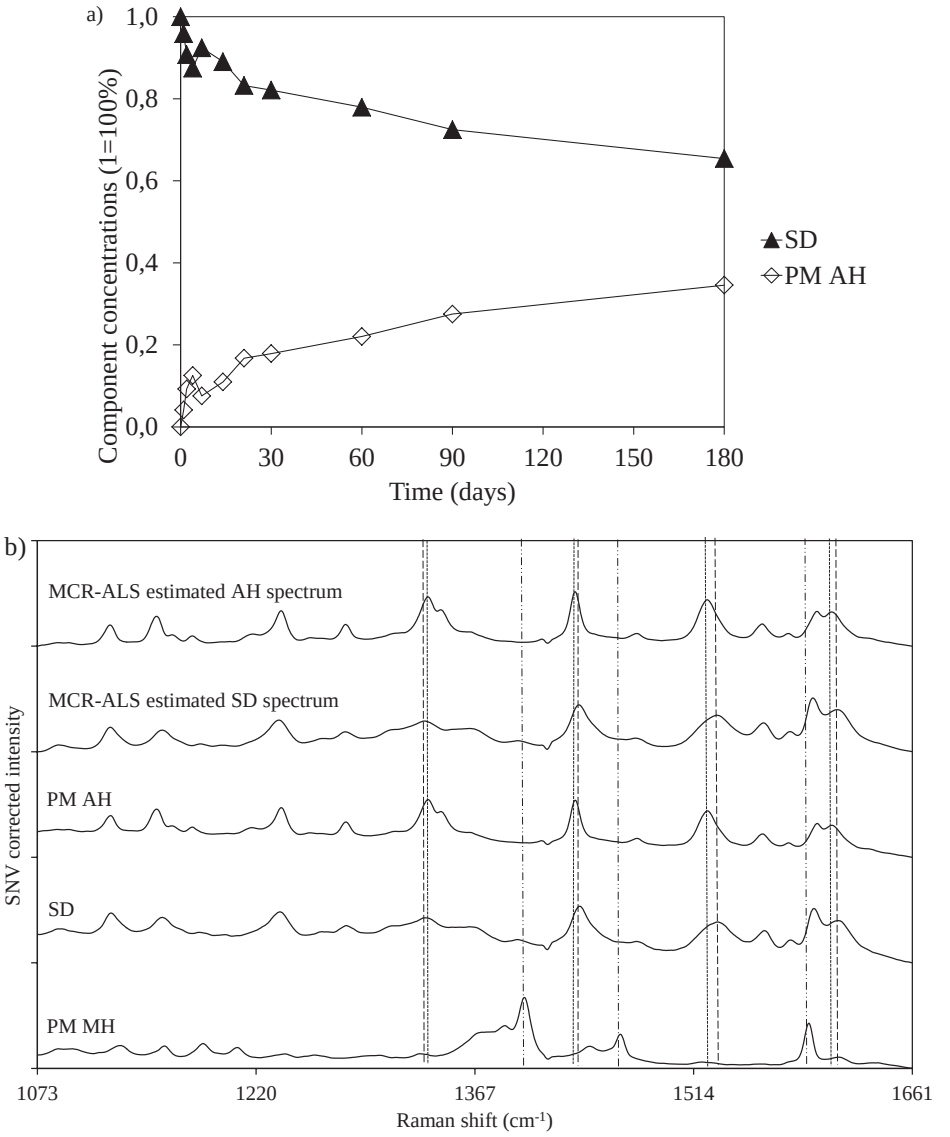

Figure 15. a) Multivariate curve resolution alternating least squares (MCR-ALS) estimated concentrations of piroxicam (PRX) solid state forms in amorphous solid dispersion (SD) samples stored at ~40% RH/25 °C. **b)** MCR-ALS estimated Raman spectra of pure components encountered in the samples stored at ~40% RH/25 °C. Legend: Solid dispersion of PRX and Soluplus® 1:4 (SD), physical mixture of PRX anhydrate I (AH) and Soluplus® (PM AH) and physical mixture of PRX monohydrate (MH) and Soluplus® (PM MH). The Raman spectra of PRX solid state forms are shown for comparison and all spectra are offset for clarity. Characteristic peaks for amorphous PRX in SD are marked with dashes (—), for AH are marked with dots (···) and for MH are marked with dashes and dots (-··) respectively.

5.3.3. Effects of "high humidity" storage conditions (II)

At higher humidity and intermediate temperature conditions (~75% RH / 25 °C), clear signs of premature crystallization of PRX in SDs as AH was observed after a short-term aging period (Fig. 16). The characteristic NH stretching vibration band of PRX AH in the ATR-FTIR spectrum was displayed at 3337 cm^{-1} already after one day storage (Fig. 16).

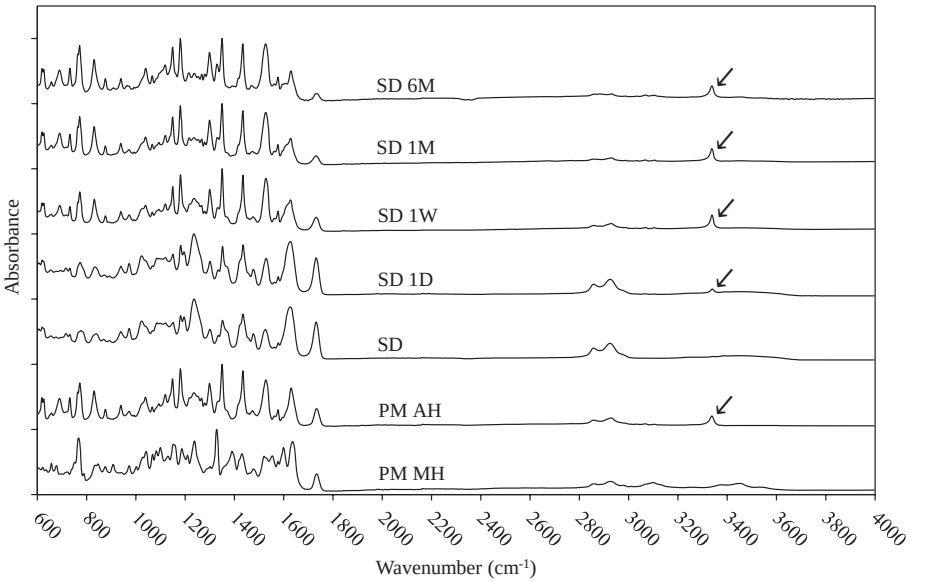

Figure 16. ATR-FTIR spectra of amorphous solid dispersions of piroxicam (PRX) and Soluplus® 1:4 (SDs) stored at ~75% RH / 25 °C. Key: The SDs stored for one day (SD 1D), one week (SD 1W), one month (SD 1M) and for six months (SD 6M). The respective spectrum of SD immediately after preparation, physical mixture of PRX anhydrate I (AH) and Soluplus® 1:4 (PM AH), and physical mixture of PRX monohydrate (MH) and Soluplus® 1:4 (PM MH) are shown as references. The arrows indicate the N-H stretching vibration band of PRX at 3337 cm^{-1}. All spectra are offset for clarity.

In the PCA plots, the Raman spectra for the aged SD samples (stored at high humidity-intermediate temperature conditions for one month) line up on a vector that points from the dot representing the Raman spectrum of SD towards the dot representing the Raman spectrum of PM AH (Figs. 13a). This suggests that after one month's storage most of the amorphous PRX had recrystallized as AH. The dots representing the Raman spectra for the SD samples stored at high humidity-intermediate temperature conditions for longer than one month line up on a vector that points from the dot representing the Raman spectrum of AH towards the dot that represents the Raman spectrum of PM MH (Figs. 13a). The present results indicated that even one month's storage at high humidity and intermediate temperature caused AH to recrystallize as MH.

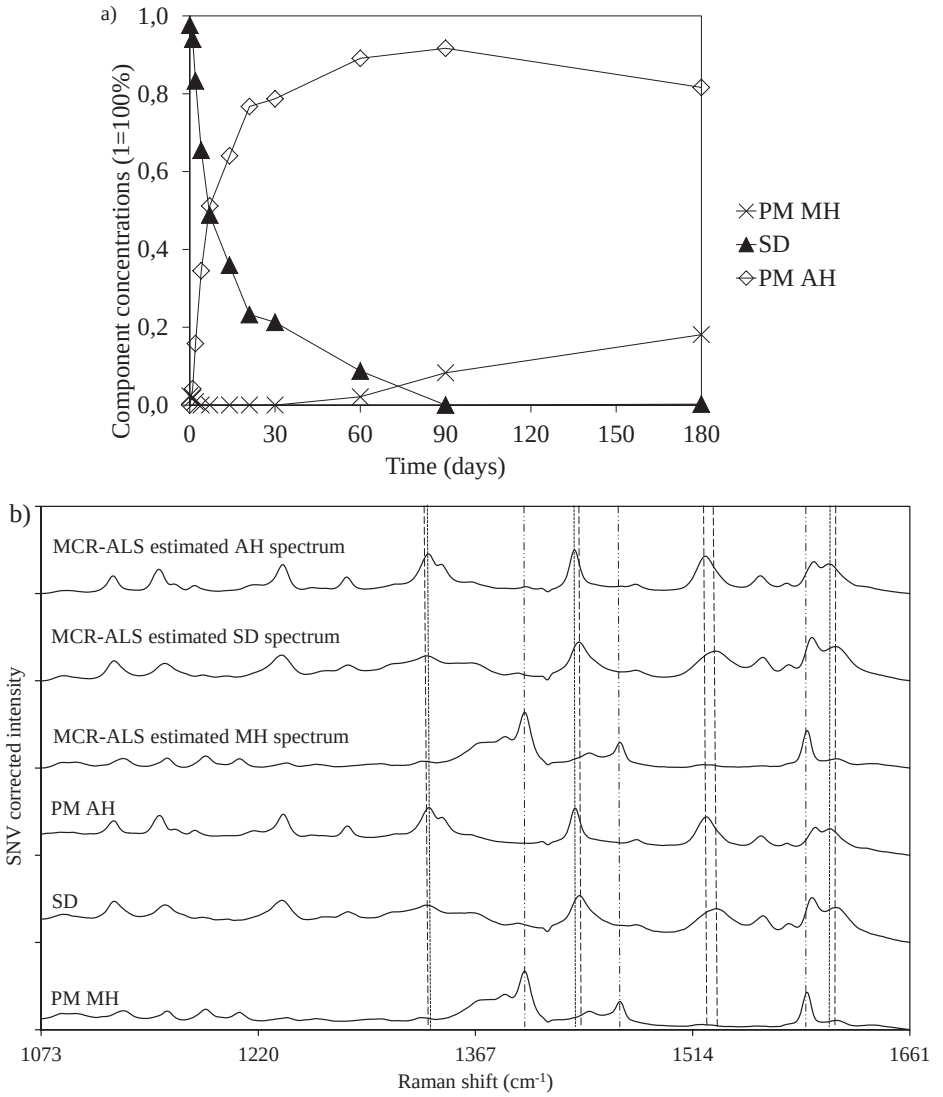

Figure 17. a) Multivariate curve resolution alternating least squares (MCR-ALS) calculated concentrations of PRX solid state forms in SD stored at ~75% RH/25 °C and **b)** MCR-ALS estimated Raman spectra of pure components encountered in the samples stored at ~75% RH/25 °C. Legend: Solid dispersion of PRX and Soluplus® 1:4 (SD), physical mixture of PRX anhydrate I (AH) and Soluplus® (PM AH) and physical mixture of PRX monohydrate (MH) and Soluplus® (PM MH). The Raman spectra of PRX solid state forms are shown for comparison and all spectra are offset for clarity. Characteristic peaks for amorphous PRX in SD are marked with dashes (—), for AH are marked with dots (···) and for MH are marked with dashes and dots (-··) respectively.

Raman spectroscopy combined with MCR-ALS confirmed the results obtained with ATR-FTIR and Raman spectroscopy together with PCA (Figs 17a and 17b). During a short-term storage for one day and one month, approximately 20% and 80% of PRX crystallized as AH, respectively. The recrystallization as PRX MH was detected after one month storage and after six months storage the amount of MH increased up to approximately 20%. The amount of PRX AH started to decrease after three months storage and this suggests that not only amorphous PRX is crystallizing as MH but also PRX AH recrystallizes as MH (Fig. 17a). The comparison of MCR-ALS and PCA models for Raman spectra obtained with the SD samples stored at ~75% RH / 25 °C verified that the MCR-ALS was preforming reasonably well in terms of fit. The PCA model for the Raman spectra of the corresponding aged SD samples used three PCs for describing 99.9% of the total variation in the data (data not shown). The MCR-ALS also needed three components to describe 97.6% of the total variation in the data.

5.3.4. Comparison of different storage conditions (II)

The present SDs were physically stable in a powder form at ~0% RH / 6 °C ("low humidity-low temperature") and ~0% / 25 °C ("low humidity-intermediate temperature") for at least six months. These SDs, however, are physically unstable at higher humidity conditions (~40% RH / 25 °C and ~75% RH / 25 °C) since amorphous PRX crystallizes out firstly as a AH and subsequently as MH within 2–3 months. It is evident that the absorbed water acts as a plasticizer in the SDs and thus increases the molecular mobility of amorphous PRX leading to premature crystallization. Hydrogen bonding between PRX and a carrier polymer (Soluplus®) is not strong enough to stabilize PRX in amorphous form at higher humidity conditions. Recrystallization as MH under 75% RH conditions probably does not occur via AH in the bulk material since AH has to be dissolved in order to allow this to take place as AH and MH have completely different unit cell structures (Kojic-Prodic and Ruzic-Toros, 1982; Reck et al., 1988; Reck and Laban, 1990). As the amount of condensed water is higher on the surface of powder particles, it is evident that there is enough free water available to dissolve not only amorphous PRX but also crystalline PRX. This is obviously one reason, why the decrease in intensity of characteristic AH N-H stretching band (in the aged SD samples – ATR-FTIR spectra) was observed only with the SD samples stored at ~75% RH / 25 °C (Fig. 16).

5.3.5. Dissolution behavior of stored piroxicam solid dispersions (II)

The dissolution profile of PRX obtained with the SDs exposed to different humidity and temperature storage conditions depended on the crystallization of PRX during the stability study (Fig. 18a, 18b and 18c). In addition, the amount of PRX converted to the crystalline state during storage and the crystal form itself were also important factors affecting the dissolution. This is in agreement with the earlier findings on the dissolution behavior of recrystallized amorphous SDs prepared with Soluplus® and cinnarizine (Tian et al., 2014). After one week's storage, only the SD samples stored at high humidity and intermediate temperature conditions showed decreased dissolution rate (Fig. 18a). After one month's storage, the SD samples stored at intermediate humidity and temperature conditions also exhibited a slightly decreased PRX dissolution rate compared to that obtained with the fresh SDs immediately after preparation (Fig. 18b). After six months' storage, the SD samples stored at intermediate humidity and temperature and high humidity and intermediate temperature showed markedly decreased dissolution rate, while the samples stored under low humidity conditions displayed similar characteristics to the fresh SDs (Fig. 18c). The present dissolution results are in line with the ATR-FTIR and Raman spectroscopy analyses of solid-state changes of PRX in the SDs during a short-term storage.

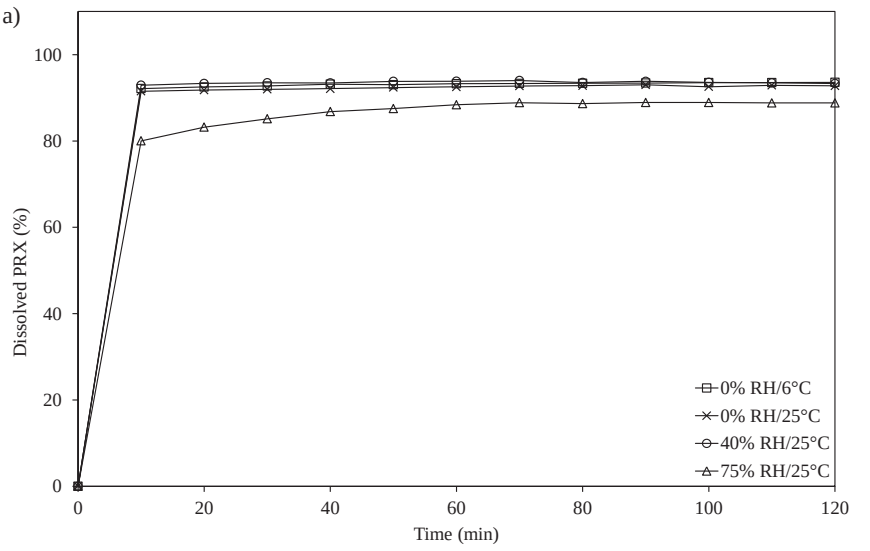

Figure 18.

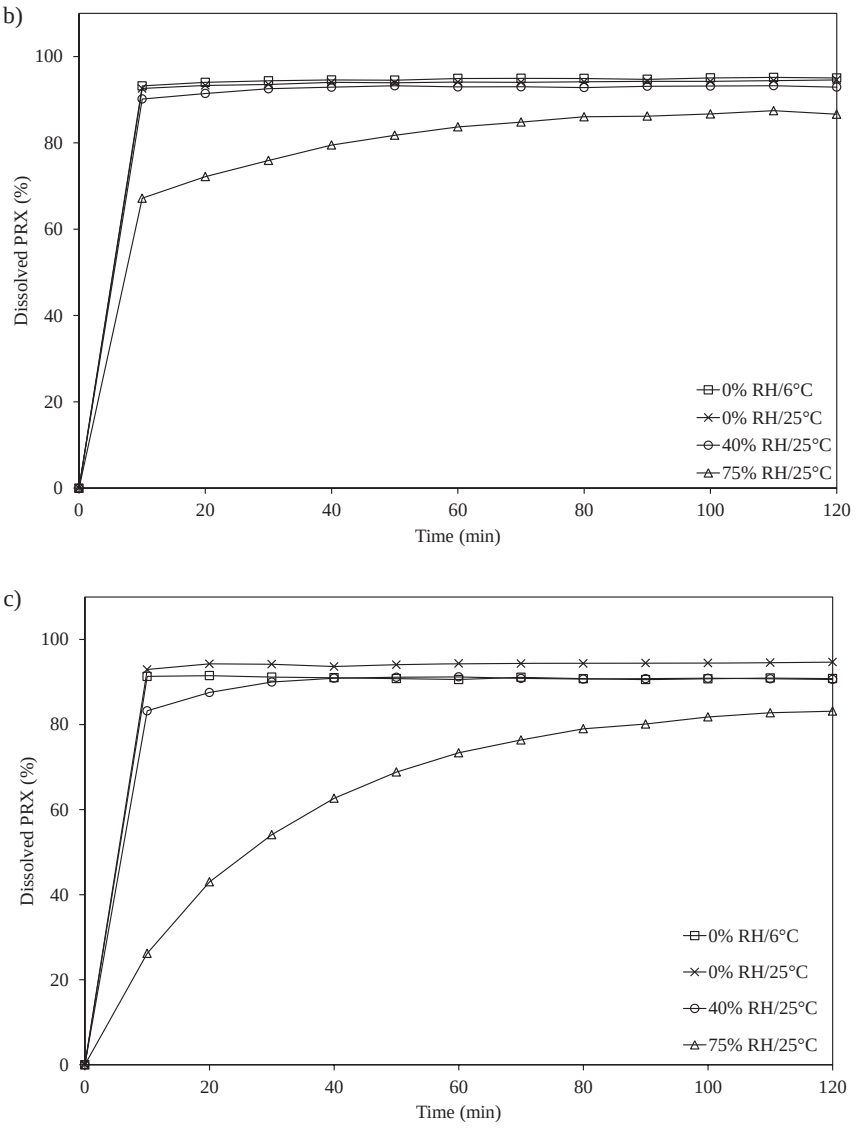

Figure 18. a) Dissolution profiles of the PRX solid dispersions (SDs)(as powders), stored at different conditions for one week, in 900 ml of hydrochloric acid buffer (pH 1.2) at 37 °C (n = 3). Average standard error was ±0.62% and is not shown for clearance purposes. **b)** Dissolution profiles of the PRX solid dispersions (SDs)(as powders) stored at different conditions for one month in 900 ml of hydrochloric acid buffer (pH 1.2) at 37 °C (n = 3). Average standard error was ±0.39% and is not shown for clearance purposes. **c)** Dissolution profiles of the PRX solid dispersions (SDs)(as powders) stored at different conditions for six months in 900 ml of hydrochloric acid buffer (pH 1.2) at 37 °C (n = 3). Average standard error was ±0.79% and is not shown for clearance purposes.

5.4. Physical solid state stability of piroxicam during processing (III)

5.4.1. Solid-state transformations of piroxicam in aqueous drug-layer coating (III)

Raman spectroscopy enabled to identify the solid-state forms of PRX also during and after drug-layer coating of pellets (Figs. 19a, 19b and 19c).

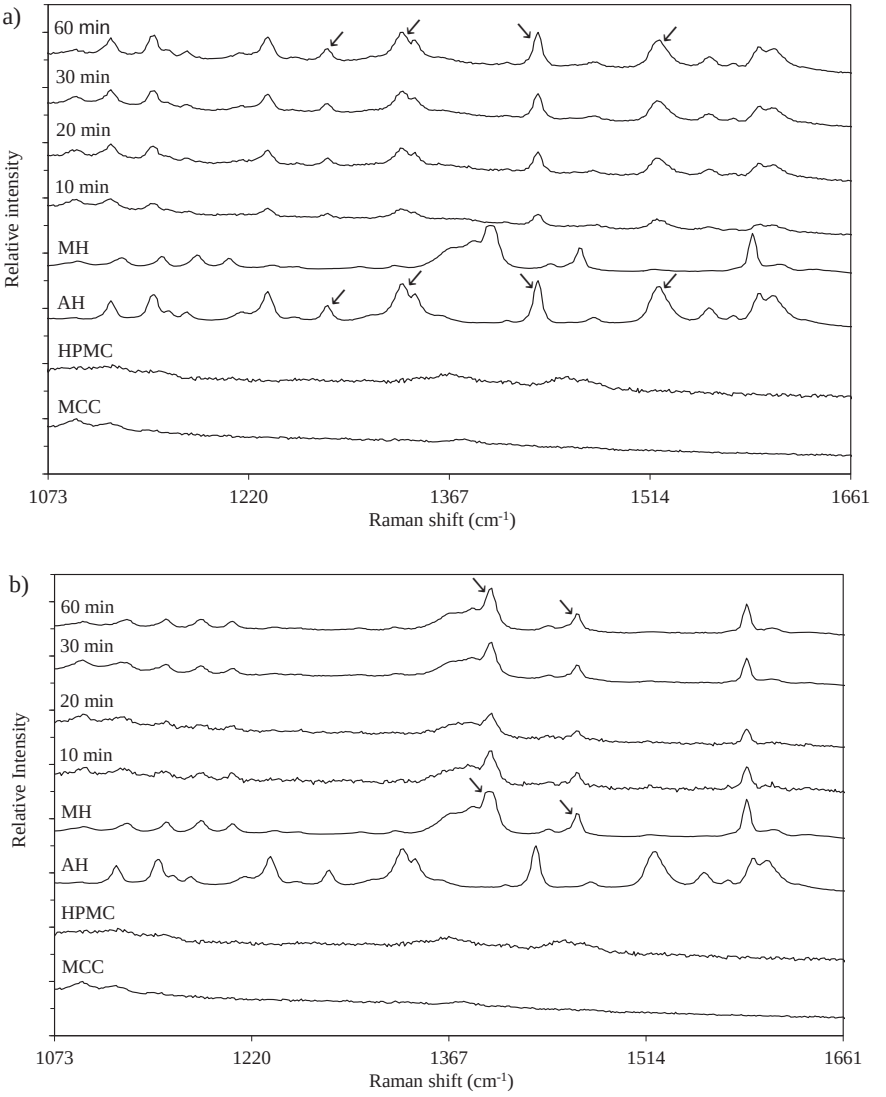

Figure 19

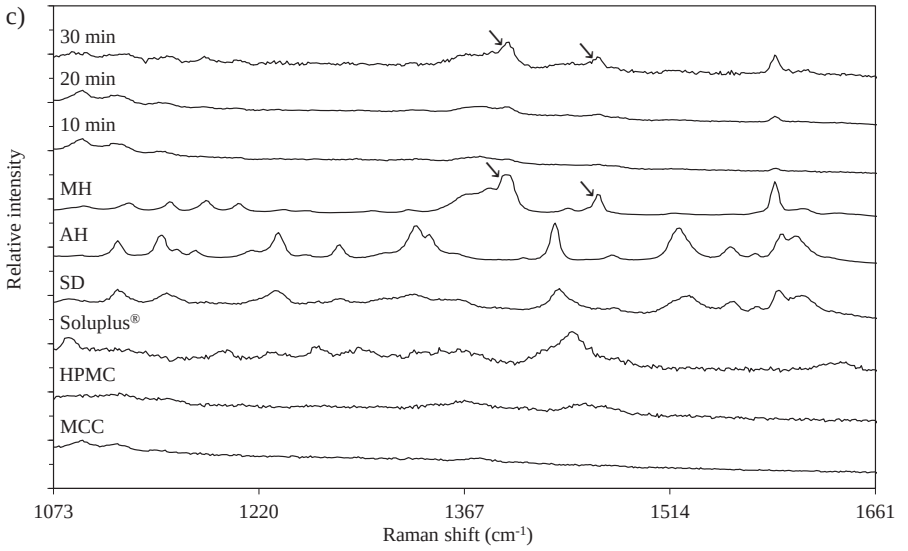

Figure 19. Raman spectra of neutral pellets drug-layer coated with **(a)** PRX anhydrate form I (AH), **(b)** PRX monohydrate (MH), **(c)** amorphous PRX as a solid dispersion (SD) of PRX and Soluplus® 1:4. Multiple Raman spectra were taken at 10, 20, 30 and 60 minutes. Raman spectra of microcrystalline cellulose (MCC); hydroxypropyl methylcellulose (HPMC); Soluplus®, amorphous PRX as a solid dispersion (SD) of PRX and Soluplus® 1:4, PRX anhydrate form I (AH) and PRX monohydrate (MH) are shown for comparison. All spectra are normalized and off-set for clarity. Arrows point to characteristic Raman peaks of AH, MH and SD.

Aqueous-based drug-layer coating of pellets has been widely used for manufacturing controlled drug release multiple-unit systems for e.g. oral pulsatile and/or sustained-release applications (Ensslin et al., 2009; Heinicke and Schwartz, 2004; Möschwitzer and Müller, 2006; Rahman et al., 2006; Sinchaipanid et al., 2004; Tian et al., 2008). The manufacturing in a fluid-bed or air-suspension process involves application of drug-polymer mixture coating layers on the pellet cores using a spray-atomization technique, and subsequent drying of the coated solids. As given process involves elevated temperature and suspending of the agent beeing coated in liquid it is vital to monitor the solid state form during coating.

Excipients, HPMC and MCC, did not interfere with the detection of PRX forms since their Raman peak intensity was quite low compared to PRX ones (Figs. 19a, 19b and 19c). The results of Raman spectroscopy revealed that different solid-state forms of PRX behaved differently during the drug-layer coating of pellets (Figs. 19a, 19b and 19c). AH and MH were found to be more stable forms than SD in aqueous-based drug-layer coating. The amorphous PRX (SD) was unstable and its crystallization as MH was identified with Raman spectroscopy already after 10 minutes of drug-layer coating of pellets (Fig. 19c). The results showed that AH and MH did not transform to any other solid

state form within a 1-hour aqueous drug-layer coating of pellets (Figs. 19a and 19b), thus revealing that AH and MH were stable in aqueous HPMC solution and during coating. In previous studies, AH has been shown to undergo transformation to MH during solubility testing (Jinno et al., 2000) and dissolution (Naelapää et al., 2012) measurements. The hydrate formation of PRX in pure distilled water has been reported to occur within 55 minutes in slurry testing (Paaver et al., 2012). In the present study, probably the presence of HPMC inhibited or slowed down the solid-state transformation from AH to MH. As expected, MH remained unchanged since MH is the most stable form of PRX in aqueous conditions (Sheth et al., 2004c).

5.4.2. Drug-layer coating efficiency (III)

Good correlations were obtained between the drug-layer coating time (10, 20, 30 and 60 minutes) and Raman peak intensity of AH (Fig. 19a) and MH (Fig. 19b). The characteristic PRX peaks in Raman spectrum were much less visible during the first phases of coating (10, 20 and 30 minutes) with SD because the percentage of PRX by weight in SD coating suspension was lower (Fig. 19c). However, Raman spectroscopy can be used to draw conclusions about the drug-layer coating efficiency. The longer coating time resulted in the higher intensity of the characteristic PRX peaks and therefore better coating efficiency. Similar results have been obtained by Wirges et al during coating of the tablets (Wirges et al., 2013). The improved coating efficiency was also verified by the weight gain of pellets during coating experiments (Table 1), and from SEM micrographs (Figs. 20a, 20b and 20c). As can be seen from Table 1, the percentage weight increase (%) in drug-layer coated neutral pellets (vs uncoated pellets) was quite similar for pellets coated with AH and for pellets coated with MH (SD values are not shown due to different testing conditions). Moreover, longer coating time resulted in higher coating efficiency (%) (Table 1). In addition, SEM micrographs revealed the change of pellets surface to more homogeneous together with longer coating time thus without any change in pellet surface morphology.

Plasticizers are most commonly used in coating solutions for improving the film formation and the mechanical properties of the film coat. Plasticizers are known to alter polymer chain interactions and make the hard and brittle coatings more flexible and rubber-like (Billmeyer, 1971). According to the literature, some drugs (e.g. ibuprofen) can have a significant solid-state plasticization effect on pharmaceutical film coatings (Wu and McGinity, 2001). In the present study, no external plasticizer was used in the drug-layer coatings. It is interesting to note, that different PRX solid-state forms itself showed different plasticizing properties. When AH and MH were used, both forms together with HPMC allowed to produce easily removable coatings on the coating chamber walls and pellets revealed more smooth surfaces.

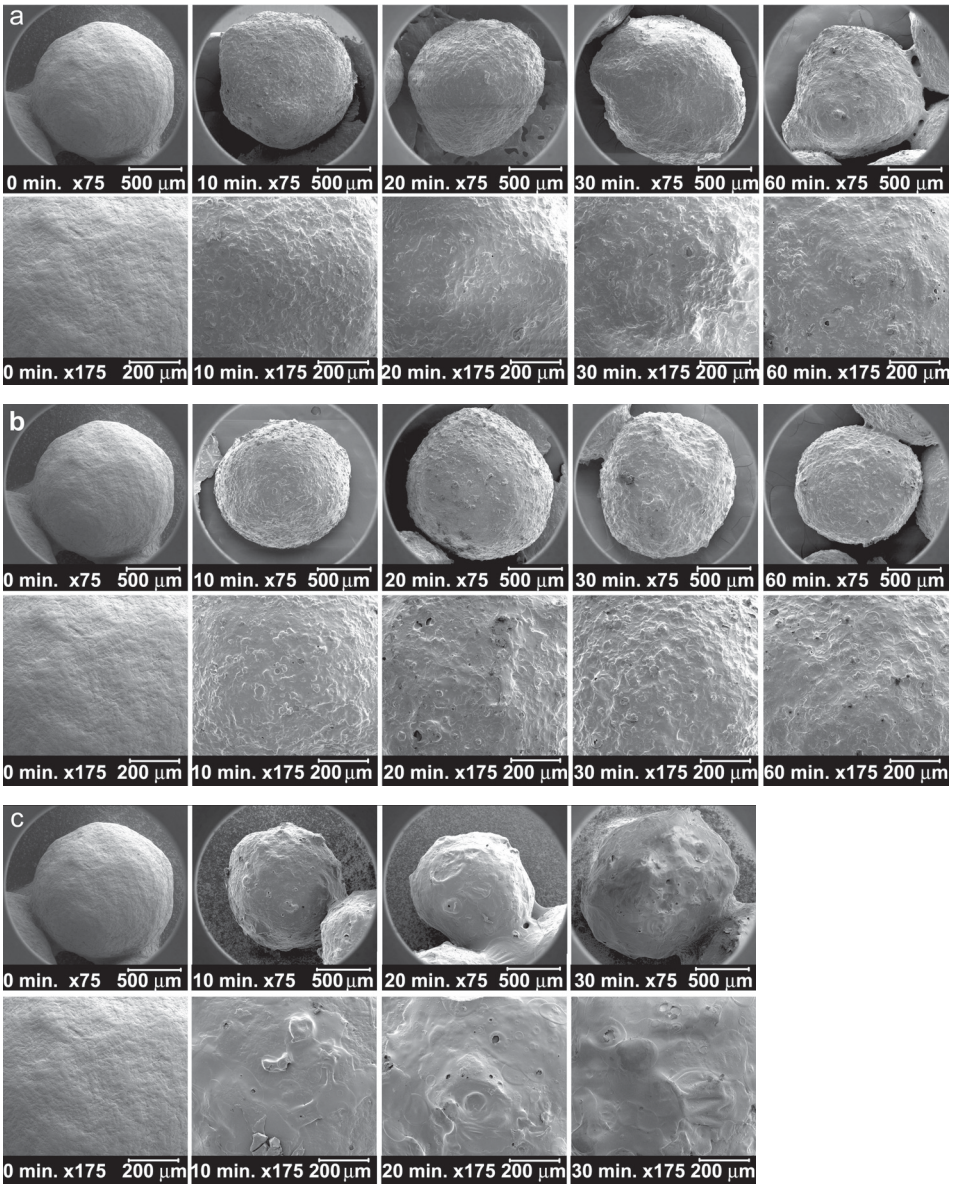

Figure 20. Scanning electron micrographs (SEM) of neutral pellets drug-layer coated with **(a)** PRX anhydrate form I (AH), **(b)** PRX monohydrate (MH) and **(c)** amorphous PRX as a solid dispersion (SD) of PRX and Soluplus® 1:4. From left to right: uncoated neutral pellet, and neutral pellets upon coating after specified time-points (minutes). Upper row: single pellet (magnification 75×). Bottom row: the surface of a single pellet (175×).

Surprisingly, SD did not show this kind of property obviously due to the addition of Soluplus®, which seemed to have quite cohesive properties in water solutions and poor plasticizing characteristics. Furthermore, the SD drug-layer coated pellets showed more rough surface compared to the pellets coated with AH or MH (Figs. 20a, 20b and 20c). It is evident that during drug-layer coating of pellets with SD, an uncontrolled crystallization of MH occurs onto the surface of pellets, and this MH probably has totally different crystal properties (such as morphology) compared to MH prepared by specified recrystallization procedure. The aqueous HPMC coating solution which contained crystallized MH had most likely different density and viscosity, and this resulted in different coating adhesion, porosity, uniformity and thickness. In addition, other factors such as sticking of the pellets to each other and onto the coating chamber wall may cause coating surface roughness variation during fluidization coating. According to the literature, the mechanical stress developed during a coating process and gravitational forces may cause coating non-uniformity (thickness uniformity) on different sides of the pellets (Haddish-Berhane et al., 2006).

Table 1. The theoretical percentage weight increase (%), the weight increase (%) in drug-layer coated neutral pellets (*vs* uncoated pellets) and coating efficiency (%) of pellets during drug-layer coating of pellets at different time points. The neutral pellets are drug-layer coated with different solid-state forms of piroxicam (PRX): PRX anhydrate form I (AH), PRX monohydrate (MH). Amorphous PRX (SD) values are not shown due to different testing conditions.

Coating time (min)	Theoretical weight increase (%)	AH weight increase (%)	AH coating efficiency (%)	MH weight increase (%)	MH coating efficiency (%)
10	2.6	0.9	35.3	1.1	44.2
20	5.2	3.4	65.6	4.5	87.5
30	7.7	7.9	102.4	6.3	81.9
60	15.4	14.2	93.2	12.8	83.4

5.4.3. Solid-state transformations of piroxicam in free films (III)

Raman spectroscopy enabled monitoring different PRX solid-state forms and the amount of AH and/or MH also in free films (Figs. 21a, 21b and 21c).

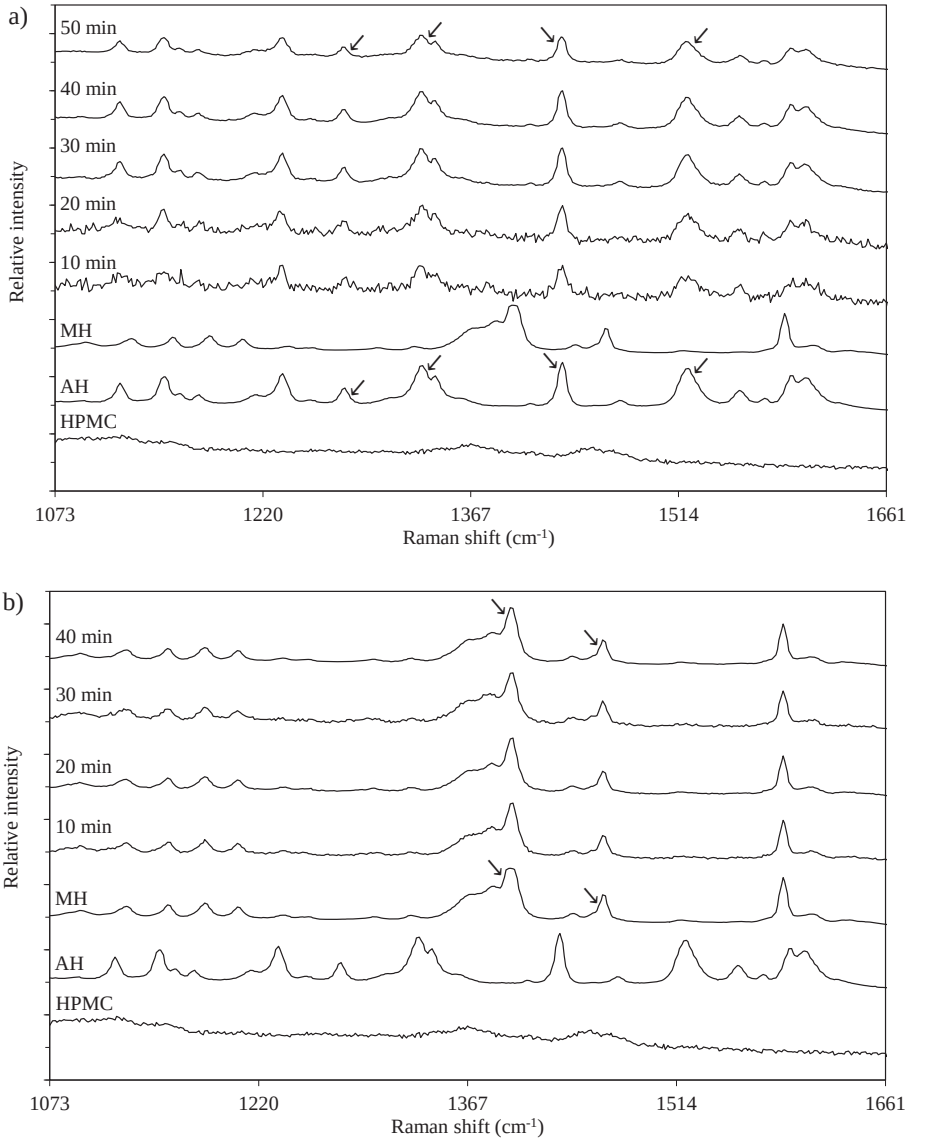

Figure 21

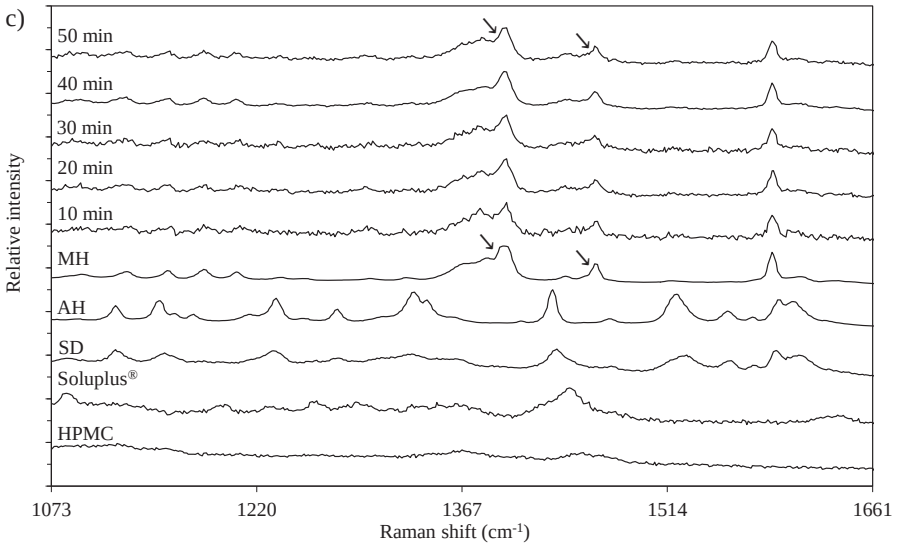

Figure 21. Raman spectra of **(a)** PRX anhydrate form I (AH) free films; **(b)** PRX monohydrate (MH) free films; **(c)** amorphous PRX as a solid dispersion (SD) of PRX and Soluplus® 1:4 free films during drying after specified time-periods (minutes). Raman spectra of hydroxypropyl methylcellulose (HPMC), PRX anhydrate form I (AH), PRX monohydrate (MH) and Soluplus® are shown for comparison. Arrows point to characteristic Raman peaks of AH, MH and SD.

The vibrational spectroscopy results obtained by monitoring the drying stage of drug-loaded free films verified those results achieved in a drug-layer coating process of the pellets. It was found that in both cases AH and MH remained stable during a drying stage and that amorphous PRX (SD) crystallized out as MH within the first minutes of drying (Figs 21a, 21b and 21c). As water vaporized during the drying of free films, the relative amount of PRX increased in free films and this can be seen in the increased intensity of Raman signal and reduction of noise (Figs. 21a, 21b and 21c).

5.4.4. Thermal properties of the drug-layer coatings and free films (III)

DSC was used to understand the interaction between the solid-state forms of PRX and HPMC, and to verify the solid-state transformations during drug-layer coating and in free films. As seen in Figure 22, pure PRX solid-state forms, Soluplus® and HPMC show characteristic thermal behavior.

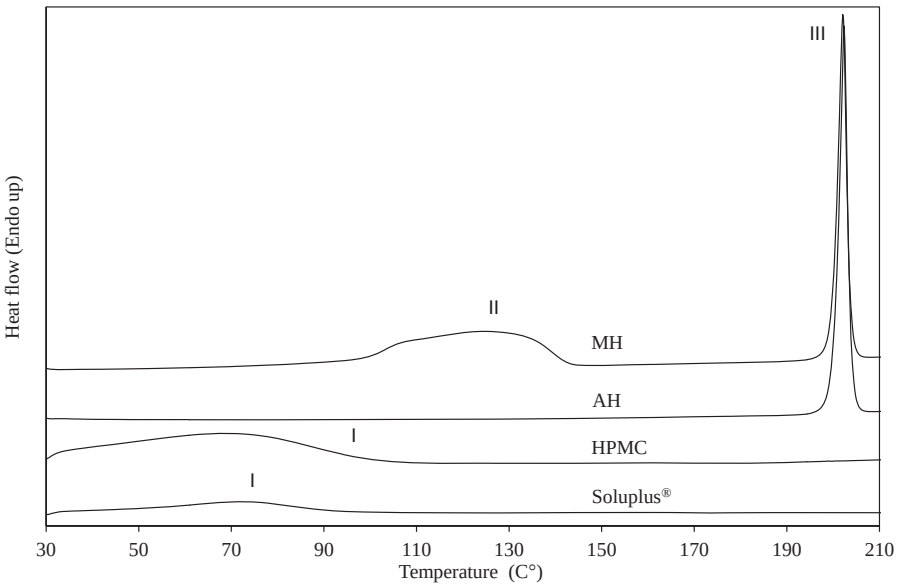

Figure 22. Differential scanning calorimetry (DSC) thermograms of Soluplus®, hydroxypropyl methylcellulose (HPMC), PRX anhydrate form I (AH) and PRX monohydrate (MH). Key: amorphous solid dispersion of PRX and Soluplus® 1:4 (SD), PRX anhydrate form I (AH), and PRX monohydrate (MH), dehydration endotherm of polymer (I), dehydration endotherm of MH (II), fusion endotherm of AH (III):

The melting temperature of AH and dehydration temperature of MH are in good agreement with the respective temperature values reported in the literature (Kogermann et al., 2007a; Kogermann et al., 2011; Vrečer et al., 2003). SD did not show any glass transition temperature (Tg), but this was obviously due to an overlap with the water desorption endotherm as described previously. Similarly, the DSC thermogram of pure HPMC carrier polymer showed only dehydration endotherm and did not reveal any Tg for the polymer. According to McPhillips et al. (1999), the conventional DSC is not able to detect the characteristic Tg for HPMC, but a modulated-temperature DSC shows the Tg at approximately 162 ºC (McPhillips et al., 1999).

The DSC thermograms of AH and MH layer coatings collected from the specific site of a coating chamber wall at different timepoints (30 and 60 minutes) showed coating time independent characteristics (Fig. 23).

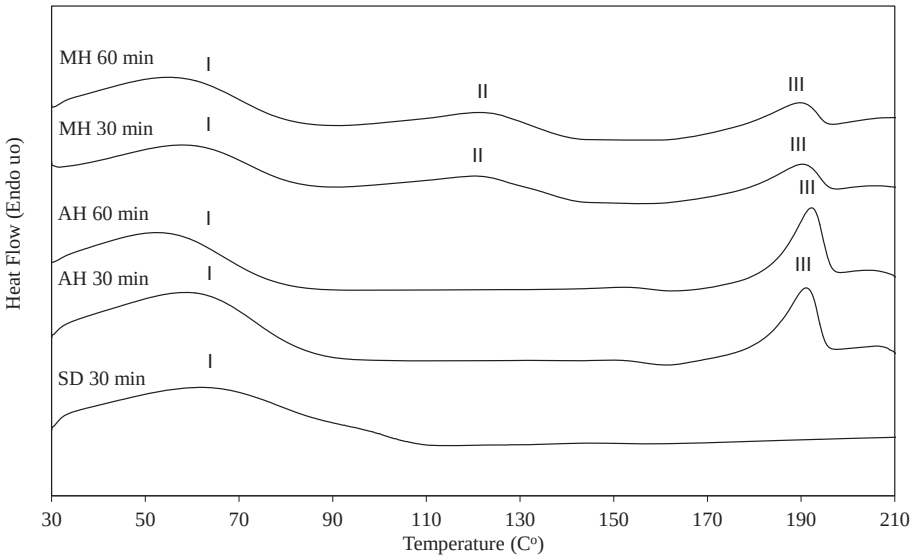

Figure 23. Differential scanning calorimetry (DSC) thermograms of drug-loaded coatings with piroxicam (PRX) solid state forms taken after specific time periods upon coating (minutes). Key: amorphous PRX as a solid dispersion (SD) of PRX and Soluplus® 1:4, PRX anhydrate form I (AH), and PRX monohydrate (MH), dehydration endotherm of polymer (I), dehydration endotherm of MH (II), fusion endotherm of AH (III).

This is quite expected result as no solid state transformation was observed and also the precentage (w/w) of AH or MH in dried coatings is expected to remain constant throughout the coating process. The melting endotherm of AH coating after 30 and 60 minutes of coating was at 190 °C and 191 °C, respectively. The decrease in melting temperature compared to the melting temperature of pure AH could be attributed to the specific interaction of polymer and drug molecules. In addition, both thermograms displayed a broad endotherm ranging from 30 to 90 °C which was attributed to the water desorption from HPMC. Both thermograms of MH displayed very broad endotherms at a range of 90–142 °C attributed to the dehydration of MH and the subsequent melting endotherm of AH at 189 °C. DSC thermogram of SD showed similar thermal behavior as for pure HPMC and Soluplus®.

The DSC thermograms taken from dry drug-loaded free films showed similar characteristics to those taken from drug-layer coatings (Fig. 24). The fusion endotherms of polymer and PRX occured at slightly higher temperatures at 197 °C for AH and MH compared to the samples taken from a coating chamber. This discrepancy can be attributed to Tween 40 which was most likely present in the samples taken from a coating chamber.

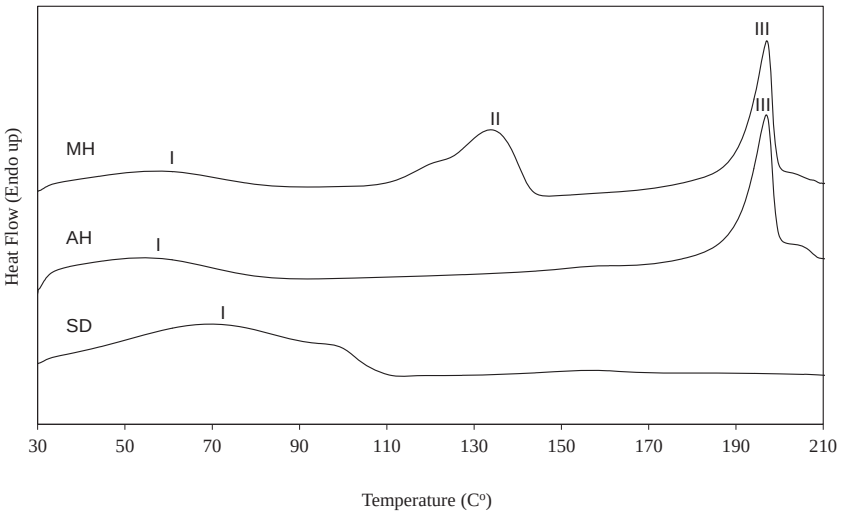

Figure 24. Differential scanning calorimetry (DSC) thermograms of drug-loaded free films with piroxicam (PRX) solid state forms taken after specified time-periods upon drying (minutes). Key: amorphous PRX as a solid dispersion (SD) of PRX and Soluplus® 1:4, PRX anhydrate form I (AH), and PRX monohydrate (MH), dehydration endotherm of polymer (I), dehydration endotherm of MH (II), fusion endotherm of AH (III)

5.4.5. Dissolution of pellets coated with different solid-state forms of piroxicam (III)

Formulated drug-layer coated pellets of PRX showed clearly faster dissolution compared to the powder and powders in a capsule forms (Figs. 8, 9 and 25).

The pellets coated with AH showed almost the highest dissolution rate (Fig. 25). Only SD introduced into dissolution medium as powder showed comparably fast rate (Fig. 9). The lowest dissolution rate was observed with the pellets coated with SD which was obviously due to the formation of MH during an aqueous drug-layer coating. Since the amount of coating polymer (HPMC) and Soluplus® in SD drug-layer coatings was quite high (compared to the amount of PRX), it is also possible that the dissolution of MH can become dependent on the diffusion rate of water molecules into the polymer and also to the diffusion of the dissolved drug molecules out of the polymer. Similarly Dukić-Ott et al. 2008 have shown that if PRX is loaded into pellet cores, the diffusion controlled drug release can be negligible due to the surrounding enteric coating (Dukić-Ott et al., 2008). The pellets coated with MH were not dissolved within the testing time of 2 hours (the plateau was not reached in the dissolution curve; Fig. 25). Comparison of the dissolution profiles of the drug-layer coated pellets for 15 minutes vs 1 hour revealed that prolonged coating increased the amount of PRX on the surface of the pellets (Fig. 25). Hence, the coating efficiency was improved with the longer coating time, and this is in agreement with previous studies with pellets coated in a fluid-bed process (Lee et al., 2011).

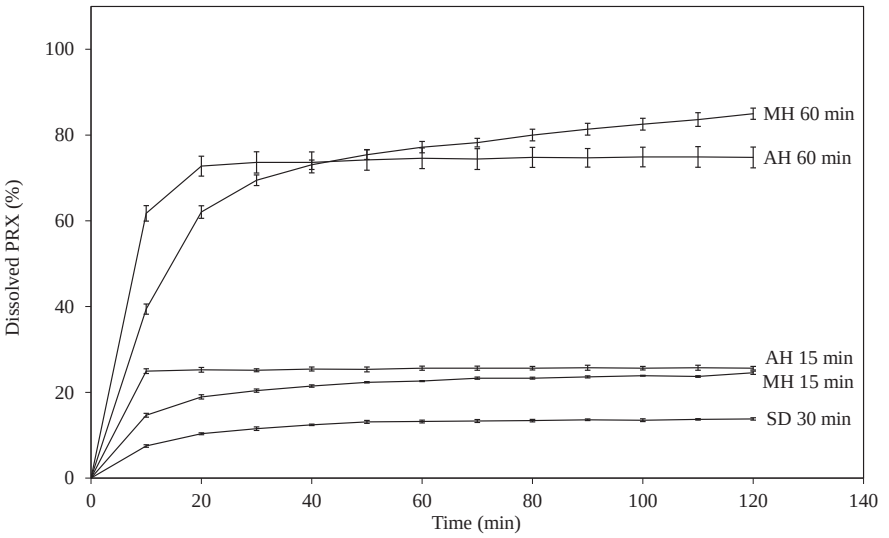

Figure 25. Dissolution profiles of drug-loaded pellets coated with different solid state forms of piroxicam (PRX) in hydrochloric acid buffer (pH 1.2). Key: pellets coated with amorphous solid dispersion (SD) for 30 minutes (SD 30 min), pellets coated with monohydrate (MH) for 15 minutes (MH 15 min), pellets coated with anhydrate form I (AH) for 15 minutes (AH 15 min), pellets coated with AH for 60 minutes (AH 60 min), pellets coated with MH for 60 minutes (MH 60 min). For dissolution test, coated pellet samples (n = 3) were closed in hard gelatin capsule shells (size 1).

The author suggest that the presence of a coating polymer, HPMC, plays a major role in improving the dissolution characteristics of PRX solid-state forms in drug-layer coated pellets. It is evident that hydrophilic HPMC could provide increased wettability of the drug-layer coatings thus accelerating the dissolution of a poorly water-soluble drug. It has been reported that HPMC may improve the solubility and dissolution along with *in vivo* bioavailability (Yamashita et al., 2003). As the drug-layer coating of pellets was not very thick, it could also be expected that an increased specific surface area increased a dissolution rate. Furthermore, in case of PRX solid-state forms as a powder, the possible agglomeration of the individual powder particles may decrease the effective surface area and thus slow down the dissolution rate.

5.5. Biopharmaceutical relevance of solid state forms and their phase transformations-pharmacokinetic studies (I)

As solid-state forms and solution-mediated phase transformations may change the oral bioavailability of poorly water-soluble APIs, the absorption of different PRX solid-state forms were compared. There were significant differences in

plasma concentrations and absorption rates after oral administration of PRX solid-state forms to rats (Fig. 26).

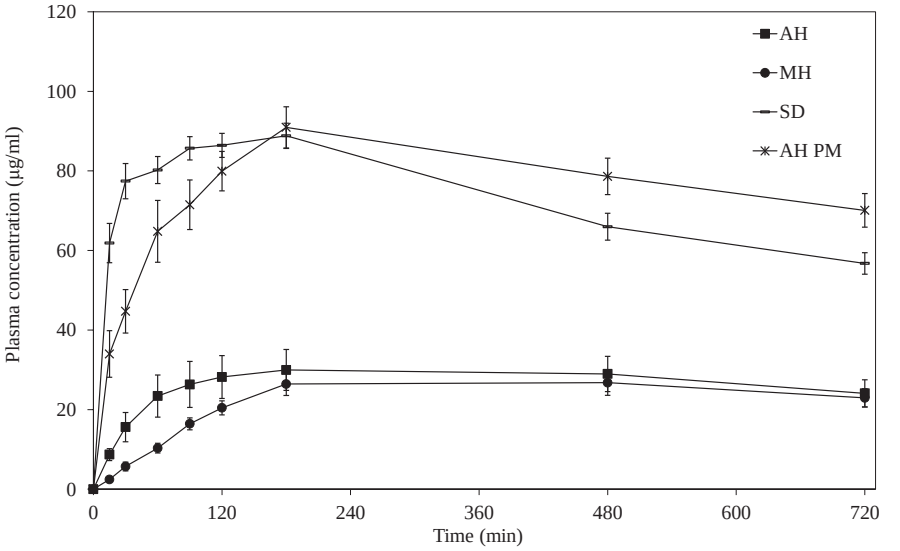

Figure 26. Plasma concentration profiles of different solid-state forms of piroxicam (PRX) after oral administration to rats (n = 6). Data are exhibited as mean (n=6)±S.E.

The PRX plasma levels were much higher after an oral administration of SD and PM AH compared to those obtained after oral administration of AH and MH to rats. After oral administration of SD, absorption was the fastest being also significantly faster than that observed after oral administration of PM AH. Furthermore, the rate and extent of absorption of drug was found to be significantly higher after oral administration of PM AH compared to that observed after oral administration of AH and MH. Also the rate of absorption of drug was found to be significantly higher after oral administration of AH compared to that observed after oral administration of MH. Several studies have investigated the effect of amorphous SD and presence of excipients on drug dissolution and presented clear advantages of amorphous SD *in vitro* (Sathigari et al., 2012; Tho et al., 2010), not so many have shown its relevance in the *in vivo* performance of a drug.

As seen in Table 2, significant differences were found in the key pharmacokinetic parameters obtained after oral administration of different PRX solid-state forms to rats. The time to reach the maximum concentration t_{max} of drug ranged from 125 ± 18 minutes (SD) to 330 ± 67 minutes (MH). The mean time of t_{max} was clearly the shortest after oral administration of SD, and the difference to the other PRX forms was statistically significant. PM showed the second shortest t_{max} mean value. The lowest rate and extent of absorption (t_{max} and C_{max} mean values) were found when AH and MH were administered by oral route to rats. Differences in the t_{max} and C_{max} mean values, however, were not

statistically significant after oral administration of AH and MH to rats. Differences in the t_{max} mean values after oral administration of MH and PM (and SD) to rats were found to be statistically significant. Bioavailability of PRX after oral administration to rats has been previously studied by Gwak et al., 2005 (Gwak et al., 2005). In their study, the plasma PRX levels after oral administration of AH to rats were clearly lower being approximately half of those plasma levels obtained in our study. The difference can be explained by different dosing of PRX.

Table 2. Pharmacokinetic parameters of piroxicam anhydrate I (AH), piroxicam monohydrate (MH), solid dispersion of AH and Soluplus® 1:4 (SD) and physical mixture of AH and Soluplus® 1:4 (PM AH). Data are expressed as mean (n=6) ± S.E.

	AH	MH	SD	PM AH
t_{max} (min)	265±69	330±67	125±18	180±0
C_{max} (μg/ml)	31.9±5.0	29.1±2.8	90.1±2.9	90.9±5.2
AUC_{0-12} (μg h/ml)	322.5±51.3	277.1±27.2	869.1±24.6	920.1±58.9
$t_{1/2}$ (h)	17.0±3.8	17.7±2.5	16.6±2.9	21.2±2.8
Cl/F (l/h)	0.007±0.002	0.007±0.001	0.004±0.001	0.003±0.001
Vd/F (l)	0.155±0.034	0.165±0.024	0.088±0.004	0.086±0.006

As regards to AH and MH, differences between the plasma concentrations of drug were statistically significant up to 90 minutes indicating faster dissolution rate and absorption of AH compared to MH to rats. As shown in Figures 8, 9 and 10, SD exhibited the highest rate and extent of dissolution *in vitro*, and this was in good agreement with the present results of the pharmacokinetic study with rats.

Based on the present results, the ranking of PRX solid-state forms according to the rate of absorption (t_{max}) after oral administration to rats decreased in the order SD (amorphous PRX), PM AH, AH and MH. Interestingly, these results were somewhat contradictory to the dissolution test results with basket method that showed higher dissolution rate for AH than PM AH (Fig. 8). This discrepancy is probably due to the differences in the solubilizing properties of Soluplus® in the hydrochloric acid buffer (pH 1.2) and gastrointestinal fluids of rat. In addition, the authors believe that these differences might also be explained by an interaction between the polymer and gelatin capsule that occurred during dissolution testing with basket method.

As seen in Table 2, the half-life of PRX was similar in all four groups, and no statistically significant differences were found between the $t_{1/2}$ mean values of different PRX solid-state forms after oral administration to rats. The mean values for Vd/F and Cl/F in the MH and AH groups were almost two times higher than those in the PM AH and SD groups, and this difference between the groups was statistically significant. This kind of discrepancy in the values of

Vd/F and Cl/F is quite expected since the values of AUC0-12 of PRX in PM and SD groups were almost three times higher than in the AH and MH groups.

The highest mean values for plasma PRX concentration (C_{max}) and $AUC_{0–12}$ were achieved after oral administration of PM AH and SD (Table 2). The mean values for C_{max} in the MH and AH groups were almost three times lower than those in the PM AH and SD groups, and this difference was statistically significant. The mean values for $AUC_{0–12}$ were more than two times smaller after oral administration of AH and MH. Differences in the mean values for $AUC_{0–12}$ were statistically significant between these two groups (PM AH/SD and AH/MH) after oral administration to rats. However, there was statistically no difference in the C_{max} and $AUC_{0–12}$ mean values between PM AH and SD groups and between AH and MH groups.

As the highest extent of absorption (C_{max} and $AUC_{0–12}$) was found after oral administration of PM AH and SD to rats it can be suggested that amorphous PRX exhibits significantly improved oral bioavailability compared to its crystalline counterparts, and that Soluplus® can act as a stabilizer and precipitation inhibitor of amorphous PRX in SD. Similar results have been obtained by Linn et al. (Linn et al., 2012) who have studied bioavailability of danazol, itraconazole and fenofibrate on beagle dogs in solid solutions and physical mixtures with Soluplus®.

The presence of polymer in a PMs with PRX (PM AH) improved the dissolution and bioavailability in a lower extent compared to SD. These results indicate that the presence of amorphous PRX in SDs leads to increased dissolution. Although it was verified for SD that a rapid amorphous to MH solid-state transformation occurred in hydrochloric acid buffer (slurry test, publication I, Figure 11b), SD still provided the best bioavailability. It is likely that amorphous drug will dissolve rapidly and the solution becomes supersaturated with respect to crystalline MH without any crystallization (i.e., nucleation and crystal growth on the surface of amorphous drug). PRX as a BCS II drug has been reported to have a fast penetration (Ginski and Polli, 1999). This implies that dissolved PRX is absorbed before any crystallization from solution occurrs. In addition, absorption decreases the concentration (and the possible degree of supersaturation) in the gastrointestinal tract, which in turn will decrease the probability of crystallization. Consequently, and for the reasons mentioned above, it is expected that most of the drug remaining in the dissolving solid sample is in the amorphous form during *in vivo* dissolution and absorption, although the crystallization occurred within similar timescales during the slurry and *in vitro* dissolution experiments.

6. CONCLUSIONS

Present study enhanced the knowledge of water-mediated solid state transformations taking place during processing and dissolution of API. Also the effect of given changes on the performance of the API was revealed *in vitro* and *in vivo*.

1. Different solid state forms of a poorly water-soluble polymorphic drug piroxicam (PRX) were successfully prepared and it was possible to characterize the forms with Raman spectroscopy, ATR-FTIR spectroscopy, DSC and XRPD.

2. The solid-state forms can significantly influence the solubility and dissolution rate of PRX. The model drug exhibits a clear solid-state dependent dissolution. Amorphous PRX (in solid dispersion, SD) was shown to have an improved dissolution rate compared to its crystalline counterparts (PRX anhydrate form I, AH and monohydrate, MH). It was also discovered that different solid state forms have different stabilities in dissolution medium. MH and PRX in PM AH remained stable while AH and SD recrystallized as MH within 220 and 10 minutes, respectively.

3. Different solid-state forms can significantly influence the oral bioavailability of a poorly water-soluble polymorphic drug. The present model drug (PRX) exhibits a clear solid-state dependent oral absorption in rats. Amorphous PRX (in SD) was shown to have an improved oral bioavailability compared to its crystalline counterparts AH and MH). Soluplus® enhanced the oral bioavailability of PRX in rats showing the importance of formulation (polymeric excipient) on oral bioavailability of a poorly water-soluble drug.

4. The present SDs were physically stable in powder form under low humidity (~0% RH) and low to intermediate temperature (6 °C and 25 °C) conditions for at least six months. Aging at higher humidity (~40% and ~75% RH) and temperature (25 °C) caused amorphous PRX (in SDs) to crystallize as a AH or MH within one month and two to three months, respectively. In conclusion, high humidity storage conditions can greatly affect the solid-state properties (crystallization) and dissolution behavior of PRX formulated in SDs with Soluplus®.

5. Principal component analysis (PCA) and multivariate curve resolution alternating least squares (MCR-ALS) facilitated the qualitative and quantitative analysis of the Raman spectra obtained with the aged SD samples stored at different humidity and temperature conditions.

6. Water-mediated solid-state process-induced transformations (PITs) of amorphous PRX can occur during aqueous-based drug-layer coating of pellets, and solid-state change can be verified using Raman spectroscopy. AH and MH were stable during drug-layer coating, but amorphous PRX in solid dis-

persion (SD) crystallized as MH already after 10 minutes of coating. Raman spectroscopy also enabled to monitor the coating efficiency as the increase in absolute intensities of spectra matched with the weight gain. Coating efficiency was mainly dependent on a drug-layer coating time; the longer coating times resulted in improved coating uniformity. Drug-layer coated pellets of PRX exhibited improved dissolution rate compared to the powder forms of PRX.

7. REFERENCES

Aaltonen, J., M. Allesø, S. Mirza, V. Koradia, K. C. Gordon, and J. Rantanen, 2009, Solid form screening – a review.: Eur J Pharm Biopharm, v. 71, p. 23–37.

Aaltonen, J., P. Heinanen, L. Peltonen, H. Kortejarvi, V. P. Tanninen, L. Christiansen, J. Hirvonen, J. Yliruusi, and J. Rantanen, 2006, In situ measurement of solvent-mediated phase transformations during dissolution testing: J Pharm Sci, v. 95, p. 2730–7.

Aaltonen, J., K. Kogermann, C. J. Strachan, and J. Rantanen, 2007a, In-line monitoring of solid-state transitions during fluidisation: Chem Eng Sci, v. 62, p. 408–415.

Aaltonen, J., C. J. Strachan, K. Pöllänen, J. Yliruusi, and J. Rantanen, 2007b, Hyphenated spectroscopy as a polymorph screening tool.: J Pharm Biomed Anal, v. 44, p. 477–83.

Abdi, H., and L. J. Williams, 2010, Principal component analysis: Wiley Interdisciplinary Reviews: Computational Statistics, v. 2, p. 433–459.

Aguiar, A. J., J. Krc Jr., A. W. Kinkel, and J. C. Samyn, 1967, Effect of polymorphism on the absorption of chloramphenicol from chloramphenicol palmitate: Journal of Pharmaceutical Sciences, v. 56, p. 847–853.

Airaksinen, S., M. Karjalainen, N. Kivikero, S. Westermarck, A. Shevchenko, J. Rantanen, and J. Yliruusi, 2005, Excipient selection can significantly affect solid-state phase transfo: AAPS PharmSciTech, v. 6, p. E311–E322.

Allen, F. H., 2002, The Cambridge Structural Database: a quarter of a million crystal structures and rising.: Acta Crystallogr B, v. 58, p. 380–8.

Alonzo, D. E., G. G. Zhang, D. Zhou, Y. Gao, and L. S. Taylor, 2010, Understanding the behavior of amorphous pharmaceutical systems during dissolution.: Pharm Res, v. 27, p. 608–18.

Amidon, G. L., H. Lennernäs, V. P. Shah, and J. R. Crison, 1995, A theoretical basis for a biopharmaceutic drug classification: the correlation of in vitro drug product dissolution and in vivo bioavailability.: Pharm Res, v. 12, p. 413–20.

Azzouz, T., and R. Tauler, 2008, Application of multivariate curve resolution alternating least squares (MCR-ALS) to the quantitative analysis of pharmaceutical and agricultural samples: Talanta, v. 74, p. 1201–1210.

Banchero, M., L. Manna, S. Ronchetti, P. Campanelli, and A. Ferri, 2009, Supercritical solvent impregnation of piroxicam on PVP at various polymer molecular weights: J Supercrit Fluids, v. 49, p. 271–278.

Bauer, L. A., 2008, Applied Clinical Pharmacokinetics: United States of America, McGraw-Hill Companies, Inc.

Bernstein, J., 2007, Polymorphism in molecular crystals: Oxford, Oxford University Press, xiv, 410 p. p.

Bhugra, C., and M. J. Pikal, 2008, Role of thermodynamic, molecular, and kinetic factors in crystallization from the amorphous state: Journal of Pharmaceutical Sciences, v. 97, p. 1329–1349.

Billmeyer, F. V., ed., 1971, Plastics technology: Textbook of Polymer Science, 2nd ed: New York, John Wiley & Sons, 491–512 p.

Blasi, P., S. S. D`Souza, F. Selmin, and P. P. DeLuca, 2005, Plasticizing effect of water on poly(lactide-co-glycolide): Journal of Controlled Release, v. 108, p. 1–9.

Boldyreva, E. V., T. P. Shakhtshneider, H. Ahsbahs, H. Sowa, and H. Uchtmann, 2002, Effect of High Pressure on the Polymorphs of Paracetamol: Journal of Thermal Analysis and Calorimetry, v. 68, p. 437–452.

Bordner, J., J. A. Richards, P. Weeks, and E. B. Whipple, 1984, Piroxicam monohydrate: a zwitterionic form, $C_{15}H_{13}N_3O_4S*H_2O$: Acta Crystallogr, v. C40, p. 989–990.

Brouwers, J., M. E. Brewster, and P. Augustijns, 2009, Supersaturating drug delivery systems: the answer to solubility-limited oral bioavailability?: J Pharm Sci, v. 98, p. 2549–72.

Buckley, S. T., K. J. Frank, G. Fricker, and M. Brandl, 2013, Biopharmaceutical classification of poorly soluble drugs with respect to "enabling formulations": Eur J Pharm Sci, v. 50, p. 8–16.

Bugay, D. E., 2001, Characterization of the solid-state: spectroscopic techniques: Advanced Drug Delivery Reviews, v. 48, p. 43–65.

Burger, A., and R. Ramberger, 1979, On the polymorphism of pharmaceuticals and other molecular crystals. I: Microchimica Acta, v. 72, p. 259–271.

Byrn, S., R. Pfeiffer, M. Ganey, C. Hoiberg, and G. Poochikian, 1995, Pharmaceutical Solids: A Strategic Approach to Regulatory Considerations: Pharmaceutical Research, v. 12, p. 945–954.

Chadha, R., and S. Bhandari, 2014, Drug-excipient compatibility screening – role of thermoanalytical and spectroscopic techniques: J Pharm Biomed Anal, v. 87, p. 82–97.

Chemburkar, S. R., J. Bauer, K. Deming, H. Spiwek, K. Patel, J. Morris, R. Henry, S. Spanton, W. Dziki, W. Porter, J. Quick, P. Bauer, J. Donaubauer, B. A. Narayanan, M. Soldani, D. Riley, and K. McFarland, 2000, Dealing with the Impact of Ritonavir Polymorphs on the Late Stages of Bulk Drug Process Development: Organic Process Research & Development, v. 4, p. 413–417.

Chieng, N., T. Rades, and J. Aaltonen, 2011, An overview of recent studies on the analysis of pharmaceutical polymorphs: Journal of Pharmaceutical and Biomedical Analysis, v. 55, p. 618–644.

Christensen, N. P. A., B. V. Eerdenburgh, K. Kwok, L. S. Taylor, A. D. Bond, T. Rhades, J. Rantanen, and C. Cornett, 2013, Rapid Insight into Heating-Induced Phase Transformations in the Solid State of the Calcium Salt of Atorvastatin Using Multivariate Data Analysis: Pharm Res, v. 30, p. 826–835.

Craig, D. Q. M., P. G. Royall, V. L. Kett, and M. L. Hopton, 1999, The relevance of the amorphous state to pharmaceutical dosage forms: glassy drugs and freeze dried systems: International Journal of Pharmaceutics, v. 179, p. 179–207.

Danesh, A., S. D. Connell, M. C. Davies, C. J. Roberts, S. J. Tendler, P. M. Williams, and M. J. Wilkins, 2001, An in situ dissolution study of aspirin crystal planes (100) and (001) by atomic force microscopy: Pharm Res, v. 18, p. 299–303.

Datta, S., and D. J. W. Grant, 2004, Crystal structures of drugs: advances in determination, prediction and engineering: Nature Reviews Drug Discovery, v. 3, p. 42–57.

De Beer, T. R., M. Alleso, F. Goethals, A. Coppens, Y. V. Heyden, H. L. De Diego, J. Rantanen, F. Verpoort, C. Vervaet, J. P. Remon, and W. R. Baeyens, 2007, Implementation of a process analytical technology system in a freeze-drying process using Raman spectroscopy for in-line process monitoring: Anal Chem, v. 79, p. 7992–8003.

De Beer, T. R., M. Wiggenhorn, R. Veillon, C. Debacq, Y. Mayeresse, B. Moreau, A. Burggraeve, T. Quinten, W. Friess, G. Winter, C. Vervaet, J. P. Remon, and W. R. Baeyens, 2009, Importance of using complementary process analyzers for the process monitoring, analysis, and understanding of freeze drying: Anal Chem, v. 81, p. 7639–49.

de Juan, A., and R. Tauler, 2006, Multivariate Curve Resolution (MCR) from 2000: Progress in Concepts and Applications: Critical Reviews in Analytical Chemistry, v. 36, p. 163–176.

Djuris, J., I. Nikolakakis, S. Ibric, Z. Djuric, and K. Kachrimanis, 2013, Preparation of carbamazepine-Soluplus solid dispersions by hot-melt extrusion, and prediction of drug-polymer miscibility by thermodynamic model fitting: Eur J Pharm Biopharm, v. 84, p. 228–37.

Drebushchak, V. A., T. P. Shakhtshneider, S. A. Apenina, A. S. Medvedeva, L. P. Safronova, and V. V. Boldyrev, 2006, Thermoanalytical investigation of drug-excipient interaction. Part II. Activated mixtures of piroxicam with cellulose and chitosan: J Therm Anal Calorim, v. 86, p. 303–309.

Dukić-Ott, A., T. De Beer, J. P. Remon, W. Baeyens, P. Foreman, and C. Vervaet, 2008, In-vitro and in-vivo evaluation of enteric-coated starch-based pellets prepared via extrusion/spheronisation: Eur J Pharm Biopharm, v. 70, p. 302–312.

Ensslin, S., K. P. Moll, H. Metz, M. Otz, and K. Mäder, 2009, Modulating pH-independent release from coated pellets: effect of coating composition on solubilization processes and drug release: Eur J Pharm Biopharm, v. 72, p. 111–118.

Garrido, M., I. Lazaro, M. S. Larrechi, and F. X. Rius, 2004, Multivariate resolution of rank-deficient near-infrared spectroscopy data from the reaction of curing epoxy resins using the rank augmentation strategy and multivariate curve resolution alternating least squares approach: Analytica Chimica Acta, v. 515, p. 65–73.

Garrido, M., F. X. Rius, and M. S. Larrechi, 2008, Multivariate curve resolution–alternating least squares (MCR-ALS) applied to spectroscopic data from monitoring chemical reactions processes - Springer: Analytical and Bioanalytical Chemistry, v. 390, p. 2059–2066.

Gillon, A. L., N. Feeder, R. J. Davey, and R. Storey, 2003, Hydration in Molecular CrystalsA Cambridge Structural Database Analysis: Crystal growth & Design, v. 3, p. 663–673.

Ginski, M. J., and J. E. Polli, 1999, Prediction of dissolution-absorption relationships from a dissolution/Caco-2 system: Int J Pharm, v. 177, p. 117–25.

Greco, K., and R. Bogner, 2011, Solution-mediated phase transformation: Significance during dissolution and implications for bioavailability.: J Pharm Sci.

Gupta, P., V. K. Kakumanu, and A. K. Bansal, 2004, Stability and Solubility of Celecoxib–PVP Amorphous Dispersions: A Molecular Perspective: Pharm Res, v. 21, p. 1762–1769.

Gwak, H. S., J. S. Choi, and H. K. Choi, 2005, Enhanced bioavailability of piroxicam via salt formation with ethanolamines.: Int J Pharm, v. 297, p. 156–61.

Haddish-Berhane, N., S. H. Jeong, K. Haghighi, and K. Park, 2006, Modeling film-coat non-uniformity in polymer coated pellets: A stochastic approach: Int J Pharm, v. 323, p. 64–71.

Han, J., and R. Suryanarayanan, 1998, Influence of environmental conditions on the kinetics and mechanism of dehydration of carbamazepine dihydrate: Pharm Dev Technol, v. 3, p. 587–96.

Hancock, B. C., and M. Parks, 2000, What is the True Solubility Advantage for Amorphous Pharmaceuticals?: Pharmaceutical Research, v. 17, p. 397–404.
Hancock, B. c., and G. Zografi, 1994, The Relationship Between the Glass Transition Temperature and the Water Content of Amorphous Pharmaceutical Solids – Springer: Pharmaceutical Research, v. 11, p. 471–477.
Hancock, B. C., and G. Zografi, 1997, Characteristics and significance of the amorphous state in pharmaceutical systems.: J Pharm Sci, v. 86, p. 1–12.
Haque, M. K., and Y. H. Roos, 2008, Water Plasticization and Crystallization of Lactose in Spray-dried Lactose/Protein Mixtures: Journal of Food Science, v. 69, p. FEP23–FEP29.
Heinicke, G., and J. B. Schwartz, 2004, Particle size distributions of inert spheres and pelletized pharmaceutical products by image analysis: Pharm. Dev. Technol. , v. 9, p. 359–367.
Heljo, V. P., A. Nordberg, M. Tenho, T. Virtanen, K. Jouppila, J. Salonen, S. L. Maunu, and A. M. Juppo, 2012, The Effect of Water Plasticization on the Molecular Mobility and Crystallization Tendency of Amorphous Disaccharides: Pharm Res, v. 29, p. 2684–2697.
Hickey, A. J., H. M. Mansour, M. J. Telko, Z. Xu, H. D. Smyth, T. Mulder, R. McLean, J. Langridge, and D. Papadopoulos, 2007, Physical characterization of component particles included in dry powder inhalers. I. Strategy review and static characteristics: J Pharm Sci, v. 96, p. 1282–301.
Hilden, L. R., and K. R. Morris, 2004, Physics of amorphous solids: Journal of Pharmaceutical Sciences, v. 93, p. 3–12.
Huang, L. F., and W. Q. Tong, 2004, Impact of solid state properties on developability assessment of drug candidates.: Adv Drug Deliv Rev, v. 56, p. 321–34.
Hughey, J. R., J. M. Keen, D. A. Miller, K. Kolter, N. Langley, and J. W. McGinity, 2013, The use of inorganic salts to improve the dissolution characteristics of tablets containing Soluplus®-based solid dispersions: European Journal of Pharmaceutical Sciences, v. 48, p. 758–766.
Hurst, S., C. M. Loi, J. Brodfuehrer, and A. El-Kattan, 2007, Impact of physiological, physicochemical and biopharmaceutical factors in absorption and metabolism mechanisms on the drug oral bioavailability of rats and humans.: Expert Opin Drug Metab Toxicol, v. 3, p. 469–89.
Janssens, S., and G. Van den Mooter, 2009, Review: physical chemistry of solid dispersions.: J Pharm Pharmacol, v. 61, p. 1571–86.
Jinno, J., D. Oh, J. R. Crison, and G. L. Amidon, 2000, Dissolution of ionizable water-insoluble drugs: the combined effect of pH and surfactant.: J Pharm Sci, v. 89, p. 268–74.
Jørgensen, A., J. Rantanen, M. Karjalainen, L. Khriachtchev, E. Räsänen, and J. Yliruusi, 2002, Hydrate Formation During Wet Granulation Studied by Spectroscopic Meth: Pharmaceutical Research, v. 19, p. 1285–1291.
Kawabata, Y., K. Wada, M. Nakatani, S. Yamada, and S. Onoue, 2011, Formulation design for poorly water-soluble drugs based on biopharmaceutics classification system: basic approaches and practical applications: Int J Pharm, v. 420, p. 1–10.
Khougaz, K., and S. D. Clas, 2000, Crystallization inhibition in solid dispersions of MK-0591 and poly(vinylpyrrolidone) polymers.: J Pharm Sci, v. 89, p. 1325–34.
Kogermann, K., J. Aaltonen, C. J. Strachan, K. Pöllänen, J. Heinämäki, J. Yliruusi, and J. Rantanen, 2008, Establishing quantitative in-line analysis of multiple solid-state transformations during dehydration.: J Pharm Sci, v. 97, p. 4983–99.

Kogermann, K., J. Aaltonen, C. J. Strachan, K. Pöllänen, P. Veski, J. Heinämäki, J. Yliruusi, and J. Rantanen, 2007a, Qualitative in situ analysis of multiple solid-state forms using spectroscopy and partial least squares discriminant modeling.: J Pharm Sci, v. 96, p. 1802–20.

Kogermann, K., A. Penkina, K. Predpannikova, K. Jeeger, P. Veski, J. Rantanen, and K. Naelapää, 2013, Dissolution testing of amorphous solid dispersions: International Journal of Pharmaceutics, v. 444, p. 40–46.

Kogermann, K., P. Veski, J. Rantanen, and K. Naelapää, 2011, X-ray powder diffractometry in combination with principal component analysis – a tool for monitoring solid state changes.: Eur J Pharm Sci, v. 43, p. 278–89.

Kogermann, K., J. A. Zeitler, J. Rantanen, T. Rades, P. F. Taday, M. Pepper, J. Heinämäki, and C. J. Strachan, 2007b, Investigating dehydration from compacts using terahertz pulsed, Raman and near-infrared spectroscopy: Appl Spectrosc, v. 61, p. 1265–1274.

Kojic-Prodic, B., and Z. Ruzic-Toros, 1982, Structure of piroxicam: Acta Crystallogr, v. B38, p. 2948.

Lai, F., E. Pini, G. Angioni, M. L. Manca, J. Perricci, C. Sinico, and A. M. Fadda, 2011, Nanocrystals as tool to improve piroxicam dissolution rate in novel orally disintegrating tablets: Eur. J. Pharm. Biopharm., v. 79, p. 552–558.

Lai, M. c., M. j. Hagerman, S. R. L., R. T. Borchardt, B. B. Laird, and E. M. Topp, 1999, Chemical stability of peptides in polymers. 2. Discriminating between solvent and plasticizing effects of water on peptide deamidation in poly(vinylpyrrolidone): Journal of Pharmaceutical Sciences, v. 88, p. 1081–1089.

Lee, M.-J., D.-Y. Seo, H.-E. Lee, I.-C. Wang, W.-S. Kim, M.-Y. Jeong, and G.-J. Choi, 2011, In line NIR quantification of film thickness on pharmaceutical pellets during a fluid bed coating process Int J Pharm, v. 403, p. 66–72.

Lehto, P., J. Aaltonen, M. Tenho, J. Rantanen, J. Hirvonen, V. P. Tanninen, and L. Peltonen, 2009, Solvent-mediated solid phase transformations of carbamazepine: Effects of simulated intestinal fluid and fasted state simulated intestinal fluid: J Pharm Sci, v. 98, p. 985–96.

Leuner, C., and J. Dressman, 2000, Improving drug solubility for oral delivery using solid dispersions: Eur J Pharm Biopharm, v. 50, p. 47–60.

Lim, H., and S. W. Hoag, 2013, Plasticizer Effects on Physical–Mechanical Properties of Solvent Cast Soluplus® Films – Springer: AAPS PharmSciTech, v. 14, p. 903–910.

Lin, S.-Y., 2015, Molecular perspectives on solid-state phase transformation and chemical reactivity of drugs: metoclopramide as an example: Drug Discovery Today, v. 20, p. 209–222.

Linn, M., E. M. Collnot, D. Djuric, K. Hempel, E. Fabian, K. Kolter, and C. M. Lehr, 2012, Soluplus® as an effective absorption enhancer of poorly soluble drugs in vitro and in vivo.: Eur J Pharm Sci, v. 45, p. 336–43.

Llinàs, A., and J. M. Goodman, 2008, Polymorph control: past, present and future: Drug Discovery Today, v. 13, p. 198–210.

Lohani, S., and D. J. W. Grant, 2006, Thermodynamics of Polymorphs, *in* R. Hilfiker, ed., Polymorphism in the Pharmaceutical Industry: Germany, Wiley-VCH Verlag GmbH & Co, p. 21–42.

Lu, J., and S. Rohani, 2009, Polymorphism and Crystallization of Active Pharmaceutical Ingredients (APIs): Current Medicinal Chemistry, v. 16, p. 884–905.

Marsac, P. J., S. L. Shamblin, and L. S. Taylor, 2006, Theoretical and practical approaches for prediction of drug-polymer miscibility and solubility: Pharm Res, v. 23, p. 2417–26.

McPhillips, H., D. Q. M. Craig, P. G. Royall, and V. L. Hill, 1999, Characterisation of the glass transition of HPMC using modulated temperature differential scanning calorimetry Int J Pharm, v. 180, p. 83–90.

Morris, K. R., U. J. Griesser, C. J. Eckhardt, and J. G. Stowell, 2001, Theoretical approaches to physical transformations of active pharmaceutical ingredients during manufacturing processes: Adv Drug Deliv Rev, v. 48, p. 91–114.

Murdande, S. B., M. J. Pikal, R. M. Shanker, and R. H. Bogner, 2011, Solubility advantage of amorphous pharmaceuticals, part 3: Is maximum solubility advantage experimentally attainable and sustainable?: J Pharm Sci.

Möschwitzer, J., and R. H. Müller, 2006, Spray coated pellets as carrier system for muco-adhesive drug nanocrystals: Eur. J. Pharm. Biopharm., v. 62, p. 282–287.

Naelapää, K., J. P. Boetker, P. Veski, J. Rantanen, T. Rades, and K. Kogermann, 2012, Polymorphic form of piroxicam influences the performance of amorphous material prepared by ball-milling.: Int J Pharm, v. 429, p. 69–77.

Nagy, Z. K., A. Balogh, B. Vajna, A. Farkas, G. Patyi, A. Kramarics, and G. Marosi, 2012, Comparison of electrospun and extruded Soluplus(R)-based solid dosage forms of improved dissolution: J Pharm Sci, v. 101, p. 322–32.

Newman, A., D. Engers, S. Bates, I. Ivanisevic, R. C. Kelly, and G. Zografi, 2008, Characterization of amorphous API:Polymer mixtures using X-ray powder diffraction: J Pharm Sci, v. 97, p. 4840–56.

Newman, A. W., and S. R. Byrn, 2003, Solid-state analysis of the active pharmaceutical ingredient in drug products.: Drug Discov Today, v. 8, p. 898–905.

Nikowitz, K., K. Pintye-Hódi, and G. J. Reqdon, 2013, Study of the recrystallization in coated pellets – Effect of coating on API crystallinity: Eur J Pharm Sci, v. 48, p. 563–571.

Paaver, U., A. Lust, S. Mirza, J. Rantanen, P. Veski, J. Heinämäki, and K. Kogermann, 2012, Insight into the solubility and dissolution behavior of piroxicam anhydrate and monohydrate forms.: Int J Pharm.

Petit, S., and G. Coquerel, 1996, Mechanism of Several Solid−Solid Transformations between Dihydrated and Anhydrous Copper(II) 8-Hydroxyquinolinates. Proposition for a Unified Model for the Dehydration of Molecular Crystals: Chem. Mater., v. 9, p. 2247–2258.

Rahman, N. u., K. H. Yuen, N. A. Khan, and J. W. Wong, 2006, Drug-Polymer Mixed Coating: A New Approach for Controlling Drug Release Rates in Pellets: Pharmaceutical Development and Technology, v. 11, p. 71–77.

Rasenack, N., and B. W. Muller, 2002, Crystal habit and tableting behavior: Int J Pharm, v. 244, p. 45–57.

Reck, G., G. Dietz, G. Laban, W. Günther, G. Bannier, and E. Höhne, 1988, X-ray studies on piroxicam modifications: Pharmazie, v. 43, p. 477–481.

Reck, G., and G. Laban, 1990, Prediction and establishment of a new crystalline piroxicam modification: Pharmazie, v. 45, p. 257–259.

Rodriguez-Hornedo, N., and D. Murphy, 1999, Significance of controlling crystallization mechanisms and kinetics in pharmaceutical systems: Journal of Pharmaceutical Sciences, v. 88, p. 651–660.

Rodríguez-Sponga, B., C. P Priceb, A. Jayasankara, A. J. Matzgerb, and N. r. Rodríguez-Hornedo, 2004, General principles of pharmaceutical solid polymorphism: A supramolecular perspective: Advanced Drug Delivery Reviews, v. 56, p. 241–274.

Romero-Torres, S., H. Wikstrom, E. R. Grant, and L. S. Taylor, 2007, Monitoring of mannitol phase behavior during freeze-drying using non-invasive Raman spectroscopy: PDA J Pharm Sci Technol, v. 61, p. 131–45.

Ruckebusch, C., and L. Blanchet, 2013, Multivariate curve resolution: A review of advanced and tailored applications and challenges: Analytica Chimica Acta, v. 765, p. 28–36.

Rustichelli, C., G. Gamberini, V. Ferioli, M. C. Gamberini, R. Ficarra, and S. Tommasini, 2000, Solid-state study of polymorphic drugs: carbamazepine: J Pharm Biomed Anal, v. 23, p. 41–54.

Sathigari, S. K., V. K. Radhakrishnan, V. A. Davis, D. L. Parsons, and R. J. Babu, 2012, Amorphous-state characterization of efavirenz-polymer hot-melt extrusion systems for dissolution enhancement: J Pharm Sci.

Savolainen, M., K. Kogermann, A. Heinz, J. Aaltonen, L. Peltonen, C. Strachan, and J. Yliruusi, 2009, Better understanding of dissolution behaviour of amorphous drugs by in situ solid-state analysis using Raman spectroscopy.: Eur J Pharm Biopharm, v. 71, p. 71–9.

Sekiguchi, K., and N. Obi, 1961, Studies on Absorption of Eutectic Mixture. I. A Comparison of the Behavior of Eutectic Mixture of Sulfathiazole and that of Ordinary Sulfathiazole in Man: Chemical & Pharmaceutical Bulletin, v. 9, p. 866–872.

Shakhtshneider, T. P., F. Danéde, F. Capet, J. F. Willart, M. Descamps, S. A. Myz, E. V. Boldyreva, and V. V. Boldyrev, 2007, Grinding of drugs with pharmaceutical excipients at cryogenic temperatures. Part I. Cryogenic grinding of piroxicam–polyvinylpyrrolidone mixtures: J Therm Anal Cal, v. 89, p. 699–707.

Shamma, R. N., and M. Basha, 2013, Soluplus®: A novel polymeric solubilizer for optimization of Carvedilol solid dispersions: Formulation design and effect of method of preparation: Powder Technology, v. 237, p. 406–414.

Sheth, A. R., S. Bates, F. X. Muller, and D. J. W. Grant, 2004a, Local Structure in Amorphous Phases of Piroxicam from Powder X-ray Diffractometry: Cryst Growth Des, v. 5, p. 571–578.

Sheth, A. R., S. Bates, F. X. Muller, and D. J. W. Grant, 2004b, Polymorphism in piroxicam: Crystal Growth Design, v. 4, p. 1091–1098.

Sheth, A. R., and D. J. W. Grant, 2005, Relationship between the Structure and Properties of Pharmaceutical Crystals: KONA Powder and Particle Journal, v. 23, p. 36–48.

Sheth, A. R., D. Zhou, F. X. Muller, and D. J. Grant, 2004c, Dehydration kinetics of piroxicam monohydrate and relationship to lattice energy and structure.: J Pharm Sci, v. 93, p. 3013–26.

Sinchaipanid, N., P. Chitropas, and A. Mitrevej, 2004, Influences of layering on theophylline pellet characteristics: Pharm. Dev. Technol., v. 9, p. 163–170.

Singhal, D., and W. Curatolo, 2004, Drug polymorphism and dosage form design: a practical perspective.: Adv Drug Deliv Rev, v. 56, p. 335–47.

Stephenson, G. A., R. A. Forbes, and S. M. Reutzel-Edens, 2001, Characterization of the solid state: quantitative issues: Adv Drug Deliv Rev, v. 48, p. 67–90.

Taddei, P., A. Torreggiani, and R. Simoni, 2001, Influence of environment on piroxicam polymorphism: vibrational spectroscopic study: Biopolymers (Biospectroscopy), v. 62, p. 68–78.

Tantishaiyakul, V., N. Kaewnopparat, and S. Ingkatawornwong, 1999, Properties of solid dispersions of piroxicam in polyvinylpyrrolidone.: Int J Pharm, v. 181, p. 143–51.

Tauler, R., 1995, Multivariate curve resolution applied to second order data: Chemometrics and Intelligent Laboratory Systems, v. 30, p. 133–146.

Thakral, N. K., A. R. Ray, D. Bar-Shalom, A. H. Eriksson, and D. K. Majumdar, 2011, Soluplus-Solubilized Citrated Camptothecin-A Potential Drug Delivery Strategy in Colon Cancer.: AAPS PharmSciTech.

Tho, I., B. Liepold, J. Rosenberg, M. Maegerlein, M. Brandl, and G. Fricker, 2010, Formation of nano/micro-dispersions with improved dissolution properties upon dispersion of ritonavir melt extrudate in aqueous media: Eur J Pharm Sci, v. 40, p. 25–32.

Tian, B., L. Zhang, Z. Pan, J. Gou, Y. Zhang, and X. Tang, 2014, A comparison of the effect of temperature and moisture on the solid dispersions: Aging and crystallization: Int J Pharm, v. 475, p. 385–92.

Tian, L., Y. Zhang, and X. Tang, 2008, Sustained-release pellets prepared by combination of wax matrices and double-layer coatings for extremely water-soluble drugs matrices and double-layer coating pellets: Drug Dev. Ind. Pharm., v. 34, p. 569–576.

Tishmack, P. A., D. E. Bugay, and S. R. Byrn, 2003, Solid-state nuclear magnetic resonance spectroscopy – pharmaceutical applications: J Pharm Sci, v. 92, p. 441–74.

Tsinman, K., A. Avdeef, O. Tsinman, and D. Voloboy, 2009, Powder dissolution method for estimating rotating disk intrinsic dissolution rates of low solubility drugs.: Pharm Res, v. 26, p. 2093–100.

Vasconcelos, T., B. Sarmento, and P. Costa, 2007, Solid dispersions as strategy to improve oral bioavailability of poor water soluble drugs.: Drug Discov Today, v. 12, p. 1068–75.

Vippagunta, S. R., H. G. Brittain, and D. J. W. Grant, 2001, Crystalline solids: Advanced Drug Delivery Reviews, v. 48, p. 3–26.

Vishweshwar, P., J. A. McMahon, J. A. Bis, and M. J. Zaworotko, 2006, Pharmaceutical co-crystals: J Pharm Sci, v. 95, p. 499–516.

Vrečer, F., M. Vrbinc, and A. Meden, 2003, Characterization of piroxicam crystal modifications: Int J Pharm, v. 256, p. 3–15.

Wen, H., K. R. Morris, and K. Park, 2008, Synergic effects of polymeric additives on dissolution and crystallization of acetaminophen.: Pharm Res, v. 25, p. 349–58.

Weuts, I., D. Kempen, A. Decorte, G. Verreck, J. Peeters, M. Brewster, and G. Van den Mooter, 2005, Physical stability of the amorphous state of loperamide and two fragment molecules in solid dispersions with the polymers PVP-K30 and PVP-VA64: Eur J Pharm Sci, v. 25, p. 313–20.

Wirges, M., A. Funke, P. Serno, K. K., and P. Kleinebudde, 2013, Monitoring of an active coating process for two-layer tablets-model development strategies: J Pharm Sci, v. 102, p. 556–564.

Wise, B. M., N. B. Gallagher, S. W. Butler, D. D. White Jr, and G. G. Barna, 1999, A comparison of principal component analysis, multiway principal component analysis, trilinear decomposition and parallel factor analysis for fault detection in a semiconductor etch process: Journal of Chemometrics, v. 13, p. 379–396.

Wu, C., and J. McGinity, 2001, Influence of ibuprofen as a solid-state plasticizer in Eudragit® RS 30 D on the physicochemical properties of coated beads: AAPS PharmSciTech, v. 2, p. 1–9.

Yamashita, K., T. Nakate, K. Okimoto, A. Ohike, Y. Tokunaga, R. Ibuki, K. Higaki, and T. Kimura, 2003, Establishment of new preparation method for solid dispersion formulation of tacrolimus: Int J Pharm, v. 267, p. 79–91.

Yu, L., 2001, Amorphous pharmaceutical solids: preparation, characterization and stabilization.: Adv Drug Deliv Rev, v. 48, p. 27–42.

Yu, L., S. M. Reutzel-Edens, and C. A. Mitchell, 2000, Crystallization and Polymorphism of Conformationally Flexible Molecules: Problems, Patterns, and Strategies: Organic Process Research & Development, v. 4, p. 396–402.

Yu, L. X., M. S. Furness, A. Raw, K. P. Outlaw, N. E. Nashed, E. Ramos, S. P. Miller, R. C. Adams, F. Fang, R. M. Patel, F. O. Holcombe, Jr., Y. Y. Chiu, and A. S. Hussain, 2003, Scientific considerations of pharmaceutical solid polymorphism in abbreviated new drug applications: Pharm Res, v. 20, p. 531–6.

Yu, L. X., R. A. Lionberger, A. S. Raw, R. D'Costa, H. Wu, and A. S. Hussain, 2004, Applications of process analytical technology to crystallization processes: Adv Drug Deliv Rev, v. 56, p. 349–69.

Zhang, G. G., D. Law, E. A. Schmitt, and Y. Qiu, 2004, Phase transformation considerations during process development and manufacture of solid oral dosage forms: Adv Drug Deliv Rev, v. 56, p. 371–90.

Zhao, Y., P. Inbar, H. P. Chokshi, A. W. Malick, and D. S. Choi, 2011, Prediction of the thermal phase diagram of amorphous solid dispersions by Flory-Huggins theory: J Pharm Sci, v. 100, p. 3196–207.

8. SUMMARY IN ESTONIAN

Vee mõjul toimuvad polümorfse raviaine tahke vormi muutused – nende mõju ravimpreparaadi toimele

Raviained võivad esined erinevate tahke aine vormidena (polümorfsed vormid, solvaatvorm, amorfne aine). Kristallilist ainet iseloomustab kindel korrapärane kolmedimensionaalne molekulide asetus struktuuris. Solvaatvormide puhul on lisaks raviaine molekulidele kristallstruktuuri kaasatud ka solvendi molekulid. Kui solvendi molekuliks on vesi, siis nimetatakse solvaatvormi hüdraadiks. Amorfsel ainel puudub kolmedimensionaalne kindel ja korrapärane molekulide asetus ja järjestatus struktuuris.

Erinevad tahke aine vormid võivad omada erinevaid füsikokeemilisi omadusi. Lahustuvus ja lahustumiskiirus on ühed olulisemad raviainete omadused, millest sõltub ravimpreparaadi biosaadavus ja toime organismis. Halb vesilahustuvus ning sellest lähtuv aeglane imendumine organismis on üheks suuremaks probleemiks ravimpreparaatide disainimisel, kuna järjest enam sünteesitakse vees vähe lahustuvaid uusi raviaineid. Püütakse leida erinevaid meetodeid, kuidas muuta raviaine omadusi ning parandada tema vesilahustuvust ning seeläbi tema dissolutsioonikiirust ja biosaadavust. Üheks selliseks meetodiks on kiiremini ja paremini lahustuva tahke aine vormi kasutamine.

Kui kasutada paremini lahustuvat tahke aine vormi, tuleb silmas pidada, et Burgeri reegli kohaselt on kõige paremat lahustumist omavad tahked vormid kõige ebastabiilsemad. On teada, et termodünaamiliselt on veevabas vormis olevad kristallilised raviained aktiivsemad kui hüdraatvormis ning suure tõenäosusega veevabad kristallvormid lahustuvad kiiremini kui hüdraadid. Amorfne raviaine omab kõige paremat näilist lahustuvust ja suuremat lahustumiskiirust, kuid olles väga ebastabiilne võib ta kergesti välja kristalliseeruda. Ka erinevused kristalliliste vormide (polümorfsete vormide, hüdraatvorm vs veevaba vorm) lahustuvustes ning lahustumiskiirususes võivad olla raviaine *in vivo* imendumise ning biosaadavuste erinevuste põhjusteks.

Niiskuse, temperatuuri ja mehaanilise survejõu mõjul toimuvad muutused farmatseutiliste protsesside ajal või ka säilitamisel erinevates tingimustes võivad indutseerida tahkes raviaines üleminekuid ühest vormist teise. Raviaine tahkes vormis toimuvate muutuste (näiteks hüdraadi tekkimine või amorfse vormi välja kristalliseerumine) tagajärjel võib oluliselt muutuda raviaine lahustumine ning biosaadavus organismis. Lisaks sellele võivad paljud abiained, mida kasutatakse ravimpreparaatide tootmisel, muuta tahke raviaine käitumist ning omadusi. On leitud, et osad abiained võivad suurendada raviaine lahustumiskiirust, teised aga võivad muuta raviaine dehüdratatsiooni kiirust. Samuti on leitud, et polümeerid suudavad stabiliseerida amorfseid raviaineid hoides ära nende kristallisatsiooni. Raviainete ja abiaine(te) vahelised interaktsioonid sõltuvad nii raviaine kui ka abiaine omadustest. On vaja välja uurida faasimuutuste mehhanisme nii *in vitro* kui ka *in vivo* tingimustes. On oluline välja selgitada, kuidas

erinevad abiained mõjutavad ja muudavad raviaine käitumist ja kas on võimalik abiainetega inhibeerida raviainega toimuvaid muutusi. Et disainida sobiv, stabiilne ja toimiv ravimvorm, on vaja juba preformulatsiooni käigus põhjalikult uurida raviaine omadusi ja tema interaktsioone abiainetega.

Kuna amorfne raviaine lahustub kristallilistest vormidest sageli kiiremini ja annab üleküllastatud lahuse, siis on sellele pühendatud väga suur hulk farmatseutilist uurimistööd. Paraku on amorfse vormi suurimaks probleemiks tema ebastabiilsus. Ühe lahendusena sellele probleemile on pakutud amorfsete tahkete dispersioonide kasutamist. Amorfse tahke dispersiooni puhul on raviaine molekulaarsel tasemel dispergeeritud polümeerses kandjas. Enamasti on see polümeerne kandja amfifiilsete omadustega. Amorfsed tahked dispersioonid omavad puhta raviaine amorfse vormiga võrreldes suuremat stabiilsust. Sageli tekivad raviaine ja polümeeri molekulide vahel vesiniksidemed, mis vähendavad termodünaamilist potentsiaali ja seega ka amorfse aine tendentsi välja kristalliseeruda. Polümeerne abiaine toimib ka kineetilise barjäärina takistades raviaine molekulide lähenemist distantsini, kus saaks tekkida kahe raviaine molekuli vahel vesinikside. Seega takistab polümeer tahketes dispersioonides kristallisatsioonikeskmete teket ja nende kasvamist. Amfifiilsete omadustega polümeerid on farmaatsias eelistatud, kuna need suudavad stabiliseerida amorfsest tahkest dispersioonist tekkivat üleküllastunud lahust läbi solubilisatsiooni.

Antud uurimistöös kasutatakse raviainena piroksikaami, mis on vees vähelahustuv kuid gastrointestinaaltraktist kiiresti absorbeeruv aine. Piroksikaamil on leitud kolm polümorfset vormi, monohüdraatvorm ja teda on võimalik saada ka amorfse vormina. Polümorfsetest vormidest on tavatingimustes kõige stabiilsem I vorm (AH), vesikeskkonnas on kõige stabiilsemaks vormiks aga monohüdraat (MH). Amorfset piroksikaami on võimalik valmistada näiteks vitrifikatsioonil, kuid on teada, et see on väga ebastabiilne ja kristalliseerub AH-na välja. Samuti on vitrifikatsioonil amorfse vormi valmistamine piroksikaami puhul problemaatiline, kuna sellega kaasneb osaline degradatsioon.

Polüvinüülkaprolaktaam-polüvinüülatsetaat-polüetüleeneglükool graft kopolümeer (Soluplus®) on spetsiaalselt tahkete dispersioonide valmistamiseks mõeldud uudne abiaine. Antud uurimistöös kasutati seda stabiliseerimaks piroksikaami amorfses vormis. Soluplusi® iseloomustab amfifiilne olemus ja klaasistumistemperatuur 68 °C. Soluplus® on võimeline absorbeerima õhuniiskust. 40% suhtelise õhuniiskuse juures 4% ja 75% õhuniiskuse juures 12% massist. Farmatseutilises mõttes on oluline ka Soluplusi® hägustumistemperatuur, mis on 40 °C. Elektrolüütide lisamisel lahustesse võib see langeda ja põhjustada antud polümeeriga valmistatud ravimvormi disintegratsiooni aeglustumist.

Kuna nii säilitamise, kui ka lahustumise ja farmatseutiliste protsesside ajal võivad esineda tahke aine vormi muutused, siis on oluline raviaine tahket vormi nende protsesside ajal jälgida. Järjest enam on hakatud farmaatsias tahke aine muutuste jälgimiseks kasutama võnkespektroskoopilisi meetodeid. Antud meetodid on mitte-invasiinsed ja kiired ning võimaldavad saada infot raviaine

muutuste kohta juba molekulaarsel tasemel. Kuna antud analüütiliste meetoditega kogutud spektrite analüüsimine võib olla suure saadava andmemahu tõttu keeruline, kasutatakse neid laialdaselt kombinatsioonis mitmemõõtmeliste andmeanalüüsi meetoditega- kemomeetriliste meetoditega. Neist levinuim on peakomponent analüüs (PCA), mis võimaldab kergelt illustreerida ja analüüsida spektrites olevat olulist informatsiooni. PCA on matemaatiline toiming, kus muudetakse suures andmestikus esinevad omavahel korrelatsioonis olevad spektrite erisused väikese arvulisteks ja kergelt hoomatavateks peakomponentideks, mis pole omavahel korrelatsioonis. Iga mudeli poolt tekitatud peakomponent sisaldab endas ja kirjeldab spektrites esinevaid erinevusi. See muudab muutuste jälgimise suurte andmemahtude puhul märgatavalt lihtsamaks. Selleks, et kvantifitseerida tahke aine vormi muutuseid on võimalik kasutada näiteks mitmemõõtmelist kõverate lahutust. See meetod lahutab ainete segudest mõõdetud spektrid koostisosade spektriteks ja selle alusel arvutab välja segu komponentide kontsentratsioonid.

Antud uurimustöös keskenduti piroksikaami tahke aine vormide (veevaba piroksikaami I vorm (AH), piroksikaam monohüdraat (MH), piroksikaami ja Soluplusi® amorfne tahke dispersioon vahekorras 1 osa 4-le (SD)) muutuste uurimisele nii pikaajalise säilitamise, lahustumise ajal kui ka farmatseutilise protsessi ajal (pelletite katmise näitel). Samuti tehti kindlaks antud muutuste olulisus nii *in vitro* dissolutsioonitesti ajal kui *in vivo* loomkatsetes. Selleks, et teha kindlaks Soluplussi® enda toime raviaine käitumisele, kaasati uurimistöösse ka kristallilise piroksikaam AH ja Soluplussi® heterogeenne segu vahekorras 1 osa 4-le (PM AH). Uurimistöö tulemused annavad võimaluse aru saada raviaine tahke vormi muutustest ja selle olulisusest ravimpreparaadi kvaliteedile ja toimele organismis.

UURINGU EESMÄRGID

Käesoleva uurimistöö spetsiifilised eesmärgid olid järgmised:

- Valmistada ja tuvastada erinevad piroksikaami tahke aine vormid
- Teha kindlaks piroksikaami erinevate tahke aine vormide mõju raviaine *in vitro* lahustumiskiirusele ja teha kindlaks piroksikaami erinevate tahke aine vormide stabiilsus lahustumiskeskkonnas
- Teha kindlaks piroksikaami erinevate tahke aine vormide *in vivo* biosaadavus rottidel
- Teha kindlaks piroksikaami ja Soluplusi® tahke dispersiooni füüsikaline stabiilsus säilitamisel ja teha kindlaks võimaliku kristallisatsiooni mõju lahustumisele.
- Viia läbi antud tahke dispersiooni rekrisalliseerumise kvalitatiivne ja kvantitatiivne analüüs kasutades vastavalt peakomponent analüüsi ja mitmemõõtmelist kõverate lahutamist.
- Teha kindlaks piroksikaami tahke aine vormide stabiilsus pelletite katmisel antud tahke aine vormide suspensioonidega.

MATERJALID JA MEETODID

AH-d kasutati tootja (Letco Medical inc., USA) poolt saadud vormis ning MH saadi AH ümberkristalliseerimisel kuumast veest. SD valmistati lahusti aurustamise meetodil. Selleks lahustati AH ja Soluplus® atsetoonis ning saadud segu aurutati kuivaks 40 °C juures. PM AH valmistati AH ja Soluplusi® segamisel uhmris kasutades geomeetrilise lahjenduse põhimõtet.

Tahke aine vormid tehti kindlaks kasutades Raman spektroskoopiat, Fourier transformeerivat infrapuna spektroskoopiat (FTIR), pulberröntgendifraktomeetriat (XRPD) ja diferentsiaalset skaneerivat kalorimeetriat (DSC).

Pulbri vormis tahke ainete lahustumiskiirus ja tahke aine vormide vabanemine kapslitest tehti kindlaks dissolutsioontesti esimese ja teise meetodiga. Raviaine kontsentratsioon lahuses määrati UV spektrofotomeetriga. Uurimaks raviaine stabiilsust vabanemiskeskkonnas viidi läbi katse, kus raviaine tahke aine vormide stabiilsus kontsentreeritud suspensioonidena tehti kindlaks Raman spektroskoobi abil.

Lühiajaline säilitamiskatse (6 kuud) viidi läbi neljas erinevas keskonnas: ~0% RH / 6°C, ~0% RH / 25°C, ~40% RH / 25°C ja ~75% RH / 25°C. Proove analüüsiti kasutades Raman spektroskoopiat ja FTIR spektroskoopiat. Raman spektrite andmeanalüüs viidi läbi kasutades peakomponent analüüsi ja mitmemõõtmelist kõverate lahutamist.

Mikrokristallilisest tselluloosist pelletite katmine raviaine suspensioonidega (sisaldas 4% raviainet kristalliliste vormide puhul ja 2% SD puhul) viidi läbi miniatuurse katmismasinaga. Katmissuspensioonidele oli lisatud 5% (w/w) hüdroksüpropüülmetüültselluloosi. Pelletite pinnal oleva tahke aine vormi määramiseks katmise ajal kasutati Raman spektroskoopiat. Pelletite pinnaomaduste uurimine viidi läbi skaneeriva elektronmikroskoobiga (SEM).

Piroksikaami tahke aine vormide biosaadavuse uuring viidi läbi kasutades isaseid *Wistar* rotte. Igas katsegrupis oli 6 rotti. Piroksikaami tahke aine vormid manustati suspensioonina kasutades maosisest sondi. Vereplasma kontsentratsioonid tehti kindlaks kasutades kõrgefektiivset vedelikkromatograafiat.

UURINGU TULEMUSED JA ARUTELU

Piroksikaami tahke aine vormide tuvastamiseks kasutati XRPD, Raman spektroskoopiat, FT-IR spektroskoopiat ja DSC. XRPD abil mõõdetud AH ja PM AH difraktogrammid vastasid Cambridge struktuuride andmebaasi (CSD) alusel arvutatud teoreetilisele AH difraktogrammile ja MH difraktogramm vastas teoreetilisele MH difraktogrammile. Selle alusel võib järeldada, et meie poolt kasutatavad tahke aine vormid vastasid eeldatavatele vormidele. SD difraktogrammi alusel oli võimalik tuvastada piroksikaami amorfne vorm, kuna esines iseloomulik amorfne “halo”– puudusid iseloomulikud kristallilise aine peegeldused difraktogrammis. Lisaks oli võimalik tuvastada piroksikaami tahke aine vormid kasutades Raman spektroskoopiat ja FTIR spektroskoopiat. Mõlema

meetodi puhul ilmnesid spektrites muutused, mis vastasid kirjanduses varem kirjeldatudele. Infrapuna spektroskoopia võimaldas tuvastada ka vesiniksidemete tekkimise piroksikaami ja Soluplusi® vahel SD-s. Vesiniksidemete esinemine piroksikaami ja Soluplusi® molekuli vahel viitab sellele, et tekkis molekulaarsel tasemel dispersioon. Samuti lubab see eeldada amorfse faasi paranenud füüsikalist stabiilsust.

Kõige kiiremini vabanes dissolutsioonitestides kapslitest piroksikaami tahke aine vormidest SD. Raviaine vabanemiskiiruselt paremuselt teine tulemus oli võimalik saavutada AH-ga ja kõige aeglasem vabanemiskiirus saavutati, kui kasutati MH-d. PM AH puhul jäi vabanemise kiirus AH ja MH vahepeale. Selle alusel võib väita, et amorfne vorm võimaldas oluliselt kiirendada raviaine lahustumist. MH kõige aeglasem lahustumine oli eelduspärane, kuna on teada, et MH on vesikeskkonnas kõige stabiilsem vorm, mistõttu peaks tal olema kõige madalam lahustuvus ja kõige aeglasem lahustumine.

Piroksikaami tahke aine vormide füüsikalise stabiilsuse uurimiseks lahustumiskeskonnas viidi läbi vastavate suspensioonide uurimine kasutades Raman spektroskoopiat. Testi tulemusel tuvastati, et SD-st kristalliseerub piroksikaam MH välja 10 minuti jooksul. AH puhul toimub see protsess 220 minuti jooksul. AH rekristalliseerumist iseloomustab viite-aeg 80 minutit, mis kulub MH suhtes üleküllastatud lahuse tekkimisele. MH ja PM AH olid antud katse tingimustel stabiilsed kaheksa tunni jooksul. Seega Soluplus® ei ole võimeline stabiliseerima piroksikaami amorfset vormi väga üleküllastunud lahuse puhul, küll aga on ta võimeline stabiliseerima veevaba AH vastavatel tingimustel. Võimalik kristallisatsioon võib ka selgitada SD lahustumise teatavat aeglustumist dissolutsioonitestides.

In vivo biosaadavuse katse viidi läbi manustades rottidele (n=6) piroksikaami tahke aine vorme vesi-suspensioonina kasutades maosisest sondi. Kõige kiirem vereplasma maksimumkontsentratsioon saavutati SD puhul (125±18 minutit). Erinevalt *in vitro* dissolutsioonitestidest saavutas kiiruselt teise tulemuse PM AH (180±0 minutit). Vereplasma maksimumkontsentratsiooni saavutamise kiiruselt kõige aeglasema tulemuse andis MH (330±67 minutit). AH andis plasma maksimum kontsentratsiooni saavutamise kiiruse mõttes vahepealse tulemuse (265±69 minutit). Vereplasma maksimum kontsentratsioonilt olid SD ja PM AH peaaegu samaväärsed, samas, kui AH ja MH andsid umbes kolm korda madalama maksimum kontsentratsiooni. Samuti oli SD ja PM AH biosaadavus uuritava ajavahemiku jooksul ($AUC_{0–12}$) umbes kolm korda kõrgem, kui AH-l ja MH-l. Kuna piroksikaam on halvasti lahustuv kuid kiiresti absorbeeruv raviaine, siis on eelduspärane, et kõige kiiremini lahustuv ravimvorm annab ka kõige kiiremini vereplasmas maksimum kontsentratsiooni. Vereplasma maksimum kontsentratsiooni ja biosaadavuse kolmekordse erinevuse tõenäoliseks põhjuseks on SD ja PM AH ravimvormides olev Soluplus®. Kuna roti seedekulglas on vedeliku maht suhteliselt väike, siis arvatavasti Soluplussi ® solubiliseerivad omadused mõjutavad oluliselt biosaadavust organismis.

Uurimaks SD füüsikalist stabiilsust säilitati proove erinevate õhuniiskuse tingimustes kuni kuus kuud. Teatud kindlates ajapunktides koguti proovide Raman ja FTIR spektrid. Selleks, et viia läbi füüsikalise stabiilsuse katse andmete analüüs kasutati peakomponentanalüüsi ja mitmemõõtmelist kõverate lahutamist. Peakomponentanalüüs võimaldas läbi viia kvalitatiivse analüüsi ja mitmemõõtmeline kõverate lahutamine võimaldas läbi viia kvalitatiivse analüüsi. SD oli ~0% suhtelise õhuniiskuse juures stabiilne vähemalt kuus kuud. ~40% suhtelise õhuniiskuse juures oli võimalik tuvastada SD kristalliseerumine AH-na neli päeva peale katse algust. ~75% õhuniiskuse juures oli tuvastatav SD kristalliseerumine AH-na juba esimese päeva jooksul. Kuu aega peale katse algust oli tuvastatav SD kristalliseerumine MH-na. Kuna kõrgema õhuniiskuse juures absorbeeritud vesi võib käituda plastifikaatorina suurendades polümeeri ahelate liikumist, siis see võib vähendada Soluplussi® stabiliseerivaid omadusi, mistõttu toimus raviaine välja kristalliseerumine tahkest dispersioonist.

Uurimaks raviaine tahke vormi füüsikalist stabiilsust farmatseutilise tootmisprotsessi ajal viidi läbi katse, kus mikrokristallilisest tselluloosist pelleteid kaeti piroksikaami tahke aine vormide vesi-suspensioonidega. Tahke aine vormi füüsikalist stabiilsust uuriti kasutades Raman spektroskoopiat. Kui AH ja MH jäid katmisprotsessi ajal stabiilseks, siis SD kristalliseerus välja katmiseprotsessi esimese kümne minuti jooksul MH-na. AH võime säilitada oma veevaba kristallvorm vesikeskkonnas on selgitatav katte kuivamise piisava kiirusega, mistõttu ei jõudnud rekristallisatsioon toimuda. Samuti võis omada stabiliseerivat toimet katmissuspensioonis sisalduv hüdroksüpropüülmetüültselluloos. Kui AH ja MH-ga läbi viidud katmisprotsessi tulemusena saadi ühtlane kate, siis SD-ga kaetud pelletitest tehtud SEM piltidel oli näha pelletite pinnal suuri defekte. Tekkinud katte ebaühtlus on selgitatav Soluplussi® kohesiivsete omadustega, mistõttu ei omanud pelleti pinnal tekkiv kate piisavat plastilisust, et protsessi käigus tasanduda.

Kõige kiiremini vabanes raviainet AH-ga kaetud pelletitest. See oli isegi kiirem, kui amorfse piroksikaami vabanemine kapslitesse paigutatud SD-st. Selle tõenäoliseks põhjuseks oli see, et kate pelletite peal oli suhteliselt õhuke, mistõttu aine eripind oli üsna suur. Samuti võis lahustumisele kaasa aidata katte koostises olev hüdroksüpropüülmetüültselluloos. Kõige aeglasemalt vabanes raviaine SD-ga kaetud pelletitetelt. See oli ka eeldatav, kuna oli toimunud amorfse aine välja kristalliseerumine MH-na ja katte koostises olev Soluplus® ei disintegreeru antud tingimustes.

JÄRELDUSED

- Kasutatud meetoditega õnnestus valmistada ja tuvastada erinevad piroksikaami tahke aine vormid
- Kõige paremad lahustumisomadused olid amorfsel piroksikaamil tahkes dispersioonis. Kõige halvemad lahustumisomadused olid MH-l. AH ja

amorfne piroksikaam olid lahustumiskeskkonnas ebastabiilsed kristalliseerudes MH-na vastavalt 10 ja 220 minuti jooksul.

- Kõige parem biosaadavus ja kõige kiirem vereplasma kontsentratsioon rottidel saavutati SD-ga. PM AH andis paremuselt teise tulemuse, samas kui MH oli kõige madalama biosaadavusega ja samuti saabus MH puhul vereplasma maksimum kontsentratsioon kõige aeglasemalt.
- Piroksikaami ja Soluplussi® tahke dispersioon oli füüsikaliselt stabiilne madala õhuniiskusega tingimustes säilitamisel. Keskmise ja kõrge suhtelise õhuniiskusega tingimustel toimus amorfse piroksikaami kristalliseerumine vastavalt AH ja MH-na.
- Peakomponent analüüsi ja mitmemõõtmeline kõverate lahutamine võimaldasid viia läbi antud tahke dispersiooni krisalliseerumise kvalitatiivne ja kvantitatiivne analüüs. Proovides, kus oli toimunud kristallisatsioon vähenes lahustumiskiirus märgatavalt võrreldeds SD-ga.
- AH ja MH olid stabiilsed pelletite katmisel samas kui SD kristalliseerus MH-na.

9. ACKNOWLEDGEMENTS

The studies encompassed in given dissertation were mainly performed in the Department of Pharmacy, Faculty of Medicine, University of Tartu and Division of Pharmaceutical Chemistry and Technology, Faculty of Pharmacy, University of Helsinki. The XRPD experiments and SEM experiments were conducted in Department of Geology, University of Tartu and Institute of Physics, University of Tartu, respectively. This work is part of the grant project no ETF7980 and the targeted financing project no SF0180042s09, and partly financed by the projects IUT02-24 and TK117. The Estonian Science Foundation, Estonian Ministry of Education and Research and The Estonian Academy of Sciences are acknowledged for financial support. This research was also financially supported by the NordForsk, the Academy of Finland and European Social Fund's Doctoral Studies and Internationalisation Program DoRa.

My deepest gratitude goes to:

- My supervisors Researcher Karin Kogermann and Professor Peep Veski, who are thanked for their help, advice and support.
- Professor Jyrki Tapio Heinämäki, who is thanked for his substantial contribution to given studies and support.
- Professor Jouko Yliruusi, Professor Clare Strachan and Associate Professor Jaakko Aaltonen from University of Helsinki, who are thanked for acting as supervisors during my visit there.
- Researcher Ivo Laidmäe and Assistant Andres Meos, who are acknowledged for their help in conducting the bioavailability study and HPLC measurements, respectively.
- Assistant Professor Satu Lakio, who is thanked for her help in conducting the coating experiments.
- Dr Vallo Matto, who is acknowledged for fruitful discussions and his help in conducting the animal experiments.
- Dr Jaan Aruväli (Department of Geology, University of Tartu) who is acknowledged for his help in conducting the XRPD experiments.
- Professor Väino Sammelselg and Dr Jekaterina Kozlova from Institute of Physics, University of Tartu, who are acknowledged for conducting the SEM experiments.
- Dr Kai Õkva, who is thanked for her help in conducting the animal experiments.
- Undergraduate students Mirja Palo, Julia Vintsevits, Julia Sinkova, Nadezda Ruina, Maarja-Liisa Lokk, Karoli Pungas and Laura Viidik, who are thanked for their help and patience.
- All the colleagues from Department of Pharmacy, Faculty of Medicine, University of Tartu and Division of Pharmaceutical Chemistry and Technology, Faculty of Pharmacy, University of Helsinki are thanked for creating friendly atmosphere and their help, advice and support.

- Reviewers Associate Professor Uno Mäeorg and Senior Researcher Meeme Utt, who are thanked for their contribution in improving given manuscript.
- Opponent Professor Guy Van Den Mooter, who is thanked for in-depth review of given manuscript and thorough discussion.
- My family and friends, who are thanked for their endless support throughout my studies.

PUBLICATIONS

CURRICULUM VITAE

Name	Andres Lust
Date of birth	February 6, 1985, Estonia
Address	Department of Pharmacy, University of Tartu Nooruse 1, 50411, Tartu, Estonia
Phone	+372 737 5291
E-mail	andres.lust@ut.ee

Education

2001–2004	Hugo Treffner Gymnasium
2004–2010	University of Tartu, Faculty of Medicine, Department of Pharmacy
2010–2015	University of Tartu, Faculty of Medicine, PhD studies

Professional employment

2013–	University of Tartu, Department of Pharmacy, specialist

Research interests and activity

Solid state properties of pharmaceutical substances and possible interactions with excipients.

Co-author of six original publications

ELULOOKIRJELDUS

Nimi	Andres Lust
Sünniaeg	6. veebruar 1985.a., Ülenurme vald, Eesti
Aadress	Farmaatsia instituut, Arstiteaduskond, Tartu Ülikool Nooruse 1, 50411, Tartu, Eesti
Telefon	+372 737 5291
E-mail	andres.lust@ut.ee

Hariduskäik

2001–2004	Hugo Treffneri Gümnaasium
2004–2010	Tartu Ülikool, Arstiteaduskond, proviisori õppekava
2010–	Tartu Ülikool, Arstiteaduskond, doktorant farmaatsia erialal

Erialane teenistuskäik

2013–	Tartu Ülikool, farmaatsia instituut, spetsialist

Teadustegevus

Uurimisvaldkond:
Tahkete raviainete füsikokeemilised omadused ja võimalikud interaktsioonid abiainetega.
Kaasautor kuues teaduspublikatsioonis.

DISSERTATIONES MEDICINAE UNIVERSITATIS TARTUENSIS

1. **Heidi-Ingrid Maaroos.** The natural course of gastric ulcer in connection with chronic gastritis and *Helicobacter pylori*. Tartu, 1991.
2. **Mihkel Zilmer.** Na-pump in normal and tumorous brain tissues: Structural, functional and tumorigenesis aspects. Tartu, 1991.
3. **Eero Vasar.** Role of cholecystokinin receptors in the regulation of behaviour and in the action of haloperidol and diazepam. Tartu, 1992.
4. **Tiina Talvik.** Hypoxic-ischaemic brain damage in neonates (clinical, biochemical and brain computed tomographical investigation). Tartu, 1992.
5. **Ants Peetsalu.** Vagotomy in duodenal ulcer disease: A study of gastric acidity, serum pepsinogen I, gastric mucosal histology and *Helicobacter pylori*. Tartu, 1992.
6. **Marika Mikelsaar.** Evaluation of the gastrointestinal microbial ecosystem in health and disease. Tartu, 1992.
7. **Hele Everaus.** Immuno-hormonal interactions in chronic lymphocytic leukaemia and multiple myeloma. Tartu, 1993.
8. **Ruth Mikelsaar.** Etiological factors of diseases in genetically consulted children and newborn screening: dissertation for the commencement of the degree of doctor of medical sciences. Tartu, 1993.
9. **Agu Tamm.** On metabolic action of intestinal microflora: clinical aspects. Tartu, 1993.
10. **Katrin Gross.** Multiple sclerosis in South-Estonia (epidemiological and computed tomographical investigations). Tartu, 1993.
11. **Oivi Uibo.** Childhood coeliac disease in Estonia: occurrence, screening, diagnosis and clinical characterization. Tartu, 1994.
12. **Viiu Tuulik.** The functional disorders of central nervous system of chemistry workers. Tartu, 1994.
13. **Margus Viigimaa.** Primary haemostasis, antiaggregative and anticoagulant treatment of acute myocardial infarction. Tartu, 1994.
14. **Rein Kolk.** Atrial versus ventricular pacing in patients with sick sinus syndrome. Tartu, 1994.
15. **Toomas Podar.** Incidence of childhood onset type 1 diabetes mellitus in Estonia. Tartu, 1994.
16. **Kiira Subi.** The laboratory surveillance of the acute respiratory viral infections in Estonia. Tartu, 1995.
17. **Irja Lutsar.** Infections of the central nervous system in children (epidemiologic, diagnostic and therapeutic aspects, long term outcome). Tartu, 1995.
18. **Aavo Lang.** The role of dopamine, 5-hydroxytryptamine, sigma and NMDA receptors in the action of antipsychotic drugs. Tartu, 1995.
19. **Andrus Arak.** Factors influencing the survival of patients after radical surgery for gastric cancer. Tartu, 1996.
20. **Tõnis Karki.** Quantitative composition of the human lactoflora and method for its examination. Tartu, 1996.

21. **Reet Mändar.** Vaginal microflora during pregnancy and its transmission to newborn. Tartu, 1996.
22. **Triin Remmel.** Primary biliary cirrhosis in Estonia: epidemiology, clinical characterization and prognostication of the course of the disease. Tartu, 1996.
23. **Toomas Kivastik.** Mechanisms of drug addiction: focus on positive reinforcing properties of morphine. Tartu, 1996.
24. **Paavo Pokk.** Stress due to sleep deprivation: focus on $GABA_A$ receptor-chloride ionophore complex. Tartu, 1996.
25. **Kristina Allikmets.** Renin system activity in essential hypertension. Associations with atherothrombogenic cardiovascular risk factors and with the efficacy of calcium antagonist treatment. Tartu, 1996.
26. **Triin Parik.** Oxidative stress in essential hypertension: Associations with metabolic disturbances and the effects of calcium antagonist treatment. Tartu, 1996.
27. **Svetlana Päi.** Factors promoting heterogeneity of the course of rheumatoid arthritis. Tartu, 1997.
28. **Maarike Sallo.** Studies on habitual physical activity and aerobic fitness in 4 to 10 years old children. Tartu, 1997.
29. **Paul Naaber.** *Clostridium difficile* infection and intestinal microbial ecology. Tartu, 1997.
30. **Rein Pähkla.** Studies in pinoline pharmacology. Tartu, 1997.
31. **Andrus Juhan Voitk.** Outpatient laparoscopic cholecystectomy. Tartu, 1997.
32. **Joel Starkopf.** Oxidative stress and ischaemia-reperfusion of the heart. Tartu, 1997.
33. **Janika Kõrv.** Incidence, case-fatality and outcome of stroke. Tartu, 1998.
34. **Ülla Linnamägi.** Changes in local cerebral blood flow and lipid peroxidation following lead exposure in experiment. Tartu, 1998.
35. **Ave Minajeva.** Sarcoplasmic reticulum function: comparison of atrial and ventricular myocardium. Tartu, 1998.
36. **Oleg Milenin.** Reconstruction of cervical part of esophagus by revascularised ileal autografts in dogs. A new complex multistage method. Tartu, 1998.
37. **Sergei Pakriev.** Prevalence of depression, harmful use of alcohol and alcohol dependence among rural population in Udmurtia. Tartu, 1998.
38. **Allen Kaasik.** Thyroid hormone control over β-adrenergic signalling system in rat atria. Tartu, 1998.
39. **Vallo Matto.** Pharmacological studies on anxiogenic and antiaggressive properties of antidepressants. Tartu, 1998.
40. **Maire Vasar.** Allergic diseases and bronchial hyperreactivity in Estonian children in relation to environmental influences. Tartu, 1998.
41. **Kaja Julge.** Humoral immune responses to allergens in early childhood. Tartu, 1998.
42. **Heli Grünberg.** The cardiovascular risk of Estonian schoolchildren. A cross-sectional study of 9-, 12- and 15-year-old children. Tartu, 1998.

43. **Epp Sepp.** Formation of intestinal microbial ecosystem in children. Tartu, 1998.
44. **Mai Ots.** Characteristics of the progression of human and experimental glomerulopathies. Tartu, 1998.
45. **Tiina Ristimäe.** Heart rate variability in patients with coronary artery disease. Tartu, 1998.
46. **Leho Kõiv.** Reaction of the sympatho-adrenal and hypothalamo-pituitary-adrenocortical system in the acute stage of head injury. Tartu, 1998.
47. **Bela Adojaan.** Immune and genetic factors of childhood onset IDDM in Estonia. An epidemiological study. Tartu, 1999.
48. **Jakov Shlik.** Psychophysiological effects of cholecystokinin in humans. Tartu, 1999.
49. **Kai Kisand.** Autoantibodies against dehydrogenases of α-ketoacids. Tartu, 1999.
50. **Toomas Marandi.** Drug treatment of depression in Estonia. Tartu, 1999.
51. **Ants Kask.** Behavioural studies on neuropeptide Y. Tartu, 1999.
52. **Ello-Rahel Karelson.** Modulation of adenylate cyclase activity in the rat hippocampus by neuropeptide galanin and its chimeric analogs. Tartu, 1999.
53. **Tanel Laisaar.** Treatment of pleural empyema — special reference to intrapleural therapy with streptokinase and surgical treatment modalities. Tartu, 1999.
54. **Eve Pihl.** Cardiovascular risk factors in middle-aged former athletes. Tartu, 1999.
55. **Katrin Õunap.** Phenylketonuria in Estonia: incidence, newborn screening, diagnosis, clinical characterization and genotype/phenotype correlation. Tartu, 1999.
56. **Siiri Kõljalg.** *Acinetobacter* – an important nosocomial pathogen. Tartu, 1999.
57. **Helle Karro.** Reproductive health and pregnancy outcome in Estonia: association with different factors. Tartu, 1999.
58. **Heili Varendi.** Behavioral effects observed in human newborns during exposure to naturally occurring odors. Tartu, 1999.
59. **Anneli Beilmann.** Epidemiology of epilepsy in children and adolescents in Estonia. Prevalence, incidence, and clinical characteristics. Tartu, 1999.
60. **Vallo Volke.** Pharmacological and biochemical studies on nitric oxide in the regulation of behaviour. Tartu, 1999.
61. **Pilvi Ilves.** Hypoxic-ischaemic encephalopathy in asphyxiated term infants. A prospective clinical, biochemical, ultrasonographical study. Tartu, 1999.
62. **Anti Kalda.** Oxygen-glucose deprivation-induced neuronal death and its pharmacological prevention in cerebellar granule cells. Tartu, 1999.
63. **Eve-Irene Lepist.** Oral peptide prodrugs – studies on stability and absorption. Tartu, 2000.
64. **Jana Kivastik.** Lung function in Estonian schoolchildren: relationship with anthropometric indices and respiratory symptomas, reference values for dynamic spirometry. Tartu, 2000.

65. **Karin Kull.** Inflammatory bowel disease: an immunogenetic study. Tartu, 2000.
66. **Kaire Innos.** Epidemiological resources in Estonia: data sources, their quality and feasibility of cohort studies. Tartu, 2000.
67. **Tamara Vorobjova.** Immune response to *Helicobacter pylori* and its association with dynamics of chronic gastritis and epithelial cell turnover in antrum and corpus. Tartu, 2001.
68. **Ruth Kalda.** Structure and outcome of family practice quality in the changing health care system of Estonia. Tartu, 2001.
69. **Annika Krüüner.** *Mycobacterium tuberculosis* – spread and drug resistance in Estonia. Tartu, 2001.
70. **Marlit Veldi.** Obstructive Sleep Apnoea: Computerized Endopharyngeal Myotonometry of the Soft Palate and Lingual Musculature. Tartu, 2001.
71. **Anneli Uusküla.** Epidemiology of sexually transmitted diseases in Estonia in 1990–2000. Tartu, 2001.
72. **Ade Kallas.** Characterization of antibodies to coagulation factor VIII. Tartu, 2002.
73. **Heidi Annuk.** Selection of medicinal plants and intestinal lactobacilli as antimicrobil components for functional foods. Tartu, 2002.
74. **Aet Lukmann**. Early rehabilitation of patients with ischaemic heart disease after surgical revascularization of the myocardium: assessment of health-related quality of life, cardiopulmonary reserve and oxidative stress. A clinical study. Tartu, 2002.
75. **Maigi Eisen.** Pathogenesis of Contact Dermatitis: participation of Oxidative Stress. A clinical – biochemical study. Tartu, 2002.
76. **Piret Hussar.** Histology of the post-traumatic bone repair in rats. Elaboration and use of a new standardized experimental model – bicortical perfora-

    2002.
77. **Tõnu Rätsep.** Aneurysmal subarachnoid haemorrhage: Noninvasive monitoring of cerebral haemodynamics. Tartu, 2002.
78. **Marju Herodes.** Quality of life of people with epilepsy in Estonia. Tartu, 2003.
79. **Katre Maasalu.** Changes in bone quality due to age and genetic disorders and their clinical expressions in Estonia. Tartu, 2003.
80. **Toomas Sillakivi.** Perforated peptic ulcer in Estonia: epidemiology, risk factors and relations with *Helicobacter pylori*. Tartu, 2003.
81. **Leena Puksa.** Late responses in motor nerve conduction studies. F and A waves in normal subjects and patients with neuropathies. Tartu, 2003.
82. **Krista Lõivukene**. *Helicobacter pylori* in gastric microbial ecology and its antimicrobial susceptibility pattern. Tartu, 2003.
83. **Helgi Kolk.** Dyspepsia and *Helicobacter pylori* infection: the diagnostic value of symptoms, treatment and follow-up of patients referred for upper gastrointestinal endoscopy by family physicians. Tartu, 2003.

84. **Helena Soomer.** Validation of identification and age estimation methods in forensic odontology. Tartu, 2003.
85. **Kersti Oselin.** Studies on the human MDR1, MRP1, and MRP2 ABC transporters: functional relevance of the genetic polymorphisms in the *MDR1* and *MRP1* gene. Tartu, 2003.
86. **Jaan Soplepmann.** Peptic ulcer haemorrhage in Estonia: epidemiology, prognostic factors, treatment and outcome. Tartu, 2003.
87. **Margot Peetsalu.** Long-term follow-up after vagotomy in duodenal ulcer disease: recurrent ulcer, changes in the function, morphology and *Helicobacter pylori* colonisation of the gastric mucosa. Tartu, 2003.
88. **Kersti Klaamas.** Humoral immune response to *Helicobacter pylori* a study of host-dependent and microbial factors. Tartu, 2003.
89. **Pille Taba.** Epidemiology of Parkinson's disease in Tartu, Estonia. Prevalence, incidence, clinical characteristics, and pharmacoepidemiology. Tartu, 2003.
90. **Alar Veraksitš**. Characterization of behavioural and biochemical phenotype of cholecystokinin-2 receptor deficient mice: changes in the function of the dopamine and endopioidergic system. Tartu, 2003.
91. **Ingrid Kalev.** CC-chemokine receptor 5 (CCR5) gene polymorphism in Estonians and in patients with Type I and Type II diabetes mellitus. Tartu, 2003.
92. **Lumme Kadaja.** Molecular approach to the regulation of mitochondrial function in oxidative muscle cells. Tartu, 2003.
93. **Aive Liigant**. Epidemiology of primary central nervous system tumours in Estonia from 1986 to 1996. Clinical characteristics, incidence, survival and prognostic factors. Tartu, 2004.
94. **Andres, Kulla.** Molecular characteristics of mesenchymal stroma in human astrocytic gliomas. Tartu, 2004.
95. **Mari Järvelaid.** Health damaging risk behaviours in adolescence. Tartu, 2004.
96. **Ülle Pechter.** Progression prevention strategies in chronic renal failure and hypertension. An experimental and clinical study. Tartu, 2004.
97. **Gunnar Tasa.** Polymorphic glutathione S-transferases – biology and role in modifying genetic susceptibility to senile cataract and primary open angle glaucoma. Tartu, 2004.
98. **Tuuli Käämbre.** Intracellular energetic unit: structural and functional aspects. Tartu, 2004.
99. **Vitali Vassiljev.** Influence of nitric oxide syntase inhibitors on the effects of ethanol after acute and chronic ethanol administration and withdrawal. Tartu, 2004.
100. **Aune Rehema.** Assessment of nonhaem ferrous iron and glutathione redox ratio as markers of pathogeneticity of oxidative stress in different clinical groups. Tartu, 2004.
101. **Evelin Seppet.** Interaction of mitochondria and ATPases in oxidative muscle cells in normal and pathological conditions. Tartu, 2004.

102. **Eduard Maron.** Serotonin function in panic disorder: from clinical experiments to brain imaging and genetics. Tartu, 2004.
103. **Marje Oona.** *Helicobacter pylori* infection in children: epidemiological and therapeutic aspects. Tartu, 2004.
104. **Kersti Kokk.** Regulation of active and passive molecular transport in the testis. Tartu, 2005.
105. **Vladimir Järv.** Cross-sectional imaging for pretreatment evaluation and follow-up of pelvic malignant tumours. Tartu, 2005.
106. **Andre Õun.** Epidemiology of adult epilepsy in Tartu, Estonia. Incidence, prevalence and medical treatment. Tartu, 2005.
107. **Piibe Muda.** Homocysteine and hypertension: associations between homocysteine and essential hypertension in treated and untreated hypertensive patients with and without coronary artery disease. Tartu, 2005.
108. **Külli Kingo.** The interleukin-10 family cytokines gene polymorphisms in plaque psoriasis. Tartu, 2005.
109. **Mati Merila.** Anatomy and clinical relevance of the glenohumeral joint capsule and ligaments. Tartu, 2005.
110. **Epp Songisepp**. Evaluation of technological and functional properties of the new probiotic *Lactobacillus fermentum* ME-3. Tartu, 2005.
111. **Tiia Ainla.** Acute myocardial infarction in Estonia: clinical characteristics, management and outcome. Tartu, 2005.
112. **Andres Sell.** Determining the minimum local anaesthetic requirements for hip replacement surgery under spinal anaesthesia – a study employing a spinal catheter. Tartu, 2005.
113. **Tiia Tamme.** Epidemiology of odontogenic tumours in Estonia. Pathogenesis and clinical behaviour of ameloblastoma. Tartu, 2005.
114. **Triine Annus**. Allergy in Estonian schoolchildren: time trends and characteristics. Tartu, 2005.
115. **Tiia Voor.** Microorganisms in infancy and development of allergy: comparison of Estonian and Swedish children. Tartu, 2005.
116. **Priit Kasenõmm.** Indicators for tonsillectomy in adults with recurrent tonsillitis – clinical, microbiological and pathomorphological investigations. Tartu, 2005.
117. **Eva Zusinaite.** Hepatitis C virus: genotype identification and interactions between viral proteases. Tartu, 2005.
118. **Piret Kõll.** Oral lactoflora in chronic periodontitis and periodontal health. Tartu, 2006.
119. **Tiina Stelmach.** Epidemiology of cerebral palsy and unfavourable neurodevelopmental outcome in child population of Tartu city and county, Estonia Prevalence, clinical features and risk factors. Tartu, 2006.
120. **Katrin Pudersell.** Tropane alkaloid production and riboflavine excretion in the field and tissue cultures of henbane (*Hyoscyamus niger* L.). Tartu, 2006.
121. **Külli Jaako.** Studies on the role of neurogenesis in brain plasticity. Tartu, 2006.

122. **Aare Märtson.** Lower limb lengthening: experimental studies of bone regeneration and long-term clinical results. Tartu, 2006.
123. **Heli Tähepõld.** Patient consultation in family medicine. Tartu, 2006.
124. **Stanislav Liskmann.** Peri-implant disease: pathogenesis, diagnosis and treatment in view of both inflammation and oxidative stress profiling. Tartu, 2006.
125. **Ruth Rudissaar.** Neuropharmacology of atypical antipsychotics and an animal model of psychosis. Tartu, 2006.
126. **Helena Andreson.** Diversity of *Helicobacter pylori* genotypes in Estonian patients with chronic inflammatory gastric diseases. Tartu, 2006.
127. **Katrin Pruus.** Mechanism of action of antidepressants: aspects of serotoninergic system and its interaction with glutamate. Tartu, 2006.
128. **Priit Põder.** Clinical and experimental investigation: relationship of ischaemia/reperfusion injury with oxidative stress in abdominal aortic aneurysm repair and in extracranial brain artery endarterectomy and possibilities of protection against ischaemia using a glutathione analogue in a rat model of global brain ischaemia. Tartu, 2006.
129. **Marika Tammaru.** Patient-reported outcome measurement in rheumatoid arthritis. Tartu, 2006.
130. **Tiia Reimand.** Down syndrome in Estonia. Tartu, 2006.
131. **Diva Eensoo.** Risk-taking in traffic and Markers of Risk-Taking Behaviour in Schoolchildren and Car Drivers. Tartu, 2007.
132. **Riina Vibo.** The third stroke registry in Tartu, Estonia from 2001 to 2003: incidence, case-fatality, risk factors and long-term outcome. Tartu, 2007.
133. **Chris Pruunsild.** Juvenile idiopathic arthritis in children in Estonia. Tartu, 2007.
134. **Eve Õiglane-Šlik.** Angelman and Prader-Willi syndromes in Estonia. Tartu, 2007.
135. **Kadri Haller.** Antibodies to follicle stimulating hormone. Significance in female infertility. Tartu, 2007.
136. **Pille Ööpik.** Management of depression in family medicine. Tartu, 2007.
137. **Jaak Kals.** Endothelial function and arterial stiffness in patients with atherosclerosis and in healthy subjects. Tartu, 2007.
138. **Priit Kampus.** Impact of inflammation, oxidative stress and age on arterial stiffness and carotid artery intima-media thickness. Tartu, 2007.
139. **Margus Punab.** Male fertility and its risk factors in Estonia. Tartu, 2007.
140. **Alar Toom**. Heterotopic ossification after total hip arthroplasty: clinical and pathogenetic investigation. Tartu, 2007.
141. **Lea Pehme.** Epidemiology of tuberculosis in Estonia 1991–2003 with special regard to extrapulmonary tuberculosis and delay in diagnosis of pulmonary tuberculosis. Tartu, 2007.
142. **Juri Karjagin.** The pharmacokinetics of metronidazole and meropenem in septic shock. Tartu, 2007.
143. **Inga Talvik.** Inflicted traumatic brain injury shaken baby syndrome in Estonia – epidemiology and outcome. Tartu, 2007.

144. **Tarvo Rajasalu.** Autoimmune diabetes: an immunological study of type 1 diabetes in humans and in a model of experimental diabetes (in RIP-B7.1 mice). Tartu, 2007.
145. **Inga Karu.** Ischaemia-reperfusion injury of the heart during coronary surgery: a clinical study investigating the effect of hyperoxia. Tartu, 2007.
146. **Peeter Padrik.** Renal cell carcinoma: Changes in natural history and treatment of metastatic disease. Tartu, 2007.
147. **Neve Vendt**. Iron deficiency and iron deficiency anaemia in infants aged 9 to 12 months in Estonia. Tartu, 2008.
148. **Lenne-Triin Heidmets.** The effects of neurotoxins on brain plasticity: focus on neural Cell Adhesion Molecule. Tartu, 2008.
149. **Paul Korrovits.** Asymptomatic inflammatory prostatitis: prevalence, etiological factors, diagnostic tools. Tartu, 2008.
150. **Annika Reintam.** Gastrointestinal failure in intensive care patients. Tartu, 2008.
151. **Kristiina Roots.** Cationic regulation of Na-pump in the normal, Alzheimer's and CCK_2 receptor-deficient brain. Tartu, 2008.
152. **Helen Puusepp.** The genetic causes of mental retardation in Estonia: fragile X syndrome and creatine transporter defect. Tartu, 2009.
153. **Kristiina Rull.** Human chorionic gonadotropin beta genes and recurrent miscarriage: expression and variation study. Tartu, 2009.
154. **Margus Eimre.** Organization of energy transfer and feedback regulation in oxidative muscle cells. Tartu, 2009.
155. **Maire Link.** Transcription factors FoxP3 and AIRE: autoantibody associations. Tartu, 2009.
156. **Kai Haldre.** Sexual health and behaviour of young women in Estonia. Tartu, 2009.
157. **Kaur Liivak.** Classical form of congenital adrenal hyperplasia due to 21-hydroxylase deficiency in Estonia: incidence, genotype and phenotype with special attention to short-term growth and 24-hour blood pressure. Tartu, 2009.
158. **Kersti Ehrlich.** Antioxidative glutathione analogues (UPF peptides) – molecular design, structure-activity relationships and testing the protective properties. Tartu, 2009.
159. **Anneli Rätsep.** Type 2 diabetes care in family medicine. Tartu, 2009.
160. **Silver Türk.** Etiopathogenetic aspects of chronic prostatitis: role of mycoplasmas, coryneform bacteria and oxidative stress. Tartu, 2009.
161. **Kaire Heilman.** Risk markers for cardiovascular disease and low bone mineral density in children with type 1 diabetes. Tartu, 2009.
162. **Kristi Rüütel.** HIV-epidemic in Estonia: injecting drug use and quality of life of people living with HIV. Tartu, 2009.
163. **Triin Eller.** Immune markers in major depression and in antidepressive treatment. Tartu, 2009.

164. **Siim Suutre.** The role of TGF-β isoforms and osteoprogenitor cells in the pathogenesis of heterotopic ossification. An experimental and clinical study of hip arthroplasty. Tartu, 2010.
165. **Kai Kliiman.** Highly drug-resistant tuberculosis in Estonia: Risk factors and predictors of poor treatment outcome. Tartu, 2010.
166. **Inga Villa.** Cardiovascular health-related nutrition, physical activity and fitness in Estonia. Tartu, 2010.
167. **Tõnis Org.** Molecular function of the first PHD finger domain of Autoimmune Regulator protein. Tartu, 2010.
168. **Tuuli Metsvaht.** Optimal antibacterial therapy of neonates at risk of early onset sepsis. Tartu, 2010.
169. **Jaanus Kahu.** Kidney transplantation: Studies on donor risk factors and mycophenolate mofetil. Tartu, 2010.
170. **Koit Reimand.** Autoimmunity in reproductive failure: A study on associated autoantibodies and autoantigens. Tartu, 2010.
171. **Mart Kull.** Impact of vitamin D and hypolactasia on bone mineral density: a population based study in Estonia. Tartu, 2010.
172. **Rael Laugesaar.** Stroke in children – epidemiology and risk factors. Tartu, 2010.
173. **Mark Braschinsky.** Epidemiology and quality of life issues of hereditary spastic paraplegia in Estonia and implemention of genetic analysis in everyday neurologic practice. Tartu, 2010.
174. **Kadri Suija.** Major depression in family medicine: associated factors, recurrence and possible intervention. Tartu, 2010.
175. **Jarno Habicht.** Health care utilisation in Estonia: socioeconomic determinants and financial burden of out-of-pocket payments. Tartu, 2010.
176. **Kristi Abram.** The prevalence and risk factors of rosacea. Subjective disease perception of rosacea patients. Tartu, 2010.
177. **Malle Kuum.** Mitochondrial and endoplasmic reticulum cation fluxes: Novel roles in cellular physiology. Tartu, 2010.
178. **Rita Teek.** The genetic causes of early onset hearing loss in Estonian children. Tartu, 2010.
179. **Daisy Volmer.** The development of community pharmacy services in Estonia – public and professional perceptions 1993–2006. Tartu, 2010.
180. **Jelena Lissitsina.** Cytogenetic causes in male infertility. Tartu, 2011.
181. **Delia Lepik.** Comparison of gunshot injuries caused from Tokarev, Makarov and Glock 19 pistols at different firing distances. Tartu, 2011.
182. **Ene-Renate Pähkla**. Factors related to the efficiency of treatment of advanced periodontitis. Tartu, 2011.
183. **Maarja Krass.** L-Arginine pathways and antidepressant action. Tartu, 2011.
184. **Taavi Lai.** Population health measures to support evidence-based health policy in Estonia. Tartu, 2011.

185. **Tiit Salum.** Similarity and difference of temperature-dependence of the brain sodium pump in normal, different neuropathological, and aberrant conditions and its possible reasons. Tartu, 2011.
186. **Tõnu Vooder**. Molecular differences and similarities between histological subtypes of non-small cell lung cancer. Tartu, 2011.
187. **Jelena Štšepetova.** The characterisation of intestinal lactic acid bacteria using bacteriological, biochemical and molecular approaches. Tartu, 2011.
188. **Radko Avi.** Natural polymorphisms and transmitted drug resistance in Estonian HIV-1 CRF06_cpx and its recombinant viruses. Tartu, 2011, 116 p.
189. **Edward Laane**. Multiparameter flow cytometry in haematological malignancies. Tartu, 2011, 152 p.
190. **Triin Jagomägi.** A study of the genetic etiology of nonsyndromic cleft lip and palate. Tartu, 2011, 158 p.
191. **Ivo Laidmäe.** Fibrin glue of fish (*Salmo salar*) origin: immunological study and development of new pharmaceutical preparation. Tartu, 2012, 150 p.
192. **Ülle Parm.** Early mucosal colonisation and its role in prediction of invasive infection in neonates at risk of early onset sepsis. Tartu, 2012, 168 p.
193. **Kaupo Teesalu.** Autoantibodies against desmin and transglutaminase 2 in celiac disease: diagnostic and functional significance. Tartu, 2012, 142 p.
194. **Maksim Zagura**. Biochemical, functional and structural profiling of arterial damage in atherosclerosis. Tartu, 2012, 162 p.
195. **Vivian Kont.** Autoimmune regulator: characterization of thymic gene regulation and promoter methylation. Tartu, 2012, 134 p.
196. **Pirje Hütt.** Functional properties, persistence, safety and efficacy of potential probiotic lactobacilli. Tartu, 2012, 246 p.
197. **Innar Tõru.** Serotonergic modulation of CCK-4- induced panic. Tartu, 2012, 132 p.
198. **Sigrid Vorobjov.** Drug use, related risk behaviour and harm reduction interventions utilization among injecting drug users in Estonia: implications for drug policy. Tartu, 2012, 120 p.
199. **Martin Serg.** Therapeutic aspects of central haemodynamics, arterial stiffness and oxidative stress in hypertension. Tartu, 2012, 156 p.
200. **Jaanika Kumm.** Molecular markers of articular tissues in early knee osteoarthritis: a population-based longitudinal study in middle-aged subjects. Tartu, 2012, 159 p.
201. **Kertu Rünkorg.** Functional changes of dopamine, endopioid and endocannabinoid systems in CCK2 receptor deficient mice. Tartu, 2012, 125 p.
202. **Mai Blöndal.** Changes in the baseline characteristics, management and outcomes of acute myocardial infarction in Estonia. Tartu, 2012, 127 p.
203. **Jana Lass.** Epidemiological and clinical aspects of medicines use in children in Estonia. Tartu, 2012, 170 p.
204. **Kai Truusalu.** Probiotic lactobacilli in experimental persistent *Salmonella* infection. Tartu, 2013, 139 p.

205. **Oksana Jagur.** Temporomandibular joint diagnostic imaging in relation to pain and bone characteristics. Long-term results of arthroscopic treatment. Tartu, 2013, 126 p.
206. **Katrin Sikk.** Manganese-ephedrone intoxication – pathogenesis of neurological damage and clinical symptomatology. Tartu, 2013, 125 p.
207. **Kai Blöndal.** Tuberculosis in Estonia with special emphasis on drug-resistant tuberculosis: Notification rate, disease recurrence and mortality. Tartu, 2013, 151 p.
208. **Marju Puurand.** Oxidative phosphorylation in different diseases of gastric mucosa. Tartu, 2013, 123 p.
209. **Aili Tagoma.** Immune activation in female infertility: Significance of autoantibodies and inflammatory mediators. Tartu, 2013, 135 p.
210. **Liis Sabre.** Epidemiology of traumatic spinal cord injury in Estonia. Brain activation in the acute phase of traumatic spinal cord injury. Tartu, 2013, 135 p.
211. **Merit Lamp.** Genetic susceptibility factors in endometriosis. Tartu, 2013, 125 p.
212. **Erik Salum.** Beneficial effects of vitamin D and angiotensin II receptor blocker on arterial damage. Tartu, 2013, 167 p.
213. **Maire Karelson.** Vitiligo: clinical aspects, quality of life and the role of melanocortin system in pathogenesis. Tartu, 2013, 153 p.
214. **Kuldar Kaljurand.** Prevalence of exfoliation syndrome in Estonia and its clinical significance. Tartu, 2013, 113 p.
215. **Raido Paasma.** Clinical study of methanol poisoning: handling large outbreaks, treatment with antidotes, and long-term outcomes. Tartu, 2013, 96 p.
216. **Anne Kleinberg.** Major depression in Estonia: prevalence, associated factors, and use of health services. Tartu, 2013, 129 p.
217. **Triin Eglit.** Obesity, impaired glucose regulation, metabolic syndrome and their associations with high-molecular-weight adiponectin levels. Tartu, 2014, 115 p.
218. **Kristo Ausmees.** Reproductive function in middle-aged males: Associations with prostate, lifestyle and couple infertility status. Tartu, 2014, 125 p.
219. **Kristi Huik.** The influence of host genetic factors on the susceptibility to HIV and HCV infections among intravenous drug users. Tartu, 2014, 144 p.
220. **Liina Tserel.** Epigenetic profiles of monocytes, monocyte-derived macrophages and dendritic cells. Tartu, 2014, 143 p.
221. **Irina Kerna.** The contribution of *ADAM12* and *CILP* genes to the development of knee osteoarthritis. Tartu, 2014, 152 p.
222. **Ingrit Liiv.** Autoimmune regulator protein interaction with DNA-dependent protein kinase and its role in apoptosis. Tartu, 2014, 143 p.
223. **Liivi Maddison.** Tissue perfusion and metabolism during intra-abdominal hypertension. Tartu, 2014, 103 p.

224. **Krista Ress.** Childhood coeliac disease in Estonia, prevalence in atopic dermatitis and immunological characterisation of coexistence. Tartu, 2014, 124 p.
225. **Kai Muru.** Prenatal screening strategies, long-term outcome of children with marked changes in maternal screening tests and the most common syndromic heart anomalies in Estonia. Tartu, 2014, 189 p.
226. **Kaja Rahu.** Morbidity and mortality among Baltic Chernobyl cleanup workers: a register-based cohort study. Tartu, 2014, 155 p.
227. **Klari Noormets.** The development of diabetes mellitus, fertility and energy metabolism disturbances in a Wfs1-deficient mouse model of Wolfram syndrome. Tartu, 2014, 132 p.
228. **Liis Toome.** Very low gestational age infants in Estonia. Tartu, 2014, 183 p.
229. **Ceith Nikkolo.** Impact of different mesh parameters on chronic pain and foreign body feeling after open inguinal hernia repair. Tartu, 2014, 132 p.
230. **Vadim Brjalin.** Chronic hepatitis C: predictors of treatment response in Estonian patients. Tartu, 2014, 122 p.
231. **Vahur Metsna.** Anterior knee pain in patients following total knee arthroplasty: the prevalence, correlation with patellar cartilage impairment and aspects of patellofemoral congruence. Tartu, 2014, 130 p.
232. **Marju Kase.** Glioblastoma multiforme: possibilities to improve treatment efficacy. Tartu, 2015, 137 p.
233. **Riina Runnel.** Oral health among elementary school children and the effects of polyol candies on the prevention of dental caries. Tartu, 2015, 112 p.
234. **Made Laanpere**. Factors influencing women's sexual health and reproductive choices in Estonia. Tartu, 2015, 176 p.